Master's thesis

NTNU
Norwegian University of Science and Technology
Faculty of Engineering
Department of Energy and Process Engineering

Thomas Svensson Moen

Mitigation of Discharge Fluctuations from Hydropower Plants by Active Measures

Master's thesis in Energy and Environmental Engineering
Supervisor: Pål-Tore Storli
January 2019

NTNU
Norwegian University of
Science and Technology

Thomas Svensson Moen

Mitigation of Discharge Fluctuations from Hydropower Plants by Active Measures

Master's thesis in Energy and Environmental Engineering
Supervisor: Pål-Tore Storli
January 2019

Norwegian University of Science and Technology
Faculty of Engineering
Department of Energy and Process Engineering

NTNU
Norwegian University of
Science and Technology

NTNU

Norwegian University
of Science and Technology

Department of Energy
and Process Engineering

EPT-M-2018-57

MASTER THESIS

for

Student Thomas Moen

Fall 2018

Mitigation of discharge fluctuations from hydropower plants by active measures

Demping av fluktuasjoner i volumstrøm fra vannkraftverk ved aktive tiltak

Background

A lot of hydropower plants have an upper reservoir making them highly suited for power balancing and highly variable power production. However, a lot of these power plants have outlet to a river, and the discharge fluctuations in the river caused by highly flexible power production might give unacceptable environmental impacts.
A technical solution has been proposed which will mitigate such discharge fluctuations, making highly flexible operation possible in theory. The solution consist of a cavern established in connection with the tailrace tunnel that will act as a temporary water storage reservoir. Active use of pressurized air in the cavern will influence the dynamics in the waterway, and mitigate the fluctuations.

Objective: Simulation of this active measure to find out if it is technically possible to obtain the desired effect at Nea power plant owned and operated by Statkraft.

The following tasks are to be considered:

1. Literature study on system dynamics and turbine operation

2. Establish a numerical model for simulation of the proposed new technology at Nea power plant. The model should aim to include a compressor and the governing of this to find out if this will enable the desired mitigation of the discharge fluctuations

3. Perform simulations of operation at Nea power plant, operation that will be specified by considerations intended to highlight the benefits of the system

-- ” --

Within 14 days of receiving the written text on the master thesis, the candidate shall submit a research plan for his project to the department.

When the thesis is evaluated, emphasis is put on processing of the results, and that they are presented in tabular and/or graphic form in a clear manner, and that they are analyzed carefully.

The thesis should be formulated as a research report with summary both in English and Norwegian, conclusion, literature references, table of contents etc. During the preparation of the text, the candidate should make an effort to produce a well-structured and easily readable report. In order to ease the evaluation of the thesis, it is important that the cross-references are correct. In the making of the report, strong emphasis should be placed on both a thorough discussion of the results and an orderly presentation.

The candidate is requested to initiate and keep close contact with his/her academic supervisor(s) throughout the working period. The candidate must follow the rules and regulations of NTNU as well as passive directions given by the Department of Energy and Process Engineering.

Risk assessment of the candidate's work shall be carried out according to the department's procedures. The risk assessment must be documented and included as part of the final report. Events related to the candidate's work adversely affecting the health, safety or security, must be documented and included as part of the final report. If the documentation on risk assessment represents a large number of pages, the full version is to be submitted electronically to the supervisor and an excerpt is included in the report.

Pursuant to "Regulations concerning the supplementary provisions to the technology study program/Master of Science" at NTNU §20, the Department reserves the permission to utilize all the results and data for teaching and research purposes as well as in future publications.

The final report is to be submitted digitally in INSPERA. An executive summary of the thesis including title, student's name, supervisor's name, year, department name, and NTNU's logo and name, shall be submitted to the department as a separate pdf file. Based on an agreement with the supervisor, the final report and other material and documents may be given to the supervisor in digital format.

☐ Work to be done in lab (Water power lab, Fluids engineering lab, Thermal engineering lab)
☐ Field work

Department of Energy and Process Engineering, 13. August 2018

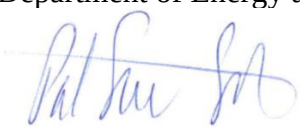

Pål-Tore Storli
Academic Supervisor

Co-supervisor: Bjørnar Svingen

NTNU

Preface

This Master's thesis is written during the autumn of 2018 at the Waterpower Laboratory at NTNU. My previous, unpublished, project work on the same topic provided me with some guidance on how this Master's thesis should be developed, as well as some experience with the LVTrans simulation tool.

First of all, thanks to Statkraft for letting me use Bratsberg hydropower plant as a case, and especially thanks to Karl Henry Andersen and Erik Jacques Wiborg for providing specific data and information about Bratsberg. I would like to thank my main supervisor Pål-Tore Selbo Storli for all your help and our weekly meetings and discussions. Your feedback have been crucial for the direction this project has taken, and I have always left your office with more motivation than I had when i came in. In addition, I am deeply grateful to my co-supervisor Bjørnar Svingen for the help with LVTrans. By answering some of my many questions, you have saved me a lot of time and effort. I would also like to thank NTNU Professor Lars Eirik Bakken for some key-information regarding compressors and their complex nature. Moreover, I owe a debt of gratitude to Julia Bådsvik for proofreading the thesis during the critical final stages of completion.

Everyone at the Waterpower Laboratory deserves a token of appreciation for creating such an inclusive and safe environment. Especially thanks to all my fellow students for enjoyable times and a lots of fun.

Most of all, thanks to my dear Astrid for always being supportive and inspiring in so many ways. I am truly grateful for having you in my life.

At last, thanks to my family for my good genes, although they came in more handy in sports than fluid mechanics.

Thomas Svensson Moen

Trondheim, January 2019

Abstract

As wind power and solar photovoltaic (PV) continues to develop, an increasing part of the total energy production mix comes from fluctuating intermittent energy sources. This generates the need for stable energy providers that can help balance the total energy supply. The flexibility of hydropower, considering both energy storage capacity and quick response time, makes hydroelectric production highly suitable to counteract changes in other renewable sources. In addition to the appealing abilities, hydropower have the advantage of already being a well-established method of power production. However, there are several challenges related to the development of future hydropower systems, and increased flexibility in hydropower plants (HPPs) with an outlet to a river is one of the qualities future hydropower needs. In these HPPs, the highly fluctuating flows from varying power production, known as hydropeaking, can have a detrimental impact on the river ecosystem. The rate of change in discharge flow is one of the main problems to juvenile fish in particular, where stranding and unintended drifting threatens the living conditions. To increase the hydroelectric flexibility while limiting the effect on the adjacent watercourses, the concept idea of ACUR LE, the Air Cushion Underground Reservoir (Low Energy), is investigated in more detail. ACUR LE is a pressure-regulated water storage volume of great dimensions in connection with the tailrace tunnel of a HPP. With the use of valves and compressors between an air adit and ACUR LE, the air pressure is regulated to adjust the ratio of water and air in the chamber at all times. As increasing air pressure is directly related to the volume flow out of the chamber, the total hydropower discharge to the river can be controlled.

In this Master's thesis, ACUR LE is successfully developed as a hydropower element in the toolkit of the LVTrans simulation program, utilized in LabVIEW. To describe the system dynamics for various amounts of air in ACUR LE, the polytropic relation for pressure and volume is used with the assumption of adiabatic behavior. The compressor and valve are taken into consideration as their assumed limitations on volume flow are included in the element. The case HPP Bratsberg is modeled in LVTrans with and without ACUR LE and simulated for different scenarios such as startup, shutdown and flood control. The simulations demonstrate how ACUR LE successfully mitigates fluctuations from varying power operating procedures. In a startup scenario, the power response time is reduced to seconds, while the total HPP discharge flow is controlled by ACUR LE to increase slowly during several minutes. Additionally, the HPP can shut down during one-third of time compared to the normal operating procedure, without causing unacceptable fluctuations for the adjacent river. However, due to the early stage in the development, there are many uncertainties and assumptions related to the LVTrans model and especially the implemented compressor and bypass valve. Nevertheless, the further development of ACUR LE looks promising. As a result of this Master's thesis, ACUR LE can now be regarded to be at Technology Readiness Level 3.

Sammendrag

Vindkraft og solenergi utvikles stadig og tar over for tradisjonell kraftproduksjon. Dette fører til at en større andel av produksjonen kommer fra energikilder med ukontrollerbare variasjoner i produksjonen. For å balansere strømnettet og sørge for jevn totalproduksjon til alle tider må en viss andel av energien komme fra stabile energikilder som lett kan kontrolleres. Fleksibiliteten som vannkraft gir, både gjennom energilagringskapasiteten og den raske responstiden, gjør vannkraft godt egnet for å motvirke de ukontrollerbare variasjonene fra fornybare energikilder. Vannkraften er i tillegg godt utbredt og en veletablert kilde til elektrisitet. Likevel er det utfordringer knyttet til vannkraftens fremtid, og økt fleksibilitet i spesielt kraftverkene med tilknytning til elver er nødvendig. For disse vannkraftverkene vil effektkjøring, beskrevet som svært varierende vannstand som følge av hyppige endringer i produksjonen, føre til svært alvorlige miljøpåvirkninger i elvens økosystem. Et av hovedproblemene er når store vannstandsendringer skjer i løpet av kort tid, da dette kan føre til både stranding og drifting av spesielt ungfisk. For å tilpasse fremtidig vannkraft og samtidig ivareta miljøet i elver har ideen ACUR LE blitt utviklet. ACUR LE er et stort trykkregulert vannlagringsvolum koblet til utløpstunnelen av et vannkraftverk. Ved å bruke kompressorer og ventiler kan lufttrykket i kammeret reguleres, slik at forholdet mellom luft og vann endres. En økning i lufttrykket fører til at vann presses ut av kammeret, og på denne måten kan den totale volumstrømmen ut av kraftverket kontrolleres.

Gjennom denne masteroppgaven har ACUR LE blitt utviklet som et av vannkraftelementene tilgjengelig i simuleringsprogrammet LVTrans, et programtillegg til LabVIEW. Dynamikken i selve kammeret med varierende luftmengde er beskrevet med den polytropiske sammenhengen for trykk og volum, for antatte adiabatiske forhold. Begrensninger fra kompressor og ventil er tatt hensyn til ved å inkludere begrensningene komponentene er antatt å gi til volumstrømmen. Deretter er referansekraftverket Bratsberg modellert i LVTrans med og uten ACUR LE implementert, for så å bli brukt i simuleringer for oppstart, nedstenging og flomkontroll. Simuleringene i dette prosjektet viser hvordan ACUR LE klarer å dempe variasjonene som følge av endret produksjon på en vellykket måte. I et oppstartsscenario er kraftverkets responstid redusert til få sekunder, mens den totale volumstrømmen ut av kraftverket kontrolleres av ACUR LE til å bruke flere minutter på å øke rolig. I tillegg kan kraftverket stenge ned på en tredjedel av tiden sammenliknet med normal nedstenging, uten å påføre elven nedstrøms en uakseptabel rask nedgang i volumstrøm. Simuleringene er riktignok gjennomført på et tidlig stadium i utviklingen av ACUR LE, som betyr at det er mange antagelser og usikkerheter som påvirker resultatet. Likevel er framtidsutsiktene til ACUR LE lovende. Som et resultat av denne masteroppgaven har ACUR LE blitt videreutviklet og kan nå regnes for å være på Technology Readiness Level 3.

Contents

List of Figures

List of Tables

List of Symbols

Symbol	Name	Unit
A	Area	m^2
C	Constant	-
c_p	Specific heat	$J/(kgK)$
e	Error	-
Gr	Grashof number	-
H	Pressure head	mWC
h	Pressure	mWC
h	Heat transfer coefficient	$W/(m^2K)$
K	Coefficient	-
k	Empirical constant	-
L	Length	m
l	Rock layer thickness	m
M	Manning number	-
m	Mass	kg
$\dot{m}$	Mass flow	kg
n	Polytropic exponent	-
Nu	Nusselt number	-
p	Pressure	kPa
Pr	Prandtl number	-
Q	Volume flow	m^3/s
$\dot{Q}$	Rate of change in flow	m^3/s^2
Q_{HT}	Heat transfer	kJ
R_r	Heat transfer resistance	$K\,W^{-1}$
s	Slope	m^3/s^2
T	Temperature	K
t	Time	s
Δt	Time step	s
u	Control variable	-
V	Volume	m^3
Z	Vertical distance	m
z	Datum level	m

Greek letters

α	Head loss coefficient	$1/s^2$
λ	Thermal conductivity	$W/(mK)$
μ	Dynamic viscosity	Pa s
ρ	Density	kg/m^3
τ	Time	-

Constants

κ	Adiabatic constant	1.4
g	Gravitational acceleration	$9.81\,\mathrm{m/s^2}$
R	Ideal gas constant	$8.314\,\mathrm{J/(Kmol)}$
R_{air}	Specific gas constant for air	$287.058\,\mathrm{J/(kgK)}$

List of Abbreviations

ACC	Air cushion chamber
ACUR LE	Air Cushion Underground Reservoir (Low Energy)
HPP	Hydropower plant
HGL	Hydraulic grade line
MoC	Method of Characteristics
MRHT	Modified Rational Heat Transfer
PID	Proportional-integral-derivative
PV	Photovoltaic
RHT	Rational Heat Transfer
TRL	Technological Readiness Level

Chapter 1

Introduction

1.1 The need for energy

As the world's population is forecasted to reach 9.2 billion people in 2050 [1, p. 10], the demand for energy will continue to grow. In 2017, investments in renewable power accounted for two-thirds of power generation spending [2, p. 4]. If the rise in global average temperature is to be limited to 2 degrees Celsius above the pre-industrial levels, as in line with the Paris agreement [3], renewable energy must be scaled up [4, p. 173].

The capacity of renewable power generation increased by 178 GW in 2017, where solar PV photovoltaic (PV) accounted for nearly 55 % of the new installed capacity. Regarding the remaining capacity additions, wind energy accounted for 27 % while hydropower came close to 11 %. During the last decade, the non-hydropower renewable capacity has increased more than sixfold, due to cost-competitiveness of wind power and solar PV [4, pp. 40-41]. Although the increase is positive from an environmental perspective, the intermittent and fluctuating nature of solar PV and wind power production is a fundamental disadvantage that works against ensuring a stable energy supply. Unless harnessed when available, the energy from variable renewable sources is lost. To ensure stable power supply, a part of the total energy production must always come from stable and reliable sources of energy. Hydropower has the ability to store water and produce energy whenever the power is needed, and can therefore be regarded as a more flexible option for renewable power generation.

1.2 The possibilities with hydropower

Hydropower is the most reliable, flexible, efficient and proven source of electricity there is, according to the International Energy Agency [5]. With more than a hundred years of experience and development, hydropower provides around 16 % of the worlds global electricity production. In 2017, the total hydroelectric production was estimated to be 4,185 TWh, equal to 62 % of all renewable electric production worldwide, making hydropower the leading renewable source of energy [4, pp. 41, 83]. Traditionally, hydropower plants (HPPs) are designed with a specific operating conditions in mind, such as providing a stable baseload with constant power production. With the continuously increasing amount of intermittent renewable energy sources in the energy mix, HPPs are being asked to operate more flexibly to ensure a stable power balance [6, pp. 8-9]. This development in hydroelectric production is not only a technical challenge as hydropower needs to overcome several barriers related to politics, public acceptance and financial issues. Moreover, the environmental impact must be reduced to a minimum [7, pp. 5, 28]. This is significantly

important for hydroelectric sites with adjacent rivers, where the power production directly affects the river's environment. The negative consequences of highly varying flow must be eliminated if these HPPs are to to become more flexible. With these thoughts in mind, the idea of ACUR LE has been developed.

1.3 The ACUR LE

To avoid river fluctuations from highly varying hydroelectric production, a hydro power plant's production flow should be decoupled from its total discharge flow. This is the essence of the functionality that the ACUR LE, or Air Cushion Underground Reservoir (Low Energy), provides to a hydropower system. Besides working as a surge tank in connection with the tailrace tunnel, the excavated cavern provides a volume for water storage, as illustrated in Figure 1.1. As a result of this new technology, existing power plants can be modified and operated beyond today's precautionary environmental restrictions. Storli was the first to describe the concept and its abbreviated name in *A novel concept of increasing the flexibility at power plants with outlet to river* [8].

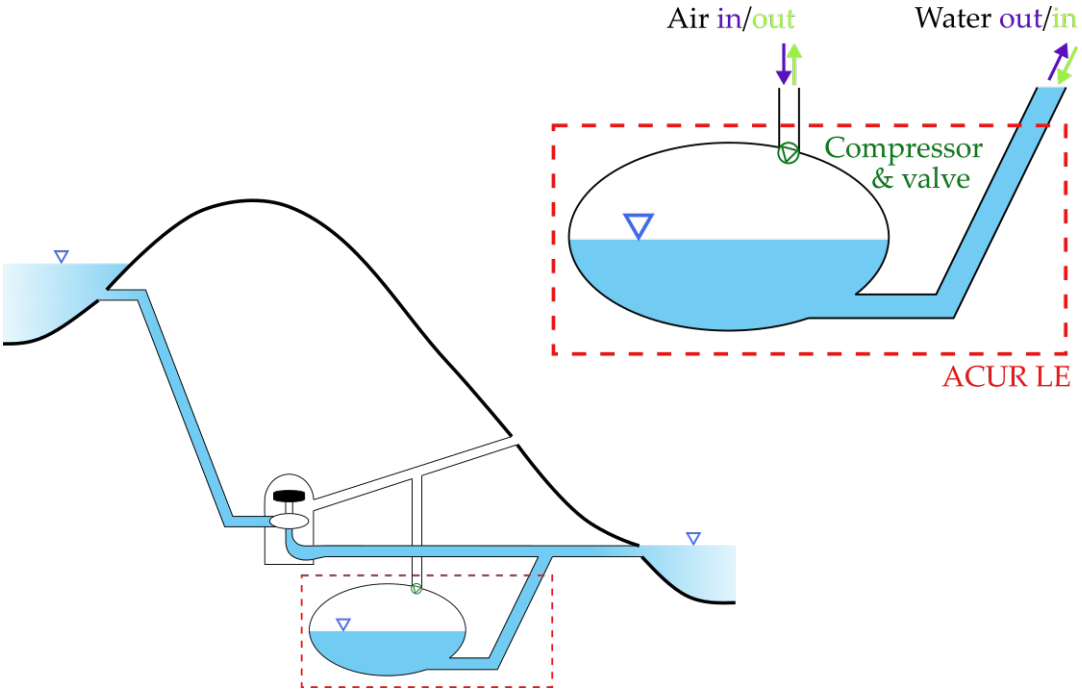

FIGURE 1.1: Principle of ACUR LE, not to scale. The illustration is redrawn from Storli [8].

An air compressor with a bypass valve is implemented in ACUR LE, as seen from Figure 1.1. By governing the amount of air in the tank, making it a pressure regulated chamber, the net flow of water in and out is controlled. In this way, the total discharge flow into the downstream river becomes a function dependent on the pressure in ACUR LE. As a result, the electricity production with its coherent flow could vary to a greater extent, since ACUR LE compensates for the changes in flow to maintain a steady total discharge.

The development of ACUR LE is a part of the HydroFlex project, aiming to increase the value of hydropower by increasing the flexibility. This project is funded by the European Union's Horizon 2020 Research and Innovation programme [9, 10].

1.4 Determining the objective

The essence of this Master's thesis is to gain more knowledge about ACUR LE, and to learn more about its related possibilities and limitations. Regarding the progression of development of this idea, the Technology Readiness Levels (TRLs) provided by The European Space Agency (ESA) is used to evaluate the current maturity [11]. Prior to this work, the technology concept and the intended applications have been formulated, which equals TRL 2. Therefore, the main objective of this thesis is to bring the concept idea to TRL 3 with simulation studies and proof-of-concept validation. To achieve this goal, the following milestones are considered:

1. Develop an accurate model of ACUR LE in the simulation tool LVTrans.
2. Simulate typical power operating procedures for the case HPP Bratsberg.
3. Evaluate the feasibility of ACUR LE and consider the outlook and possibilities for further development based on obtained knowledge.

1.5 Limiting the scope

The scope of this thesis is limited to the assessment of the technical feasibility of ACUR LE, and for this reason the economic aspect is excluded. A literature study on environmental conditions in consideration of hydropower operation will be carried out to provide motivation and background for the idea. The simulation model of ACUR LE must be developed to imitate the intended behavior based on realistic dynamic relations. To limit the scope, the complex compressor dynamics will be represented merely through the limitations on the expected operation. Further, the simulations will be based on a single case hydropower plant for different scenarios were ACUR LE is intended to make a difference.

Chapter 2

Background

2.1 Hydropower in the world today

There exist more than 45,000 dams over 15 meter and perhaps a million smaller dams globally [12, p. 323]. The transfer, redirection, and storage of water have been done for thousands of years, and today the majority of the world's accessible freshwater river systems is appropriated by humanity [13, p. 787]. Hydropower has many advantages, such as high efficiency, reliability, and flexibility, very low operating and maintenance costs, as well as a proven technology and a large storage capacity. In fact, storage hydropower is estimated to account for 96-99 % of the global storage energy capacity [4, p. 22] [14, p. ix].

Although hydropower is an old and already broadly developed source of energy, the technology is increasingly recognized as an important asset in times with further deployment of variable renewable resources such as wind power and solar PV [15, p. 4]. The stable energy supply that characterizes hydropower is a result of the ability to store energy. This quality is very useful as the surplus energy from other sources can be utilized to pump water up into reservoirs for storage and later electricity production. As of today, pumped-storage hydropower is the most cost-effective form of electric storage [5]. The remaining potential for development is still considerable, suggesting that the energy storage and production capacity will increase. The International Energy Agency foresees a doubling of global hydropower capacity by 2050, equal to nearly 2000 GW, providing a total hydroelectric production of over 7000 TWh per year [7, p. 5].

HPPs with head over 300 m are called high-head, and are of especial importance in covering peak energy supply [16, p. 643]. Regarding power production, high-head storage hydropower plants can produce electricity with shorter response time than most types of power plants [17, p. 1205]. This flexibility is crucial in the energy system to balance variable renewable electricity production, and generates the need for more hydropower development. Unfortunately, too much variable hydroelectric generation can cause detrimental impacts on adjacent river ecosystems.

2.2 Hydropeaking and natural flow variations

Hydropeaking is a form of hydroelectric production and reservoir operations where storage water is used during peaks in demand in the energy market [18, p. 5]. This results in highly variable discharges to downstream watercourses in as short as sub-daily periods. The alterations to natural flow patterns have been broadly stated and consist mainly of changes in magnitude, duration, sequence, and frequency in the river flow [19, p. 5]. For a river ecosystem, the ecological integrity is dependent on the natural dynamic characteristics [20]. A certain level of flow variability is

normal and healthy for a river. These variations are crucial for maintaining the hydraulic complexity, surface water-groundwater exchange, sediment transport, and floodplain connections. All of these variables interact and influence the nutrient and organic matter concentrations, the water temperature and biological habitats in the river bed and riparian areas [21, p. 868]. Flow variations happen on a sub-daily basis, given by naturally occurring events such as rainfall, evaporation, snowmelt or other climatic processes. These variations could typically be in the order of around 10 % of the mean daily flow [22, pp. 591-592]. Although hydropeaking may very well create flow variations within the annual range of natural flows, the result could also be greater fluctuations with unnatural flow patterns. Whereas an unregulated river has a limited number of days with a high degree of sub-daily flow fluctuations per year, hydropeaking sites have several days all year round, including the seasons with naturally small variations [23, p. 1254]. Therefore, many hydropeaking rivers can be considered to be two different rivers from an ecological perspective; One with low flow and the other with fluctuating high flow. Within the span of 24 hours or less the river biota must deal with both flow environments [24].

Hydropeaking can affect almost every living organism in a river ecosystem [25, pp. 44-45]. As sub-daily flow fluctuations become more frequent, less predictable and with larger magnitude than natural flow variations in unregulated rivers, the native biota of the river will be affected. Also, the number of species and the quantity and quality of habitats available for fish could be changed dramatically [23, p. 1257] [26, p. 317]. During shutdowns, the reduction in discharge often leads to land reclamation of submerged areas in the river, meaning that the water level decreases to expose parts of the river bed. If the river flow reduces too fast, the fish run the risk of ending up in dry areas, either in small ponds, water pockets between rocks, or in worst case on dry land. This phenomenon is known as stranding and is one of the main problems with hydropeaking [27, p. 69]. The juvenile fish are often most affected due to their limited swimming abilities, and especially since they tend to use the shallow parts of the river. In contrast, the elderly fish uses the deeper river parts where the risk of stranding is smaller [27, p. 10]. The impact of hydropeaking is dependent on the time the flow reduction occurs, where the biggest risk of stranding is assumed to be in the winter during the daytime. The reason is probably due to the cold conditions, as well as the substrate seeking behavior in the fish. Although the stranding of fish is a problem that causes higher mortality, experiments have shown that fish stranding is not tantamount to death. In the absence of predators, fish have been observed to survive for several hours in the substrate after dewatering [28]. In addition, changing the frequency and duration of periods with land reclamation and flooding affects the flora and vegetation in the river. River bottom erosion and sediment transport are affected by changes in the water velocity [29, p. 50].

2.2.1 Measures to mitigate the effects of hydropeaking

Hydropeaking is not really considered to be compatible with environmentally hydroelectric production, but measures can be made to reduce the negative effects. These measures are divided into the following three types [16, p. 643] [19, p. 12]:

- Morphological measures
- Constructive measures
- Operational measures

Morphological measures are in-stream renovations that improve the river characteristics with areas suitable for the biotic system, and protects the river from erosion. The work can, for example, include river widening, gravel and sediment placements, as well as an installation of weirs, deflectors and cover structures [19, p. 13].

Constructive measures consist of hydraulic structures that smooth the peaking variation either by retaining the water in ponds, separating the flow between several outlet structures, or reducing the flow energy and water velocity with artificial reefs in reservoirs. As these kinds of measures consist of constructing large structures, like open-air or underground compensation basins and bypass tunnels, they are in general expensive [19, p. 13]. However, in multipurpose projects, where the target is to cover the hydroelectric demand and still enhance downstream aquatic ecology, the most effective solution would often be to construct compensating basins [30, p. 179].

Operational measures involve adjustments of the power production, with limits for maximum and minimum flow discharge. Ensuring a stable level of minimum flow is claimed to be the most important of all measures [31, p. 9]. However, to lower the risk of fish and benthos stranding, the power production should be gradually reduced to ensure an acceptable dewatering rate. In the opposite case, the production should increase slowly to reduce the risk of unintended drift of benthos and fish spawn, quick changes in water temperature, as well as ice drift during winter [27, pp. 32, 101, 135]. At times when the ecosystem is especially vulnerable, hydropeaking should be avoided entirely. Although these kinds of measures are easy to implement, they present a potential inefficient utilization of water that causes an economic loss compared to the alternative power operation without the limitations. In addition, by attenuating the magnitude of maximum discharge, slowing down the ramping rates and increasing the minimum flow, the flexibility of hydroelectric production is reduced [19, p. 17].

Ensuring a flow reduction at a slow rate of change is especially important when the river bottom dries out, as the fish tend to wait and not move for as long as possible [28, p. 619]. A study from 2003 regarding stranding of wild juvenile brown trout concluded that the acceptable dewatering speed depends on the fish size, the local site characteristics, the light conditions and the time of the year [32, p. 601]. A series of lab experiments and field tests showed that the stranding risk decreased with a dewatering rate of less than 10-15 cm/h [28, 32]. Based on this, a rule of thumb was established to prevent fish stranding, suggesting that the dewatering limit should be no more than 10 cm/h [27, p. 72].

2.3 The possibilities with ACUR LE

The concept idea ACUR LE is a combination of an operational and constructive measure. This section introduces the reader to the general concept of ACUR LE and its applications, as previously established by Storli [8]. In general, the total hydraulic power P_h produced in hydropower plants is calculated as

$$P_h = \rho g Q H \eta \tag{2.1}$$

where ρ is the density of water, g is gravitational acceleration, Q is volume flow, H is pressure head and η is efficiency. The electric power is produced in the generator, driven by the turbine. This means that a larger flow of water will increase power production, as seen from Equation 2.1. The correlation between power and flow is almost proportional since the other variables remain approximately constant.

Thus, rapid changes in power production will at the same time abruptly change the volume flow in the adjacent river.

As already established, the modern hydroelectric production should be characterized by high capacity and short response time. To achieve this, many HPPs must be upgraded to increase the installed capacity. Figure 2.1a illustrates how a fictional HPP could utilize a given amount of water for two cases with different capacities. In both scenarios the total amount of energy produced will be the same, but the case with increased capacity, seen as the green dotted lined in Figure 2.1a, will respond quicker and produce the energy within the shortest amount of time. With the current capacity, the gradients for discharge flow follows an assumed acceptable rate of change, illustrated with the purple line in Figure 2.1b. If the capacity were to increase, the river discharge would change accordingly, causing the gradient seen with the red dotted line in the figure to the right. However, with ACUR LE implemented, the total discharge flow can be controlled to follow an acceptable rate of change, given as the green dotted line in Figure 2.1b, while the power production follows the increased capacity function from Figure 2.1a. By retrofitting ACUR LE into existing HPPs, traditional plants will be able to utilize the water faster and more efficient. The higher flexibility that comes with ACUR LE makes it possible to increase the total capacity of a HPP, without creating unacceptable conditions for the ecosystem in the adjacent river.

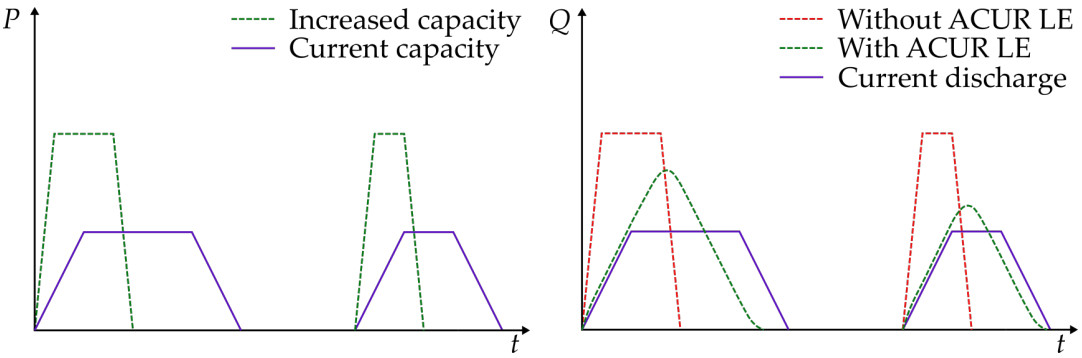

(a) Power P per time t.

(b) Discharge flow Q per time t.

FIGURE 2.1: Implementation of ACUR LE could enable acceptable flow gradients combined with increased ramp in power production. The illustration is redrawn from Storli [8].

The ability in ACUR LE to affect the discharge flow to river is made possible through the compressor and air valve, as previously seen in Figure 1.1. During the power production increase scenario, the compressor is bypassed by the valve. The pressure difference between the chamber condition and atmosphere outside of the HPP makes air flow through the valve. As the pressure in ACUR LE decreases, water from the discharge tunnel starts filling the chamber. By exploiting the sink imitating functionality of ACUR LE, the total discharge to the river is reduced. The discharge flow $Q_{Discharge}$ is no longer equal to the production flow $Q_{Production}$, but instead described as:

$$Q_{Discharge} = Q_{Production} - Q_{ACUR} \tag{2.2}$$

given that the positive direction of ACUR LE flow Q_{ACUR} is into the chamber. In the opposite case where the power production is reduced, the compressor is put to use. As the production flow is reduced, ACUR LE appears as a source of water in the pipe system. The compressor forces more air into the surge tank to increase

the pressure. As a result, water is pushed into the tailrace tunnel. By constantly governing the pressure in ACUR LE, the rate of change in the discharge flow is kept at an acceptable level. This happens as the power reduction follows a pattern that in normal HPPs would massively affect the adjacent river in unfortunate ways.

2.3.1 An economical utilization of water

From the economic perspective on hydroelectric production, water represents income. Saving water whenever electricity is cheap and producing as much as possible during high energy demand would be the most economical way to utilize storage hydropower. In cases where the river regulations prevent large rates of change in discharge, the implementation of ACUR LE would in theory enable faster changes in production flow.

Under normal circumstances, complete shutdowns for HPPs with adjacent rivers downstream are restricted to a maximum power ramping speed. This causes the volume flow decrease given by the green top line in Figure 2.2. The amount of water used during dewatering is calculated as the integral of this function. During an emergency shutdown, the flow will decrease to zero as fast as the mechanical components in the HPP are capable of. This flow reduction is given as the steep purple line, to the left in the figure, and represents a better dewatering scenario considering the economic aspect, as less water is utilized.

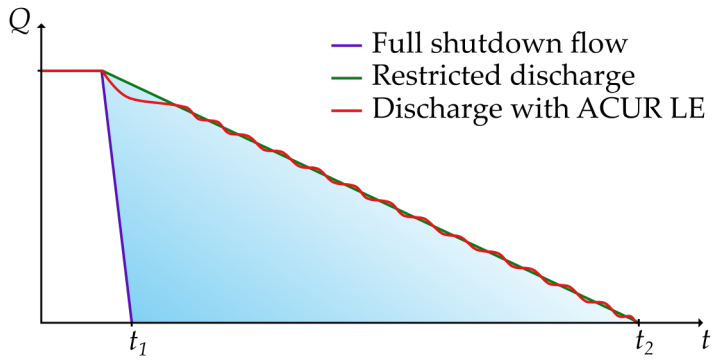

FIGURE 2.2: An illustrated example of dewatering rates in flow Q for different scenarios.

If ACUR LE were to be implemented in the power plant and work as intended, the power production could be turned off as if the adjacent river and the associated regulations and ramping restrictions did not exist. As the production flow quickly reduces to zero, equivalent to the purple line in Figure 2.2, the flow out of ACUR LE increases, making the river experience a decrease in flow equal to the red line in the figure. Comparing the cases with and without ACUR LE, the amount of water saved is calculated as the area between the green line and the purple bottom line. This water could be utilized in electricity production later when the power demand is higher.

The same principle of water utilization applies to the startup scenario. Ideally, the HPP will immediately produce electricity at design flow conditions, without having to consider the adjacent river. ACUR LE uses the water storage volume to ensure a small rate of change in discharge, while the production flow increases as fast as the mechanical equipment allows.

2.3.2 Flood controlling abilities of ACUR LE

Besides enabling higher rates of change in power production, ACUR LE could have even more advantages in HPPs regarding flood mitigation. During extreme flood situations, the storage volume ACUR LE makes up can be used to avoid the worst flood peak. In this way, one of the most destructive parts of the flood could be removed, and hopefully, the damages from the flood will be lowered. This scenario is illustrated in Figure 2.3a. Additionally, ACUR LE can be operated to manipulate regulated river flows in ways traditional hydropower plants cannot. A potential problem with highly regulated rivers is the lack of spring flood. This high and variable flow creates a great opportunity for the migration of salmon fry to the ocean, and the survival of salmon fry is assumed to be at the highest as the spring flow occurs. ACUR LE could mimic such a flow pattern at favorable occasions, creating an artificial flood as illustrated in Figure 2.3b. This operational use of ACUR LE is of especial interest for countries where both fish conditions and flood events are considered, such as in Norway.

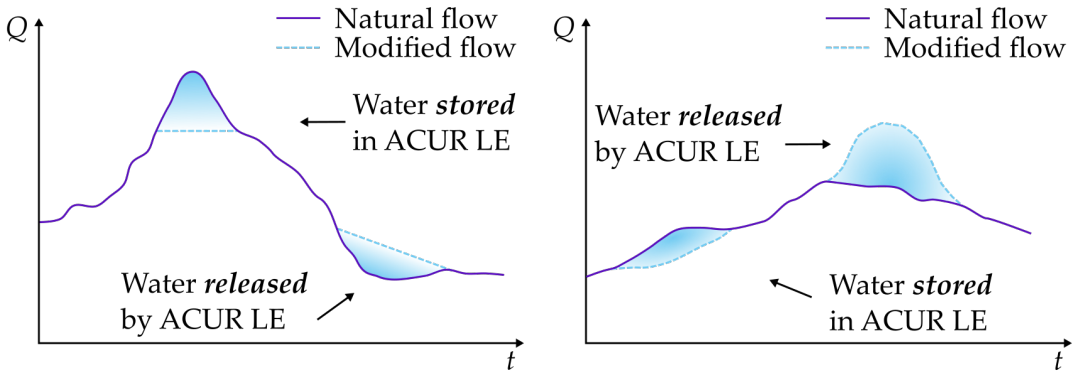

(a) Flood mitigation (b) Flood imitation

FIGURE 2.3: ACUR LE manipulates the natural river flow in two different flood scenarios. The illustration is redrawn from Storli [8].

2.4 Hydropower in Norway

In Norway, hydropower accounts for approximately 95 % all the energy production. At the beginning of 2018, the annual hydroelectric production was estimated to be 133.9 TWh from the around 1600 Norwegian HPPs [33]. The traditional regulation scheme for hydropower in Norway is to store water in the summer, to be used in energy production during the winter. A positive side effect of HPPs is some flood absence and reduced flood discharge due to the dams and regulated rivers [19, p. 27]. In the 1960s, the Norwegian hydropower development increased along with concerns regarding the environmental impact of river regulation. As the awareness of environmental issues has come to fore, the power plant licenses that stipulates rules of power operation now include conditions to reduce the environmental impact. To ensure that water discharge occurs at a slow rate of change, the license could typically contain an explanatory sentence about hydropeaking, e.g.: "The hydropower plant shall be operated according to river discharge. All changes in production shall be smooth, and hydropeaking is not allowed" [34, pp. 373-374].

In 1991, Norwegian hydroelectric production altered from supply driven to demand driven due to a new energy law [35, p. 37]. The liberalization of the energy

market gives hydropower suppliers strong incentives to behave competitively [36, p. 678]. By constantly evaluating the economic profitability of producing electricity versus storing water for later use, a hydropeaking like operation is promoted. The effects of this incentive appears in a Norwegian study from 2018. By comparing 256 small HPPs of less than 10 MW installed, the study found that hydropeaking licenses given were rarely followed [34].

The favorable conditions for hydropower in Norway have led to an impressive capacity for energy saving through approximately 370 hydroelectric storage systems. These systems often consist of several reservoirs interconnected by underground tunnels [37, p. 12]. Today, Norwegian reservoirs are assumed to hold almost 50 % of Europe's capacity for energy storage [38, 39]. This puts Norwegian hydropower forward as a potential "green battery" to accommodate sources of intermittent power all over Europe. To fulfill this idea, the total flexibility and capacity must be increased beyond the state of today. In theory, the Norwegian hydroelectric storage system can be converted to a pumped storage system at a relatively low cost, thus providing the opportunity of more energy storage [37, p. 12]. Regarding the total power production, the installed power capacity in all Norwegian HPPs amounts to approximately 32 GW [33]. This is an impressive quantity considering Norway's modest area, as 32 GW equals around 2.7 % of the global hydropower production capacity [4, p. 83]. Still, the potential for further technological development and expansion is significant. A study from 2011 states that a turbine capacity increase of 20 GW in Norwegian HPPs would be technically possible without using new regulation reservoirs or breaking the current demands for highest and lowest regulated water level [40, p. 81]. This would increase the installed capacity by over 60 %.

As the share of unregulated power production is expected to be higher in the future, the amount of hydropeaking is also expected to increase. For this reason, extensive research on hydropower is carried out in Norway [41, p. 54]. The Centre for Environmental Design of Renewable Energy (CEDREN) have projects related to pumped-storage and future hydropower design, in addition to consequences of frequent discharge flow changes in adjacent watercourses [42]. In the HydroFlex project, the main focus is the flexibility restricting bottlenecks of hydroelectric production, while the environmental impact of increased flexibility is addressed. Both turbine and generator design, as well as measures regarding the river environment, are considered to accommodate a hydropeaking scenario of 30 starts and stops per day [9].

These projects are of particular relevance for hydropower in Norway, due to the number of HPPs with an upper reservoir and adjacent river downstream. By using the data from Hamnaberg [43, pp. 239-254] in combination with the hydropower database from The Norwegian Water Resources and Energy Directorate [44], the turbine capacity of these HPPs are calculated to be approximately 5.4 GW, equal to more than 15 % of the total power capacity in Norway. To utilize these hydroelectric sites, the environmental impact on the watercourses must be reduced. An example of such a watercourse is described in further detail in the following subsection.

2.4.1 Nea-Nidelvvassdraget

Nea-Nidelvvassdraget is a watercourse in the middle part of Norway that runs from the mountain areas around Nesjøen in Sweden to Trondheimsfjorden in Trondheim [45]. The main river comes from the artificial dam Sylsjøen, finished in 1952. Between Sylsjøen and Selbusjøen, seven power stations were built until 1989 [46]. As

the additional seven power stations are located from Selbusjøen to Trondheimsfjorden, where the river is called Nidelva, the watercourse is considered to be highly regulated. The steady water flow during both summer and winter makes Nidelva one of the best locations for sports fishing in Norway [45]. Presumably, a part of the reason for the large fish population and favorable conditions is the river regulation. The river reservoirs created for the HPPs Øvre Leirfossene and Fjæremsfoss has led to the development of a fauna with species not found in typical Norwegian rivers. Further up, Svean power plant has through its transmission tunnel from lake Selbusjøen brought crustaceans and zooplankton into the river. Combined, these contributions provide an important food source for the fish and stimulate the conditions for population growth [47, p. 25]. Another benefit from river regulation is higher water temperature in the river during the winter compared to unregulated rivers. This makes the river normally free of ice, enabling more daylight to brightening the river bed and causing a long growing season for the water vegetation. However, too stable and low water flow in regulated rivers could cause problems, such as river bed sedimentation and few available spawning areas.

Nea-Nidelvvassdraget is assumed to be highly vulnerable for increasing regulation and potentially large changes in volume flow [47, p. 30]. In 1994, a report presented the effects of regulation from Bratsberg power plant in Nidelva. Rapid changes in power production was found to cause the most damage, especially as both turbines stopped and the water flow was reduced from 150 to 30 m^3/s. A gradual decrease in flow was suggested in the cases where one of the aggregates were shut down [48, p. 53].

Chapter 3

Theory

3.1 Hydropower plants in general

A hydropower plant converts the potential energy in water from reservoirs and rivers into electricity with the use of turbines and generators. The typical arrangement consists of a headrace tunnel and pressure shaft that transports the water from the reservoir to the turbine. To reduce the pressure increase in times of severe flow changes, surge tanks are installed in the headrace tunnel, as illustrated in Figure 3.1a. The alternative arrangement, seen in Figure 3.1b, uses an inclined pressure tunnel in combination with a closed surge tank, known as an air cushion chamber (ACC). After the water has run through the turbine, it is transported to the downstream reservoir or river through the tailrace tunnel. Depending on the length of this tunnel, implementation of surge tanks could be of interest [49, pp. 3-5].

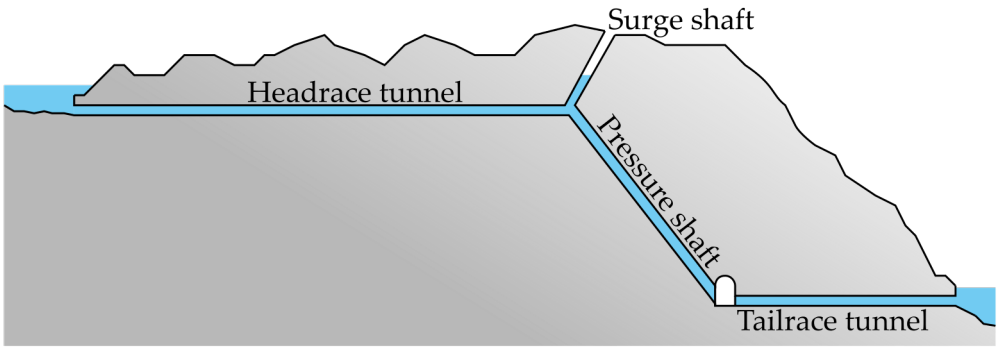

(a) HPP with surge shaft.

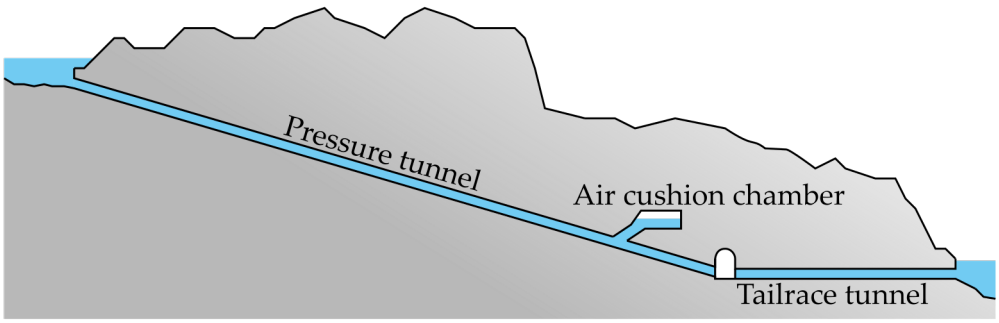

(b) HPP with air cushion chamber.

FIGURE 3.1: Illustration of two different HPP tunnel solutions.

3.2 Surge tanks

The need for surge tanks is especially recognized during startups and shutdowns for large power plants with long transmission tunnels. During operation, a sudden stop in power production forces large amounts of water to slow down, causing a phenomenon known as retardation pressure. As a result, this massive pressure built up could damage machines and equipment. To prevent this from happening, excavated areas with free water surface, called surge tanks, are established close to the turbine. This limits the amount of water that causes the pressure built up in front of the turbine [50, p. 35]. A HPP could have several surge elements, often both in the headrace and tailrace tunnel. The two most common types of surge tanks, with the hydraulic grade line HGL showing the pressure head, are illustrated in Figure 3.2.

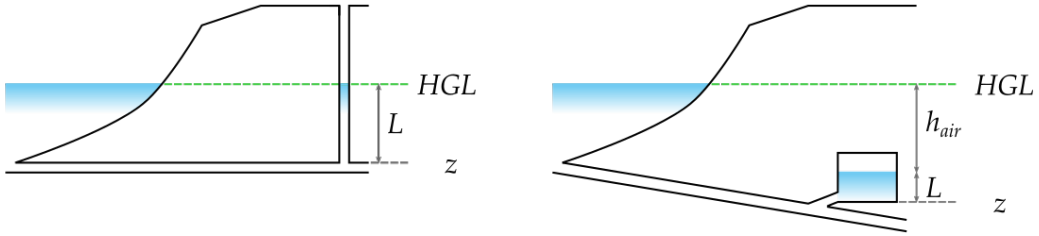

(a) Surge shaft with water length L.

(b) ACC with air pressure h_{air}.

FIGURE 3.2: Two surge tank arrangements with hydraulic grade line HGL at constant distance above the datum height z, as friction loss in tunnels are neglected.

3.2.1 Open surge tanks

The traditional surge arrangement consists of a tank, open to the atmosphere at the top and connected to the main pipeline. This type of surge element is often called a surge shaft, due to the shaft shape that extends to far above the HGL, as illustrated in Figure 3.2a. During a shutdown, the surge shaft becomes the path of least resistance for the masses of water in the headrace tunnel. Hence, the water level in the tank increases quickly, until the gravitational force of the water's own weight have fully counteracted and dampened the momentum. However, due to the inertia of the water, there is a delay in the system that causes the water level L to surpass the HGL. This delay makes the water level oscillate around the HGL while the direction of flow in the headrace tunnel changes accordingly. Likewise, a surge shaft in the tailrace tunnel will compensate for the quick change in volume flow in the same way, but the water level decreases initially during a shutdown scenario, as illustrated in Figure 3.3. During a startup scenario, equivalent but opposite oscillations will occur due to the surge elements. These so-called u-tube oscillations between the reservoir and the surge tank are eventually dampened due to friction losses in the tunnel.

Surge tanks also provide another benefit to hydropower systems regarding response time. During a quick increase in production, e.g. a startup scenario, the water from the surge tank in the headrace tunnel is utilized to accelerate the volume flow. Open surge tanks are initially dimensioned to prevent overtopping and draining during such scenarios with dramatic volume flow changes [50].

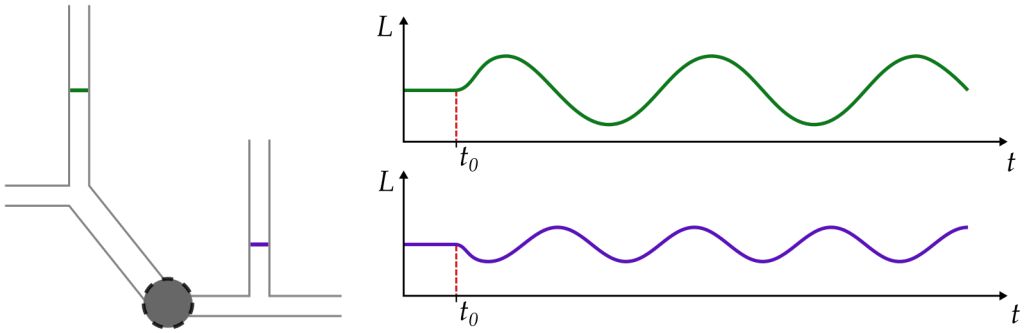

FIGURE 3.3: Illustration of a HPP with surge shafts of different dimensions in headrace and tailrace tunnel. The oscillations occur during complete shutdown.

3.2.2 Closed surge tanks

The alternative to open surge tanks is closed surge tanks, also known as air cushion chambers. These surge elements consist of a closed container partially filled with pressurized air or gas, as seen in Figure 3.2b. Like surge shafts, also ACCs can increase response time and prevent excessive pressure in adjacent tunnels, but at the cost of introducing oscillations during changes in production and flow. During a shutdown, water in the headrace tunnel increases the chamber's water level L and air pressure h_{air}, causing a greater downward force as $(h_{air} + L) > HGL$. During all operation, the absolute pressure H_{ACC} in the tunnel directly below the air cushion chamber must equal the effective pressure head at that place in the tunnel system, given by the total hydraulic grade line HGL. With the variables from Figure 3.2b, where HGL for simplicity is assumed constant, this can numerically be described as:

$$H_{ACC} = h_{air} + (z + L) = HGL \tag{3.1}$$

with

$$h_{air} = \frac{p_{air}}{\rho_w g} \tag{3.2}$$

Here, absolute pressure H_{ACC} is the sum of the chamber air pressure h_{air} and the pressure due to elevation, given as the datum height z and the water string length L. With the use of Equation 3.2, the air pressure p_{air} is divided by the density of water ρ_w and the gravitational acceleration g to obtain the pressure in meter water column. In real life, HGL decreases along the tunnel system due to the head loss caused by friction in the tunnels, but the magnitude is approximately equal to the reservoir water level in the tailrace tunnel. More importantly, HGL drops drastically over the turbine, where the head is utilized to produce electricity. In the tailrace tunnel, HGL equals the river level at the outlet but increases closer to the turbine due to the friction loss in the tunnel.

Unfortunately, there are some drawbacks for closed surge tanks. Compared to surge shafts, air cushion chambers demand more maintenance and supervision. In addition, air leakage could occur with poor rock quality [51, pp. 10-11] [52, p. 16]. However, the advantage of closed surge tanks is the flexibility that follows, considering the development of the power station and the tunnel system. With a sufficient rock quality, the headrace tunnel and the surge shaft can be replaced by a shorter

pressure tunnel, which will be cheaper [49, p. 7]. At places with unfavorable topography, the ground level above the tunnel system might be too low for surge shafts, as seen in Figure 3.1b. For these cases, the air cushion chamber is an excellent choice.

3.2.3 Deriving the stability and surge limits in surge tanks

The following theory is provided from Guttormsen [49, pp. 165-169] and is related to the oscillations caused by surge elements in hydropower systems. These oscillations are critically damped and on the limit of stability if the surge shaft area equals the Thoma area A_{Thoma}:

$$A_{Th} = \frac{L_t A_t}{2\alpha g H_e} = 0.0087 \frac{M^2 A_t^{5/3}}{H_e} \tag{3.3}$$

L_t and A_t are the length and cross-sectional area of the headrace tunnel, respectively. The effective head is given as H_e, while M is the Manning number. The expression to the right is obtain with the following expression for the loss coefficient α:

$$\alpha = \frac{L_t}{M^2 R^{4/3}} \tag{3.4}$$

where $R = 0.265\sqrt{A_t}$. The stability criterion says that the cross-sectional area in the surge tank must be larger than the Thoma area. A recommended ratio is:

$$A_s = 1.5 A_{Th} \tag{3.5}$$

where A_s is the water surface area in the open surge tank. The maximum amplitude of the oscillation that occur during fast changes in volume flow is called the surge limit and can be estimated with the following equation:

$$\Delta Z = \pm \Delta Q \sqrt{\frac{\sum (L_i / A_i)}{g A_s}} \tag{3.6}$$

Here, ΔZ is the difference in water level in the surge shaft, while ΔQ is the change in HPP production flow. The equation includes the sum of quotients of the length L_i divided by the area A_i for all tunnel sections between the free water surface in the surge tank and the closest reservoir. Regarding air cushion chambers, Equation 3.5 and 3.6 cannot be used directly with the ACC area. However, the equations can be used by estimating the ACC's equivalent surge shaft area. From Nielsen, the following equation is provided [50, p. 95]:

$$A_{eq} = \frac{1}{\frac{1}{A_{ACC}} + \frac{\kappa h_0}{V_0}} \tag{3.7}$$

while an alternative equation is given from Guttormsen [49, p. 167]:

$$A_{eq} = \frac{V_0}{\kappa h_0} \tag{3.8}$$

Here, A_{ACC} is the area, h_0 is the absolute air pressure, and V_0 is the air volume in the chamber.

3.3 The Method of Characteristics

In this thesis, the Method of Characteristics (MoC) is used to analyze unsteady flows in conduits. The equations of motion and continuity make up a pair of quasi-linear hyperbolic partial differential equations. The velocity and hydraulic grade line elevation are the dependent variables, while the two independent variables are the distance along the pipe and time. By using the MoC, these equations are transformed into four ordinary differential equations. Then a finite difference representation of the variables is found as the equations are integrated. The full derivation of the method is found in Appendix A.

There are several advantages with the MoC. The procedure is relatively simple with few approximations, and the calculations provide a physical interpretation that is simple, yet precise. In addition, the method provides a firmly established stability criterion, as well as an explicit solution, meaning that different elements that are physically removed from one another in the real system are handled independently. The primary disadvantage is the relationship of the time step-distance interval, due to the strict adherence that is required [53, pp. 37-38, 14].

3.4 Thermodynamic relations in air cushion chambers

In this section, three different methods of calculating the dynamic behavior inside an air cushion chamber are presented. To fully describe all the dynamics in ACCs during operation in an analytic way is very difficult. The common solution has been to use the polytropic relation to describe the changes between pressure and volume:

$$pV^n = C \tag{3.9}$$

Here, p and V are pressure and volume of air, respectively, n is the polytropic exponent and C is a constant. An experimental study on hydraulic transients of entrapped air pockets in water pipelines showed that the adiabatic assumptions with $n = \kappa$ where $\kappa = 1.4$ gave the closest results to the experimental values [54]. In Vereide's Ph.D. thesis on the hydraulics and thermodynamics of closed surge tanks, the same conclusion was found to apply for fast transients [55, p. 5]. At the same time, the polytropic relationship was found to be unsuccessful in modeling slow transient, as heat transfer will have a more significant effect on the thermodynamics of the system in these events.

The following theory is relevant, but not used directly in the development of ACUR LE. Therefore, the theory from here to Section 3.5 can be skipped without losing continuity. To describe the dynamics and behavior in a closed surge tank more accurately, an alternative model called the Rational Heat Transfer (RHT) method was proposed by Graze in 1968 [56]. Graze started with the equation for ideal gas:

$$pV = mRT \tag{3.10}$$

where the variables p, V, m and T correspond to pressure, volume, mass, and temperature of air, respectively, while R is the ideal gas constant. This equation is differentiated and combined with the concept of reversibility to derive the following expression for pressure change as a function of heat transfer and volume change:

$$dp = \frac{1}{V}[\kappa p dV + (\kappa - 1) dQ_{HT}] \tag{3.11}$$

Here, dp is the pressure change, $\kappa = 1.4$ is the adiabatic constant, dV is the volume change and dQ_{HT} is the change in heat transfer. This method has later been expanded by Vereide to separate between heat transfer to water (subscripted w) and rock (subscripted r), for an even more accurate result [57]. The method is called The Modified Rational Heat Transfer (MRHT) method and uses the following relations:

$$dQ_{HT} = dQ_{HT,w} + dQ_{HT,r} \tag{3.12}$$

$$dQ_{HT,w} = -h_{HT,w} A_w (T_a - T_w) dt \tag{3.13}$$

$$dQ_{HT,r} = -h_{HT,r} A_r (T_a - T_r) dt \tag{3.14}$$

where h_{HT} is heat transfer coefficient, L is the characteristic length, A is boundary surface area and T is temperature. Further, the heat transfer coefficients are calculated in the following way from Incropera and DeWitt [58]:

$$h_{HT,w} = \frac{Nu_w \lambda_a}{L_w} \tag{3.15}$$

$$h_{HT,r} = \frac{1}{\frac{1}{h_{HT,a}} + R_r} \tag{3.16}$$

$$h_{HT,a} = \frac{Nu_r \lambda_a}{L_r} \tag{3.17}$$

$$R_r = \frac{l}{\lambda_r} \tag{3.18}$$

Here, Nu is the Nusselt number, λ is thermal conductivity, R_r is heat transfer resistance and l is rock layer thickness. The final MRHT model combines Equation 3.11 with the following expression for heat transfer in closed surge tanks:

$$dQ_{HT} = \frac{Nu_w \lambda_a}{L_w} A_w (T_a - T_w) dt + \frac{1}{\frac{L_r}{Nu_r \lambda_a} + R_r} A_r (T_a - T_r) dt \tag{3.19}$$

The only unknown is the Nusselt number, which could be determined from lab experiments or field measurements. With the empirical relationship for turbulent air flow ($Gr > 10^8$), suggested by Incropera and DeWitt, Nu can be described as:

$$Nu = k \sqrt[3]{PrGr} \tag{3.20}$$

where k is an empirical constant, $Pr = c_p \mu / \lambda$ is the Prandtl number, c_p is specific heat, μ is dynamic viscosity and Gr is the Grashof number.

3.5 Compressors

Compressors come in all shapes and sizes. In this thesis, only dynamic compressors are evaluated, as they are assumed to be of most relevance for ACUR LE. The following theory about dynamic compressors is derived from McMillan [59], unless otherwise stated. In a dynamic compressor, the gas is accelerated before the increased kinetic energy is converted into gas pressure. This is done by a combination of impellers on motor-driven shafts and diffusers, meaning stationary passages

where the cross-sectional area increases. There are two main types of dynamic compressors, known as axial and centrifugal. The primary difference is the direction of the flow through the compressors. In addition, the characteristic curves of axial and centrifugal compressors are quite different, as seen in Figure 3.4.

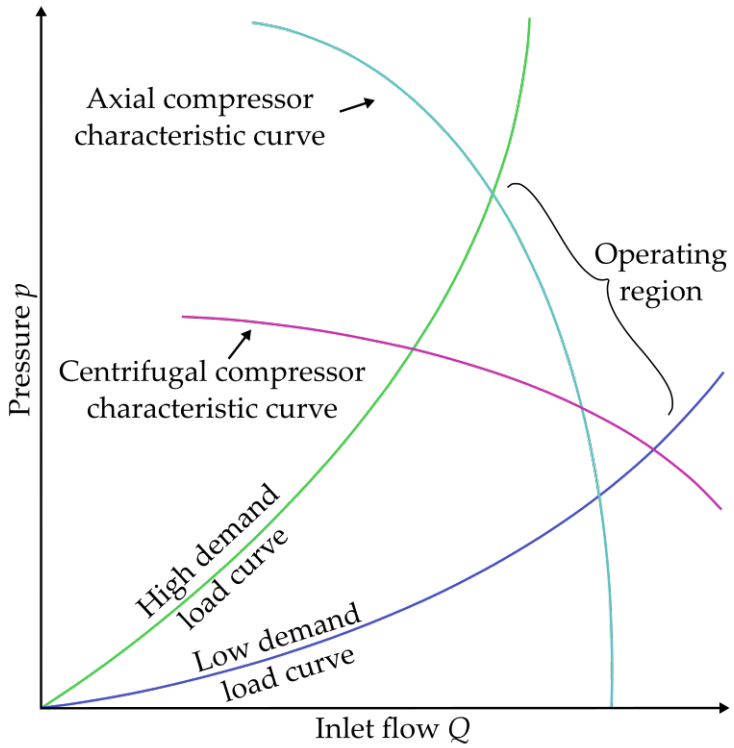

FIGURE 3.4: Illustration of typical characteristic curves of compressors. Compared to the axial compressor, the centrifugal compressor curve is flat. Redrawn from McMillan [59].

In axial compressors, the gas flows axially along the shaft. There are several sets of impellers and stationary vanes in axial compressors, where each set equals one stage in the compression process. The characteristic curve, shown in Figure 3.4, is relatively steep and more vertical than horizontal. This makes the axial compressors suited for variable pressure control with constant flow. However, there are several variables that affect the position of the characteristic curve. The vane position, speed, and suction operating conditions can be adjusted to manipulate the position of the curve. In general, the axial compressor is more efficient than the centrifugal compressor.

Dynamic compressors with radial flow direction are called centrifugal compressors. As seen in Figure 3.4, the characteristic curve is relatively flat. For perfect centrifugal compressors without any internal losses, the characteristic curve would be entirely flat as the discharge pressure would remain constant for all flows. This makes centrifugal compressors particularly suited for variable throughput control for large volumes of constant pressure. As for the axial compressor, the position of the characteristic curve for the centrifugal compressor depends on the suction operating conditions and speed. In general, centrifugal compressors are suited for cases that demand higher discharge pressure, but lower flow than axial compressors, as seen in Figure 3.5.

For both the axial and the centrifugal cases, compressor control is a challenging problem. The dynamic aspects such as lags and delays that usually occurs make

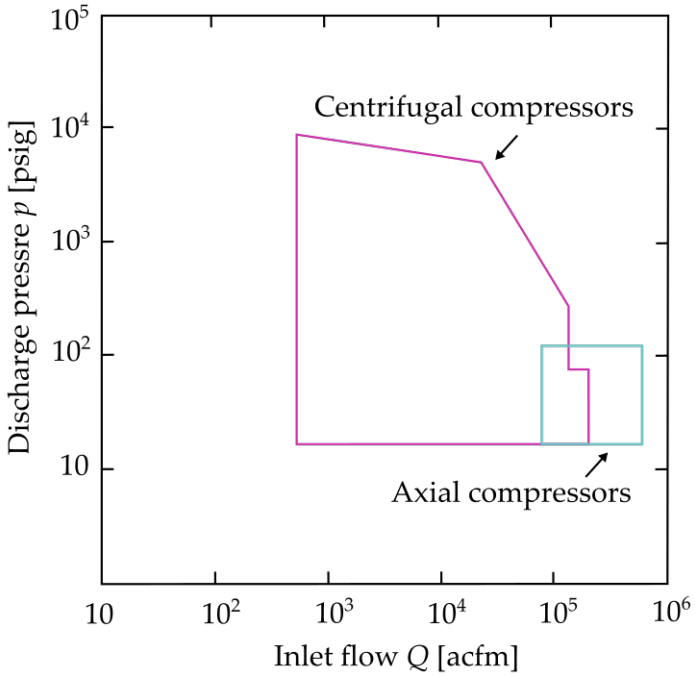

FIGURE 3.5: Typical operating ranges for compressors, where 100 psig = 70.3 mWC and 100,000 acfm = 47.2 m^3/s . Redrawn from McMillan [59].

compressors difficult and sometimes impossible to control with a simple PID approach [60, p. 380]. There exist several throughput control methods for dynamic compressors, as for example discharge throttling, suction throttling, guide vane positioning and speed control. The greatest turndown capability, meaning the width of the operating range, is achieved by guide vane positioning. As the guide vanes are adjusted further to closed position, the suction flow or the discharge pressure is decreased. With speed control, the suction flow or discharge pressure is reduced by decreasing the motor power frequency of the turbine inlet flow. Since the power needed to run the compressor is proportional to the speed squared, the power requirement reduces dramatically along with the speed. This makes speed control the most efficient control method [59].

Chapter 4

Developing the ACUR LE simulation model

This chapter describes the method used to show the potential of ACUR LE. To develop the simulation model of the concept idea, ACUR LE is decomposed to consist of three parts; the ACC with its pressure-regulated environment, the compressor with the bypass valve, and the regulator that governs the net air flow. Through these three steps, the ACUR LE model is developed as a new functional element in LVTrans, based on the given theory and assumptions. To investigate the affects of ACUR LE, scenarios for different operating procedures with the case HPP Bratsberg are developed. This particular HPP is located in Nea-Nidelvvassdraget, as seen in Figure 4.1, a watercourse where a real-life ACUR LE presumably would be of interest.

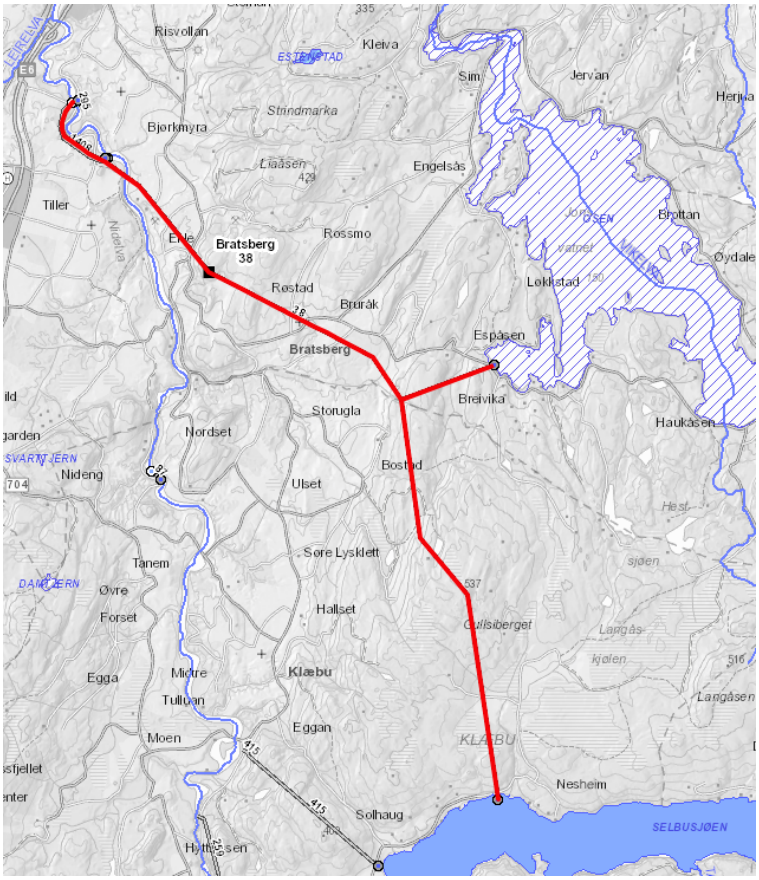

FIGURE 4.1: Bratsberg power plant in Nea-Nidelvvassdraget. Screen-shot from map provided by NVE [61].

4.1 The case power plant Bratsberg

In order to fully investigate the performance and evaluate the feasibility of ACUR LE, using a case power plant is necessary. With a reference HPP and real-life data for comparison, the simulations can be done for different production patterns with and without ACUR LE implemented. For this thesis, the power plant used as a case in the simulations is the HPP Bratsberg. This HPP is owned by Statkraft, and the following information is provided by them [62]. Bratsberg power plant is parallel to six other HPPs in Nidelva, as a part of the watercourse previously described in Section 2.4.1. The water runs from Selbusjøen through a 16 km long transmission tunnel with an average cross-sectional area of 60 m^2, discharging into Nidelva right after Leirfossene HPP, as seen from Figure 4.1. This gives a total head of 147 m, that combined with the installed capacity of 124 MW divided by two Francis turbines makes the power plant produces around 650 GWh annually. Besides transporting water from Selbusjøen further down into Nidelva, the tunnel system provides the opportunity to transport water to Jonsvatnet, as seen in Figure 4.1. In the intersection between this transportation pipe and the headrace tunnel, there exists a surge shaft. Further down, just before the penstock, an air cushion chamber is implemented. Although the headrace tunnel has two surge elements, the tailrace tunnel has none.

The operating restrictions for power production at Bratsberg is found in Table 4.1. At most times, Bratsberg uses under 13 minutes on a complete startup or shutdown. During the season for salmon fishing, the rates of change are more strict, with a startup ramp at about 1/10 of the fast startup, and shutdown ramp even lower. The operating restrictions for slow startup and shutdown are not used in the simulations.

TABLE 4.1: Operating restrictions at Bratsberg HPP.

Type of operation	Duration [min]	Difference in load [MW]
Fast startup	6	62
Fast shutdown	6	62
Slow startup	60	65
Slow shutdown	60	43

4.2 The simulation tool LVTrans

All simulations are done using the simulation tool LVTrans, a program extension to LabVIEW [63]. The program, developed by Bjørnar Svingen, utilizes the MoC to solve the differential equations for all elements in the system. With the use of this method, an approximately accurate solution can be calculated fast. The development in pressure, volume flow, and other variables can be monitored during simulation, as well as logged for later use. By using LabVIEW's interface, large hydropower plants can easily be set up to a high degree of accuracy, as all devices usually found in a HPP are included in LVTrans. Since the program has an open source code, all elements can be edited after the users own needs. The data sets with logged values from the simulations in LVTrans can easily be imported into Excel and later used by MATLAB to create figures.

The Bratsberg model setup in LVTrans, seen in Figure 4.2, is based on technical drawings and other information provided by Statkraft. To reduce the number of pipe elements, average areas are used to simplify the model. Also, the surge tanks in the headrace tunnel are modeled with average areas, instead of all the complex

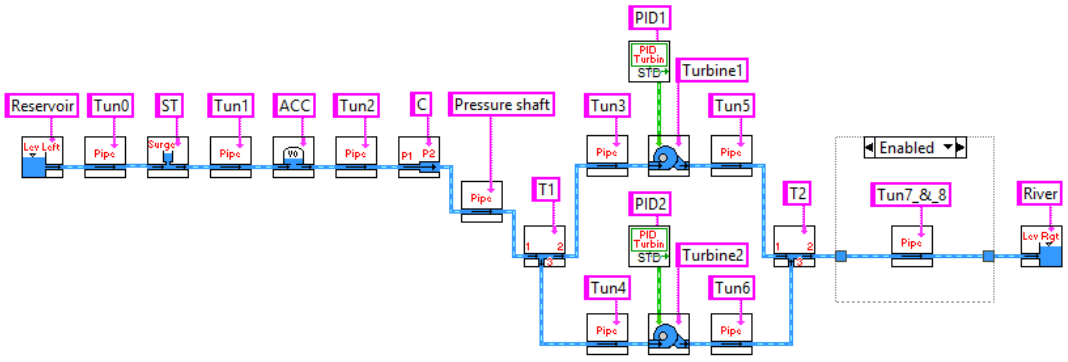

(a) The complete model setup of Bratsberg power plant with ordinary pipe tailrace tunnel.

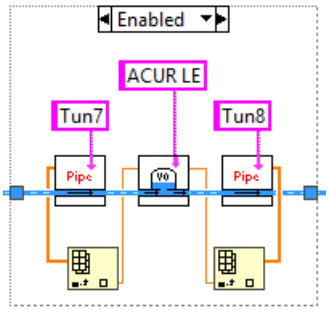

(b) Tailrace tunnel with ACUR LE element.

FIGURE 4.2: Screen-shot of model setup of Bratsberg power plant in LVTrans with two alternative tailrace tunnels.

dimensions from the technical drawings. Initially, Bratsberg is modeled both without ACUR LE, as seen in Figure 4.2a, since the real-life HPP does not have a surge element in the tailrace tunnel. However, the model setup can also include the ACUR LE element, with the alternative tailrace tunnel given in Figure 4.2b.

The ACUR LE element, seen in Figure 4.2b, combines the pressure-regulated ACC, the compressor and valve, as well as the regulator into one element. A screen-shot of the final ACUR LE element controller, used during the simulations, can be found in Appendix B, while the associated code describing the element is found in Appendix C.

4.3 Developing the pressure-regulated ACC model

The first step in the development of the ACUR LE element in LVTrans is to consider the dynamic relations in the chamber itself. Due to the resemblance to an air cushion chamber, the ACUR LE element is developed with the already-existing ACC element in LVTrans as a starting point. This element utilizes the MRHT method, as described in Section 3.4. Although accurate, the method is at the same time advanced and an unfortunate choice for the first ACUR LE model to be based on. Since the adiabatic assumption has been found to model hydraulic transients quite successfully, the dynamic behavior in the ACC is simplified to follow the polytropic relation from Equation 3.9. At this point in the development of ACUR LE, adiabatic simulations are assumed to be sufficient.

To describe the process of adding air to the chamber, an expression for the polytropic equation with specific values is derived:

$$pv^{\kappa} = p(\frac{V_{air}}{m_{air}})^{\kappa} = C(m_{air})^{\kappa} = C_{specific} \tag{4.1}$$

Here, p is the air pressure, v is the specific volume equal to the volume of air V_{air} divided by the mass of air m_{air}. Both C and $C_{specific}$ are constants. This extension of the polytropic equation was inspired by an example in *Fundamentals of Engineering Thermodynamics* by Moran and Shapiro [64, p. 157]. When new air is added to the chamber, the mass will increase, while the pressure and volume will adjust as $C_{specific}$ stays constant. By assuming this relation between pressure, volume, and mass, the following assumptions are made:

1. The ideal gas model applies for the air.
2. Heat transfer is ignored.
3. Potential and kinetic energy effects are neglected.
4. The air stored within the air compressor or connected pipes is ignored.

Although the pressure and volume of air follow Equation 4.1 as air is added or removed from the chamber, the air cushion will still follow the polytropic relation from Equation 3.9 while counteracting changes in flow and pressure in the HPP tunnel system, just as an ordinary ACC. This dynamic behavior is implemented in the code of the ACUR LE element in LVTrans, where the new amount of air is evaluated every time step, before the air pressure is adjusted according to the MoC. In general, the sum of air pressure and elevation pressure due to the water level in the ACC must equal the HGL at that exact moment, as given from Equation 3.1. With a total excavated chamber volume V_{ACC} and a constant chamber area A_{ACC}, this equals:

$$\begin{aligned} H_{ACC} &= h_{air} + (L + z) \\ &= \frac{p_{air}}{\rho_w g} + (\frac{V_{ACC} - V_{air}}{A_{ACC}} + z) \end{aligned} \tag{4.2}$$

At the beginning of every time step, the specific polytropic constant $C_{specific}$ is calculated:

$$C_{specific} = p_0 \frac{V_0}{m_0} \tag{4.3}$$

where p_0, V_0 and m_0 is the pressure, volume, and mass of air. As an amount of air is added or removed from the chamber, the ratio between pressure and volume changes while the specific polytropic constant stays constant. The new polytropic constant C_{new} is then calculated by multiplying $C_{specific}$ with the new total mass of air m_{new}:

$$C_{new} = C_{specific}(m_{new})^{\kappa} \tag{4.4}$$

The polytropic constant has now increased, meaning that the product of pressure and volume of air increases as well. These values are estimated through a process of iterations, seen in Appendix C. In short, the iteration process uses the Newton-Raphson method to estimate the new water level in the chamber, thus dividing the total chamber volume between water and air. To begin with, the new water volume $V_{iterate}$ is based on the trend in previous changes, before later being based on the

estimated water level. The polytropic equation enters the iteration as it is used to calculate the pressure change dp and new air pressure p_{new}:

$$dp = p_{new} - p_0 = C_{new}(V_{iterate}^{-\kappa} - V_0^{-\kappa}) \tag{4.5}$$

At the end of the iteration, the new air volume is determined as $V_{new} = V_{iterate}$. After the new pressure and volume are estimated, the simulations carries on to the next time step, starting with the calculation of $C_{specific}$ once again. A drawback of this method is that temperature changes are not considered. This follows the adiabatic assumption of no heat transfer, meaning that the temperature is kept constant at all times.

A MATLAB-script is developed to determine the initial values for air pressure, total volume, and water level in ACUR LE, seen in Appendix D. The script is found to be very useful in combination with LVTrans, as the initial values for ACUR LE are critical for all simulations.

4.4 Developing the compressor model

Before the compressor and bypass valve can be implemented in LVTrans, the behavior of real-life compressor must be evaluated. For ACUR LE to run as intended, the air compressor should ideally be characterized by:

- A constant output pressure at a suited medium high level.
- A high maximum throughput.
- A wide range of capable delivery flows.
- A short startup and response time.

The output pressure from the compressor does not need to be higher than the maximum air pressure in ACUR LE. This pressure can be calculated with Equation 4.2 for minimum possible water level in the chamber given by $L = 0$. As ACUR LE is connected to the tailrace tunnel where the HGL is relatively low, a 3-5 times pressure increase through the compressor would likely be enough for most cases. Far more important is the compressor's throughput. By assuming that an air flow of 1 m^3/s causes 1 m^3/s of water into the tailrace tunnel, the maximum throughput should be in the magnitude of the normal HPP production flow if ACUR LE is to counteract the largest flow changes. However, the compressor should also be able to deliver the entire range of smaller flows as well in cases with minor regulations. The startup time is of special importance, as the flexibility of ACUR LE would be very limited with a slow compressor startup.

Based on the condition of high throughput with relatively low pressure, Figure 3.5 suggests that an axial compressor is the best choice. There is a high possibility that the ACUR LE compressor must be custom made, which makes the simulation model of the compressor more difficult to establish. NTNU professor Lars Eirik Bakken was kind enough to offer some advice regarding a real-life compressor for inspiration. He suggested the axial compressor found in the General Electric (GE) LM2500+ gas turbine. From GE's own brochure describing the different gas turbines in the series, the compressor data cannot be extracted solely, as only the values for the total gas turbine process are available [65]. This means that variables such as the compressor outlet temperature are unknown. However, the average pressure

increase for the 2500 series, calculated to 21:1, is assumed to be an accurate ratio for the pressure increase through the compressor. The increase is much higher than ACUR LE needs, but could in theory easily be reduced by decreasing the number of steps in the compression process. Further, the average mass flow $\dot{m}$ is calculated to 84.26 kg/s, which makes the inlet flow Q_{in} equal to:

$$\begin{aligned} Q_{in} &= \frac{\dot{m}_{air} R_{air} T_{in}}{p_{in}} \\ &= \frac{(84.26\,\mathrm{kg\,s^{-1}})(287.058\,\mathrm{J\,kg^{-1}\,K^{-1}})(288.15\,\mathrm{K})}{101.325\,\mathrm{Pa}} \\ &= 68.79\,\mathrm{m^3/s} \end{aligned} \tag{4.6}$$

where R_{air} is the specific gas constant for air. This puts the GE compressor close to the left border in the axial compressor region in Figure 3.5. However, the ACUR LE compressor must be dimensioned according to the volume flow of pressurized air delivered after the pressure increase. By assuming a pressure ratio of 3:1 to be realistic and sufficient for the Bratsberg case, the outlet pressure $p_{out} = 3p_{in}$ gives the compressor outlet flow Q_{out} as:

$$Q_{out} = \frac{\dot{m}_{air} R_{air} T_{out}}{p_{out}} = \frac{Q_{in}}{3} = 22.93\,\mathrm{m^3/s} \tag{4.7}$$

assumption of no temperature increase, thus $T_{in} = T_{out}$. An air flow of nearly 23 $\mathrm{m^3/s}$ would not be enough for ACUR LE to work as intended, calling the need for a compressor with larger inlet throughput, or perhaps a combination of several compressors. Regardless of the number of compressors, the startup time must be considered. From their own brochure, GE claims that their gas turbines can go from cold start to full power within 10 minutes [65]. Whether or not the compressor is the limiting component during the gas turbine startups is unfortunately unknown. In addition, there is not provided any information about how quickly the air flow can change. There might be some stability issues that limits the total startup time, or there could be other unknown delays.

The advanced dynamics in compressors make them difficult to simulate exactly. Additionally, the literature provides only a restricted amount of specific compressor details and accurate performance maps, as these often are considered to be the manufacturer's proprietary information. Without knowing the real-life compressor principles of operation for sure, with the associated limitations, the compressor model in LVTrans is forced to be developed based on a fair amount of assumptions.

4.4.1 Implementing the compressor and bypass valve in LVTrans

The performance of ACUR LE is highly dependent on the flexibility regarding the flow of air into and out of the chamber. Due to the highly complex dynamics in compressors, a direct implementation of the compressor model in the MoC would be very difficult. A better solution is to include the compressor effects solely through the limitations in air flow at different times. In the ACUR LE element in LVTrans, these limitations are given as the four variables startup delay time, maximum rate of change in flow, maximum throughput, and output pressure, as seen from the ACUR LE element controller in Appendix B. These variables affect the performance of ACUR LE during a shutdown scenario as illustrated in Figure 4.3. The shutdown procedure starts at $t = t_0$, where the production flow equals the discharge to river.

Due to the startup delay, the compressor does not start until $t = t_1$. Here, the air flow through the compressor increases with the maximum rate of change until $t = t_2$, when the maximum throughput is reached. From this point on, the production must decrease according to the given maximum ramping rate. After the production flow has decreased to zero at $t = t_4$, the air flow through the compressor reduces slowly.

The compressor is for simplicity assumed to be able to vary the throughput continuously from 0 to maximum, while the compressor control method is not considered in more detail. As there might be a need to use several compressors, the flexibility in throughput is likely to be higher than for a single compressor. In addition, the compressor flow could be adjusted with bypass control, where the bypass valve returns some of the air added to the chamber, and thus reduces the net mass flow of air. This method extracts an economic penalty due to the inefficient use of energy and is the compressor control method with the lowest efficiency [66, p. 20.24].

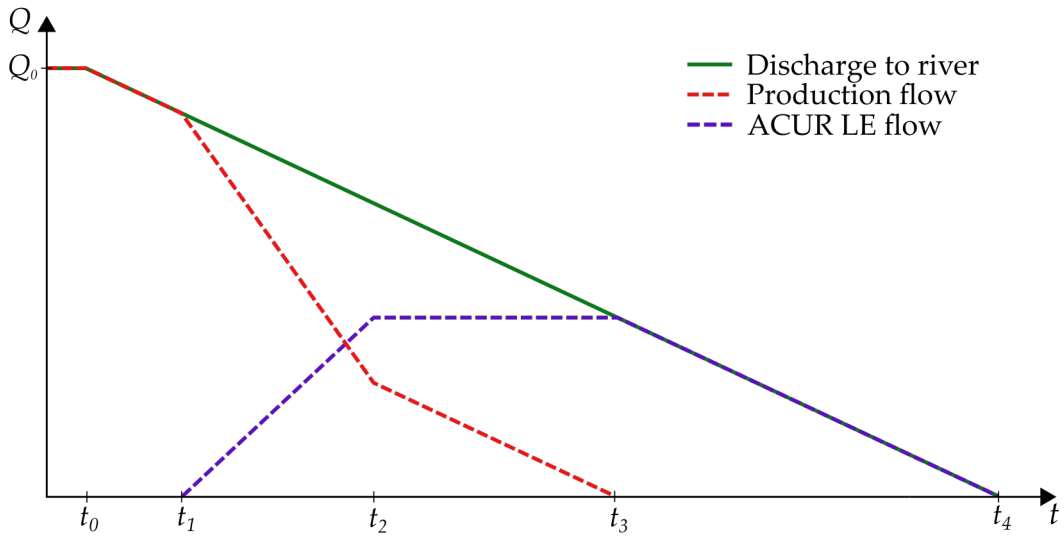

FIGURE 4.3: Illustration of how a shutdown scenario could occur with different compressor limitations taken into account.

As the dynamic behavior in the ACUR LE element is assumed to follow the polytropic equation for a specific volume, previously given in Equation 4.1, the easiest way to include the new air is through its mass. As the compressor works, the mass flow is given through the ideal gas model:

$$\dot{m} = \frac{p_a V_a}{R T_{ch}} \frac{1}{\Delta t} \tag{4.8}$$

where R is the ideal gas constant and Δt is a time step. The subscript a indicates new air condition, while ch indicates that the air temperature T_{ch} is equal to the constant ACUR LE chamber temperature. The air pressure p_a is user determined as one of the compressor limitations, but should typically be kept constant during the simulations. This leaves the volume of new air, V_a, which is determined by the regulator depending on the needed amount of air increase.

The bypassing valve is used to remove air and reduce the pressure in ACUR LE. Since the process of removing air is assumed to be equivalent to adding air, the ACUR LE element includes the valve dynamics through flow limiting variables, in the same way as for the compressor. The effect of removing air from the chamber is

calculated with an equation for the mass flow, where $p_a = p_{ch}$ since the pressure of air leaving equals the chamber pressure p_{ch}:

$$\dot{m} = \frac{p_{ch} V_a}{R T_{ch}} \frac{1}{\Delta t} \tag{4.9}$$

The air valve in the ACUR LE element in LVTrans includes both the options of a starting time delay and a maximum rate of change, seen at the ACUR LE element controller in Appendix B. However, a maximum throughput variable has not been included simply because the valve is assumed to be dimensioned to cover the largest amount of flows.

4.5 Developing the regulator model

Like the compressor and valve, the regulator is also included in the ACUR LE element. For this application, the proportional-integral-derivative (PID) controller was chosen due to its great ability to regulate in a controlled way. The PID controller is defined in the following way:

$$u(t) = K_p e(t) + K_i \int_0^t e(\tau) d\tau + K_d \frac{de(t)}{dt} \tag{4.10}$$

where $u(t)$ is the control variable, and $e(t)$ is the error, meaning the difference between actual volume flow and the setpoint volume flow. The coefficient for the proportional, integral and derivative term, given as K_p, K_i and K_d, respectively, are all non-negative and used to tune the controller to achieve optimal behavior. In the ACUR LE element code, the control variable $u(t)$ is multiplied with the expression for mass flow from Equation 4.8 and 4.9 to get the amount of air added to or removed from the chamber.

However, since the total amount of mass in the chamber varies, the effect of e.g. $u = 1$ will be higher for a chamber with a small amount of air, compared to a chamber almost entirely filled with air. For this reason, the control variable needs to be scaled to compensate for the different water level conditions. To do this, the regulation variable must be adjusted in a way that includes the amount of air in ACUR LE. A simple solution is to use the present volume of air V_{air} and the total chamber volume V_{tot}:

$$u_{new}(t) = u(t) \frac{V_{air}}{V_{tot}/2} \tag{4.11}$$

Here, $u_{new}(t)$ is the control variable adjusted for the amount of mass in the chamber. The equation is determined so that $u_{new}(t) = u(t)$ when the present air volume is half of the total volume, given as $V_{air} = V_{tot}/2$. In this way, any deviations from the middle value will be compensated.

To estimate the error $e(t)$, the regulator needs to monitor the volume flow in the tailrace tunnel. In LVTrans model setup, the volume flow magnitudes are provided to the ACUR LE element through simple connections to the adjacent pipe elements, as seen in Figure 4.2b. The flow downstream of ACUR LE is measured to find the error, while the upstream measurement reveals the actual production flow.

To take the amount of air in the chamber into account, the PID controller is tuned for a half-full chamber. This gives the best result with Equation 4.11. The PID is tuned with a manual approach where K_p is adjusted first, with the other values zero, before K_i next and at last K_d. Since the control variable directly links to the mass flow of air into or out of the chamber, there is no point of a high control variable if

the compressor or valve is not capable of delivering the intended flow. Therefore, the PID controller is tuned with the objective of keeping the control variable $u(t) \in [-1, 1]$, where $u(t) = 1$ means maximum compressor throughput, $u(t) = 0$ gives no air flow, and $u(t) = -1$ corresponds to maximum flow through the valve. In addition to this, some limitations are added to the code to make any values over 1 or under -1 equal to 1 and -1, respectively.

Further, a linear setpoint function is implemented in the model. By controlling the PID target through a function, the discharge flow out of the system can easily be changed linearly and adjusted whenever needed. The implementation of this function consists of an initial value, given as the first regulation target, and a value for the slope. After the first time step, the setpoint target Q_{target} changes according to the following function:

$$Q_{target} = Q_{oldtarget} - s\Delta t \tag{4.12}$$

where $Q_{oldtarget}$ is the target flow prior to the current time step, and s is the slope. With a positive slope value, the target function decreases. This is the typical desired way the discharge should change while the compressor works, as in a shutdown scenario. In addition to this setpoint function, the ACUR LE element developed includes the opportunity to change the slope value s or control variable $u(t)$ manually. The ACUR LE element controller also includes options for whether both the compressor and bypass valve should be used during the current simulation, or if just one of the components should regulate the air flow.

The implementation of the regulator concludes the development of the ACUR LE element in LVTrans. To investigate how the element works during different scenarios, ACUR LE must be dimensioned to fit the case HPP Bratsberg.

4.6 Setting up the simulations

All simulations are done for the Bratsberg model in LVTrans, previously illustrated in Figure 4.2. As the values for installed capacity, annual production, and maximum volume flow in Bratsberg are difficult to determine exactly, the design flow and power for normal operation is assumed to be $Q_{design} = 100\ \mathrm{m^3/s}$ and $P_{design} = 130$ MW, respectively. These values deviate from the information given in Section 4.1, but they are assumed to be a good estimate for the actual production values during normal operation. With use of Equation 2.1, the total efficiency η is then estimated to $\eta \approx 0.9$. Further, the restricted rate of change in discharge $\dot{Q}$ can be calculated as:

$$\dot{Q} = \frac{\Delta P_{OR}}{\Delta t_{OR}} \frac{Q_{design}}{P_{design}} = \frac{62\,\mathrm{MW}}{(6\,\mathrm{min} \cdot 60\,\mathrm{s})} \frac{100\,\mathrm{m^3/s}}{130\,\mathrm{MW}} = 0.1325\,\mathrm{m^3/s/s} \tag{4.13}$$

where the power ΔP_{OR} and time Δt_{OR} are the operating restrictions for fast startup and shutdown given in Table 4.1. Now the developed ACUR LE element in LVTrans can be dimensioned to fit the case HPP Bratsberg. To determine the total volume of the chamber, the total amount of water needed to cover a fast shutdown or startup is taken into account. With the use of Equation 4.13, the total time to reach 100 $\mathrm{m^3/s}$ is estimated to nearly 13 min, while an ideal startup can be assumed to take a few seconds. This means that approximately $38,000\ \mathrm{m^3}$ of water separates the ideal startup from the normal startup procedure. Compared to already existing air cushion chambers, creating a cavern of this size should be possible. Berg (1998), referred to in Røse [51, p. 9], states that most of the Norwegian air cushion chambers have a

total volume in the range of 5,000 to 15,000 m^3, with the exception of Kvilldal HPP, where the chamber volume is 110,000 m^3. From this, Bratsberg was determined to be simulated with two cases of ACUR LE volumes, as presented in Table 4.2.

The volume for Case 1 is chosen to be 25,000 m^3, representing a conservative measure with limited water storage. For Case 2, the volume is 50,000 m^3, indicating that water storage will not be the limiting factor during the simulations. In the setup of Bratsberg HPP, shown in Figure 4.2, the ACUR LE element is placed at the lowest point in the tailrace tunnel, where the vertical distance to the river reservoir is 22 m. As the total volume already is determined, the constant water surface areas in the two cases are chosen with the hydraulic grade line in mind. To ensure a chamber air pressure stays higher than the atmosphere pressure at all times, the water surface diameters given in Table 4.2 are chosen to keep the total chamber height close to, but below 22 m.

TABLE 4.2: Dimensions of ACUR LE for two cases.

	Case 1	Case 2
Volume [m^3]	25,000	50,000
Diameter [m]	40	55
Height [m]	19.89	21.05

With the dimensions of ACUR LE determined, the stability and surge abilities are evaluated based on the theory from Section 3.2.3. Regarding the stability, the areas chosen for Case 1 and 2 are not sufficiently large if ACUR LE is considered to be an air cushion chamber. This is, however, assumed not to be a problem as ACUR LE is designed to be pressure-regulated with the intention of mitigating fluctuations. The total down-surge for different flow values are estimated as well. By using Equation 3.7 and 3.8 to calculate the equivalent surge shaft area, the maximum surge becomes dependent on the volume of air. From this, a limit of minimum water volume in ACUR LE per volume flow is estimated, as presented in Appendix E.

The remaining variables related to ACUR LE and other elements in LVTrans are determined differently for startup, shutdown and flood scenarios. In the following sections, further details in the simulation setup are presented.

Startup

The startup scenarios are simulated from an initial power production of 0 MW, as well as 0 m^3/s of flow through the system. For all startup simulations, the objective is to ensure that the discharge to river increases with the appropriate rate of change for the fast Bratsberg startup condition, calculated by Equation 4.13. Therefore, the available water storage volume must be considered. To maximize the storage for water, ACUR LE is initially almost completely filled with air. As explained in Section 2.3.1, ACUR LE covers the amount of water between the production flow and the discharge to river. To avoid high rates of change in discharge, the volume of water that separates the production flow from the total discharge must be lower than the storage volume in the chamber. This determines the power setpoint function, that represent the ideal power production.

During the startup scenarios presented in the results, the production flow is typically higher than the intended discharge flow. This surplus of water in the tailrace tunnel is absorbed by ACUR LE as the regulator adjusts the valve only. In these simulations, the valve is not restricted with neither a startup delay time nor a ramping increase rate, thus enabling the HPP power to increase almost immediately.

Shutdown

In the shutdown scenarios, all variables are initially at steady state with the assumed operating conditions, before the shutdown happens after 60 s. Equivalent to the startup simulations, the objective is to ensure that the discharge to river follows the appropriate rate of change, although this time decreasing from normal operating flow with the fast shutdown condition from Table 4.1. The rate of change in power, proportional to the production flow, depends on the total amount of available water stored in ACUR LE. For this reason, the chamber is initially almost depleted of air. In addition, the restrictions related to the compressor are considered. The maximum rate of change in flow rate is somewhat arbitrary chosen to be 25 $m^3/s/min$, as exact values for the air flow increase through compressors are not found. For the Case 1 shutdown scenario in Section 5.5, the maximum compressor throughput is assumed to be 50 m^3/s. Further, the compressor is assumed to deliver a constant pressure of 30 mWC, while being able to deliver a continuous specter of flow values. The compressor startup delay time is for simplicity neglected. With all of these conditions in consideration, the power reduction in each shutdown scenario is calculated prior to simulation to ensure constant discharge to river.

Flood

Regarding the flood scenarios, only the ACUR LE dimensions from Case 2 are used in the simulations, as Case 1 is assumed to give equivalent results. These flood simulations are not based on any real-life scenarios for Bratsberg HPP or Nidelva, as they are simply performed to investigate how ACUR LE handles flood control. During the flow mitigation scenario, the surplus of water makes the river flow bypassing the HPP increase beyond normal conditions. The power plant is assumed to without the reservoir water and not produce electricity, implying that the bypass flow equals the total discharge. To simulate this scenario in LVTrans, the tailrace tunnel in Figure 4.2a is modified according to Figure 4.4. This specific setup where the bypassed river enters the end of the tailrace tunnel was necessary for the ACUR LE element to work as intended. Although the setup deviates from a real-life scenario, ACUR LE is assumed to operate equivalently to a better bypass river setup. To create a varying flood discharge, the reservoir level in the Bypass element is changed during the simulation. As the flood increases to peak values, the pressure in ACUR LE is adjusted to suck water into the tailrace tunnel. In this way, the total river discharge is reduced as ACUR LE adsorbs a part of the volume flow.

For the simulation with flood imitation, the ordinary setup from Figure 4.2b is used instead of the setup from Figure 4.4. In this simulation, the hydroelectric production is at normal conditions.

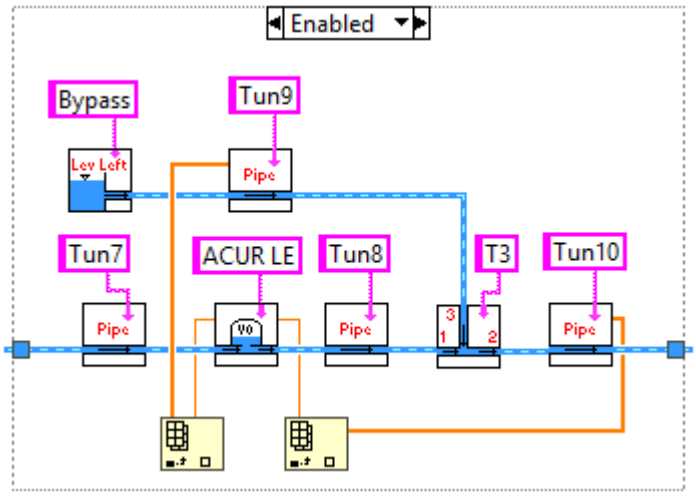

FIGURE 4.4: Modified tailrace tunnel with bypass water included for the Bratsberg model in LVTrans.

Chapter 5

Results and discussion

In this chapter, the simulation results from the different scenarios are presented and discussed. An overall discussion and comparison between the scenarios is found in Section 5.9.

5.1 Overview over performed simulations

For readability, an overview of all simulated power production scenarios is presented in Table 5.1. These simulations are done with different operating procedures for Bratsberg HPP. Furthermore, the simulations regarding flood are given in Table 5.2.

TABLE 5.1: Overview over scenarios with different operating procedures.

Description:	Type:	Case:	Results in section:
Normal Bratsberg HPP startup	Startup	1 & 2	5.2.1
Normal Bratsberg HPP shutdown	Shutdown	1 & 2	5.2.2
Immediate maximum power	Startup	1	5.3.1
Delayed maximum power	Startup	1	5.3.2
Power increase in two steps	Startup	1	5.3.3
Power increase in three steps	Startup	1	5.3.4
Case 2 startup	Startup	2	5.4
Case 1 shutdown	Shutdown	1	5.5
Case 2 shutdown	Shutdown	2	5.6
Varying power production	Regulation	2	5.7

TABLE 5.2: Overview over flood simulations.

Description:	Type:	Case:	Results in section:
Flood mitigation	Flood	2	5.8.1
Flood imitation	Flood	2	5.8.2

5.2 Simulating Bratsberg HPP with and without ACC

5.2.1 Normal Bratsberg HPP startup

A startup scenario based on the operating conditions at Bratsberg is simulated to get reference for comparison with the other startup simulation. This is done both with and without ACUR LE implemented in the LVTrans model, giving in Figure 4.2b and 4.2a, respectively. In these simulations, ACUR LE is in passive mode and not pressure regulated, thus affecting the system in the same way as an air cushion chamber would have done. The power production, seen in Figure 5.2, is for all simulations adjusted to follow the Bratsberg restriction for fast startup, given in Table 4.1, with ramping rate of 62 MW per 6 minutes. To achieve this slow increase, the turbines are started up one by one. The turbine efficiency increases with the volume flow and reaches the maximum value of 0.9 for the normal operating flow of 50 m^3/s per turbine, as seen in Figure 5.4. With this startup procedure, the total amount of energy produced is approximately 18.84 MWh.

The difference between the simulations with and without a surge element is clearly recognized as the model with the ACUR LE creates fluctuations. These fluctuations lead to a varying degree of volume flow increase, although the mean value seems to be the same as for the simulation without the surge element in the tailrace tunnel. As seen in Figure 5.1, the fluctuations differ from Case 1 and Case 2. The doubled air volume from Case 2 causes discharge oscillations with a longer wavelength, equivalent to the change in water volume in the chamber seen in Figure 5.3. Although the wavelength and frequency are different, the amplitude of discharge fluctuations in Figure 5.1 are more or less equal.

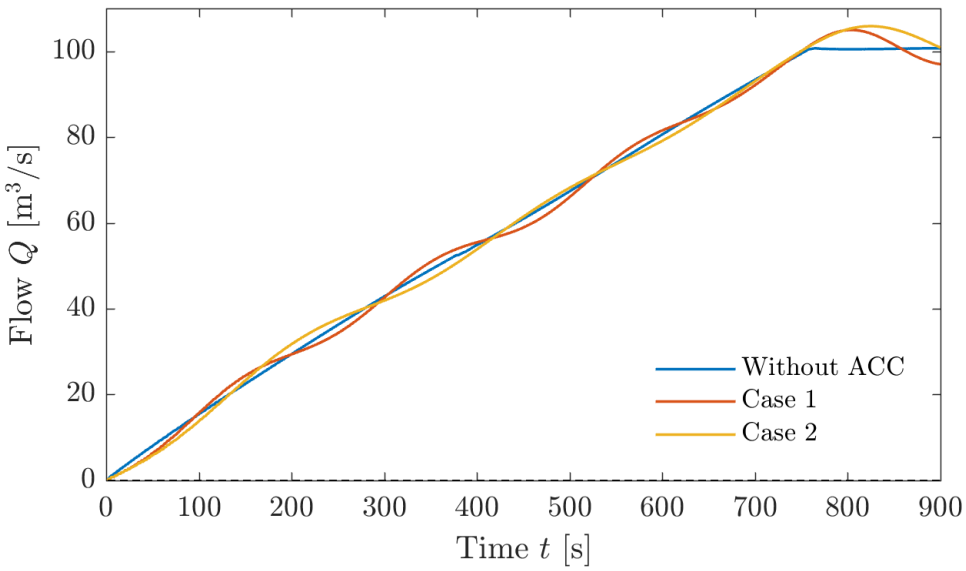

FIGURE 5.1: Linear and oscillating river discharge during startup.

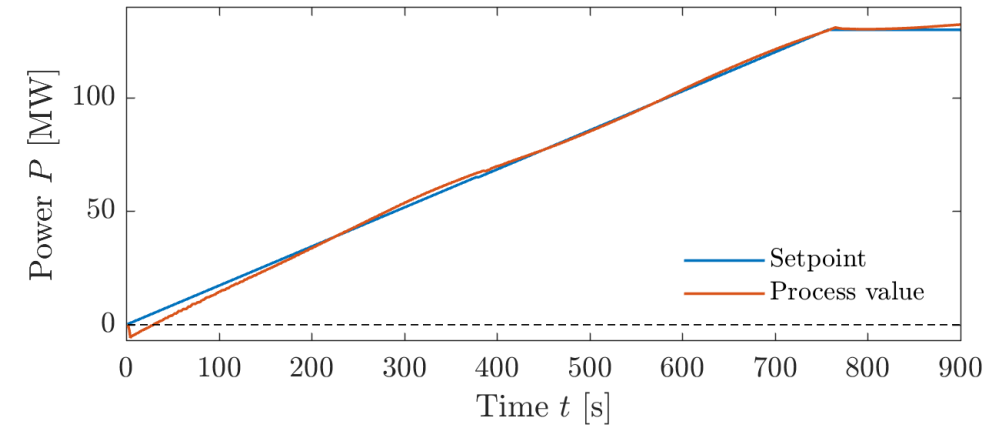

FIGURE 5.2: Power increase during startup with a total production of 18.84 MWh.

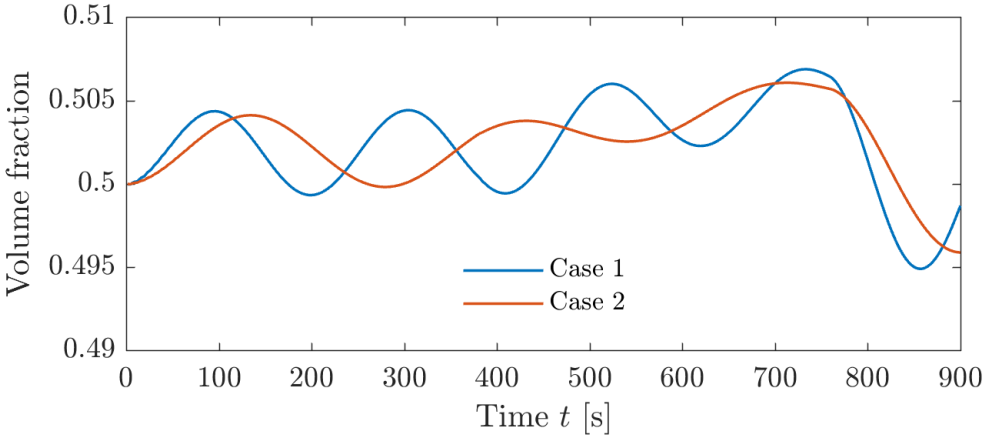

FIGURE 5.3: The volume fraction of water in ACUR LE fluctuates for the two cases.

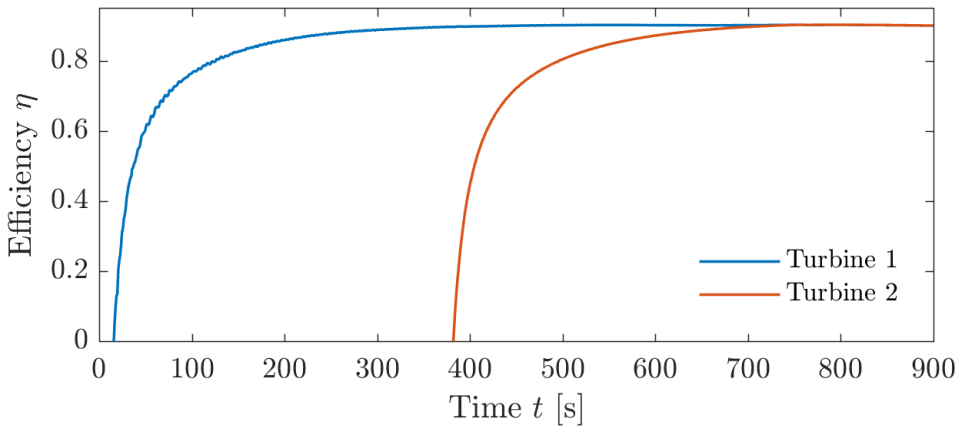

FIGURE 5.4: Total efficiency η per turbine increases slowly.

5.2.2 Normal Bratsberg HPP shutdown

The fast shutdown scenario for Bratsberg HPP is simulated according to the restriction in Table 4.1 for the Bratsberg setups in LVTrans from Figure 4.2. Like for the initial startup, the presence of ACUR LE in passive mode leads to oscillations in the discharge flow, as expected from an ACC. Both the power production and the total efficiency per turbine, given in Figure 5.6 and 5.8, respectively, are approximately reversed versions of their equivalents from the normal startup case. The process value of power is higher than the setpoint during the first 300 s, causing the HPP to produce more than intended. For the rest of the time, the energy actually produced is lower than targeted. This behavior is caused by the PID Francis element in LVTrans that governs the power production.

In the case without ACUR LE in the system, the discharge flow starts decreasing linearly along with the power. This is clearly seen in Figure 5.5 from 60 s, where the blue line instantly changes direction. For Case 1 and 2, the decrease in volume flow is delayed by a few seconds, as the red and yellow lines show respectively. This delay causes oscillations in discharge, as well as in the water level in ACUR LE, illustrated through the volume fractions in Figure 5.7

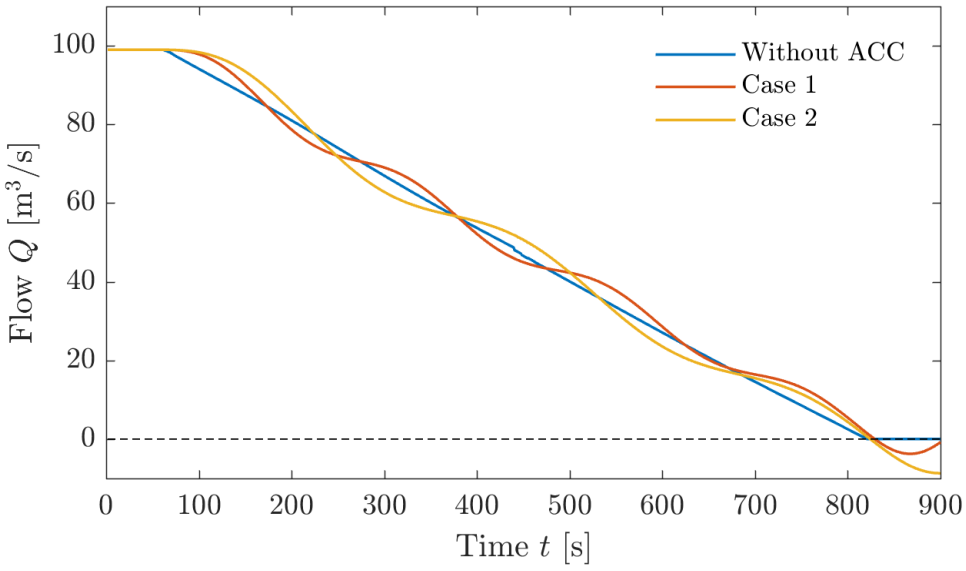

FIGURE 5.5: Linear and oscillating flow reductions for the three cases.

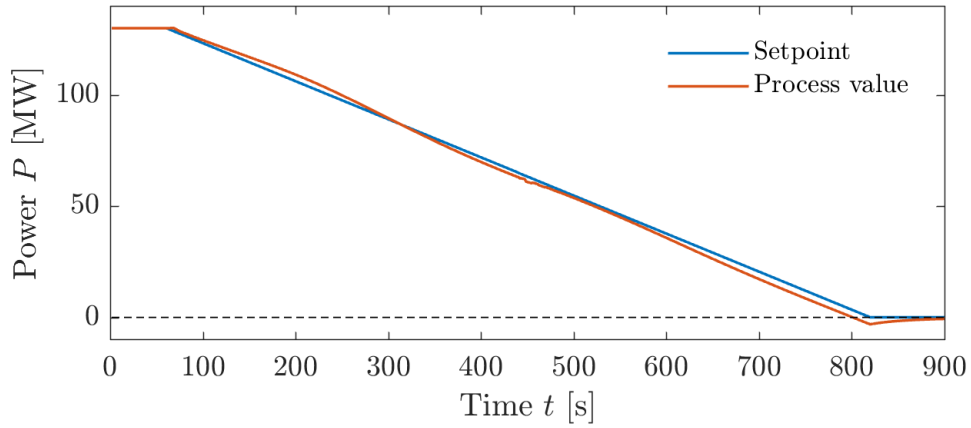

FIGURE 5.6: The power P reduces during shutdown.

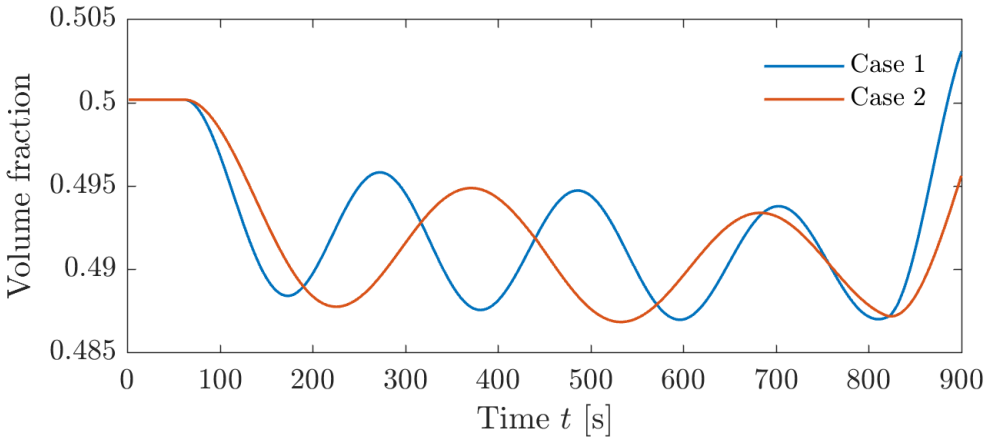

FIGURE 5.7: The fraction of water in ACUR LE changes equivalent to the water level oscillations throughout the simulation.

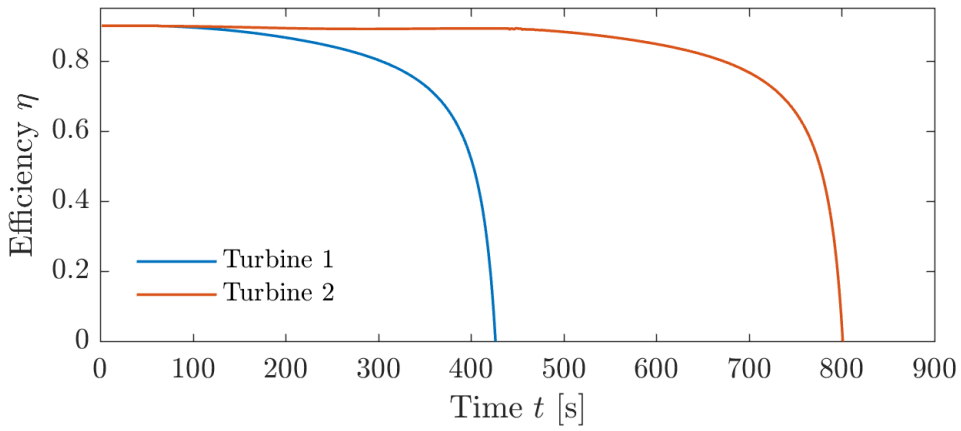

FIGURE 5.8: The efficiency η drops as the flow through the turbines decreases.

5.3 Startup scenarios for Case 1

For Case 1, where the ACUR LE volume is limited to 25,000 m^3, the water storage is too small for an ideal and fast startup. However, ACUR LE can ensure that a part of the total discharge increase follows the restricted rate of change from Equation 4.13, while the power production varies from the normal startup procedure simulated in Section 5.2.1.

5.3.1 Immediate maximum power

This scenario involves an early response to the energy demand by maximizing the power production at the beginning of the increase in discharge. The initial setpoint for power is 130 MW, as seen with the blue line in Figure 5.10. This results in a massive increase in production flow, shown in Figure 5.9, while the discharge water increases approximately according to the acceptable ramping rate from Equation 4.13. As the volume of ACUR LE is limited to cover only a certain amount of the water production flow, the production is adjusted after approximately 250 s. At this point, ACUR LE is almost entirely filled with water, seen in Figure 5.11, and the production is forced to follow the restricted ramping rate from Table 4.1. However, due to the oscillations in power, the process value, and thus the production flow from Figure 5.9, ends up being lower than intended.

At approximately 370 s, the discharge water exceeds the production flow. As only the valve is used in this startup scenario, ACUR LE is unable to force more water into the tailrace tunnel. This causes the total discharge to drop below the production flow, until ACUR LE increases the discharge above the production flow again. This oscillating pattern continues until around 570 s, where the process value for power is increasing above the setpoint, seen in Figure 5.10.

In general, the largest pressure oscillations occur during the first 300 s of the simulation, as a result of the massive increase in power and flow. The efficiency stays quite high for Turbine 1 during the entire startup, as seen in Figure 5.12, but increases slowly between 450 s and 600 s for Turbine 2. The total amount of power produced during the 15 simulated minutes is 25.77 MWh.

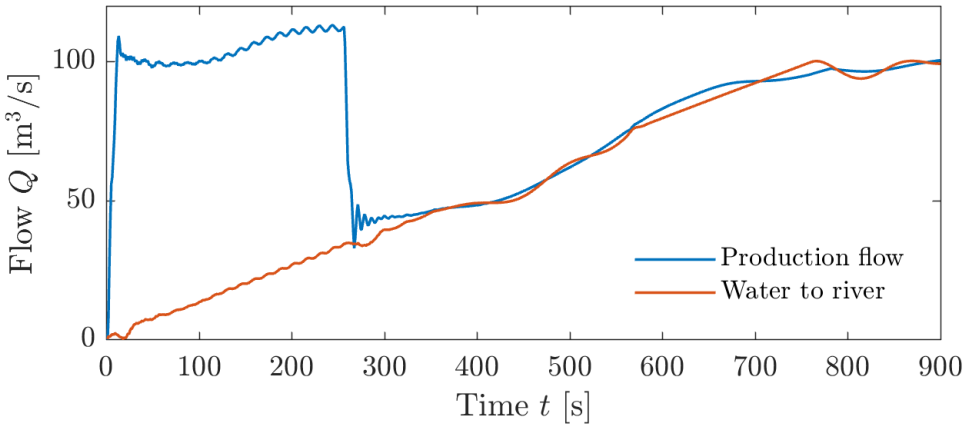

FIGURE 5.9: The river discharge increases approximately evenly, although the production flow affects the result.

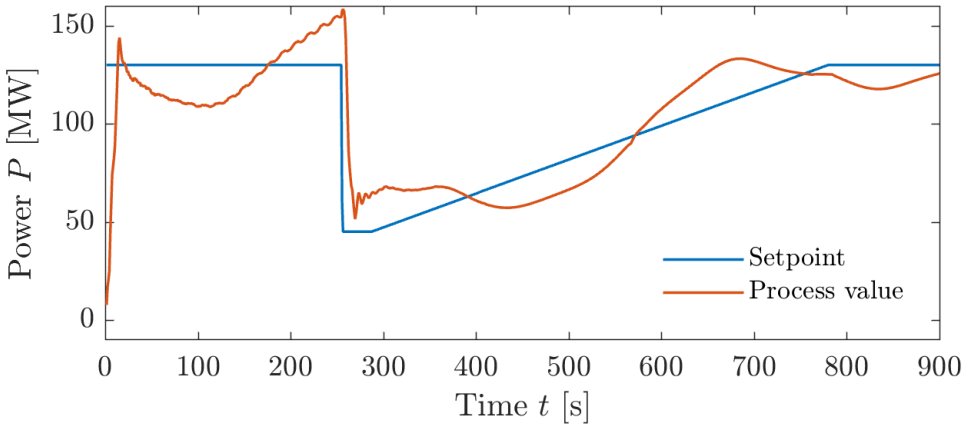

FIGURE 5.10: Maximum power is produced instantly, before the power drops and slowly increases.

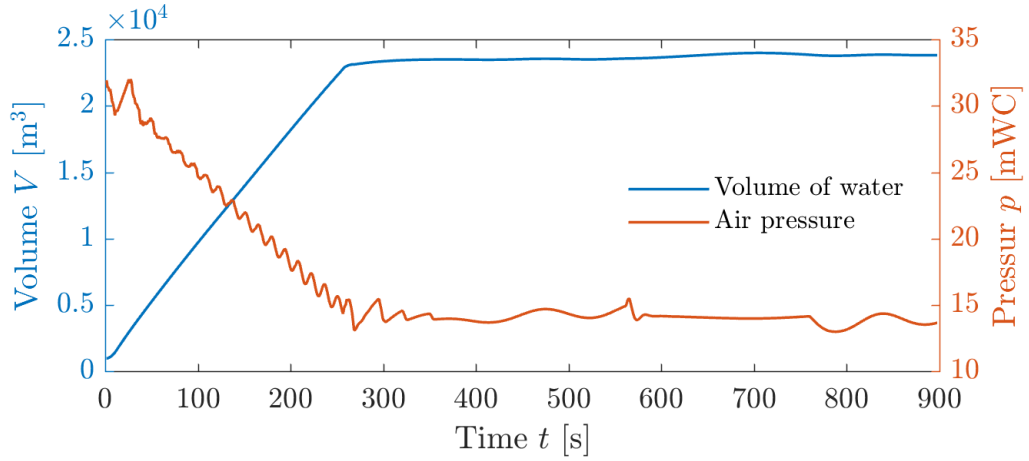

FIGURE 5.11: The water storage of ACUR LE fills up during the first 250 s.

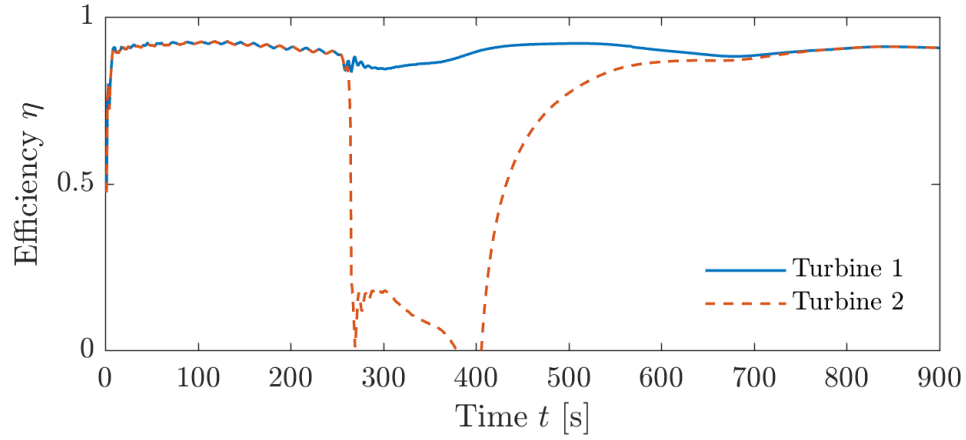

FIGURE 5.12: The efficiency η varies with the flow through the turbines.

5.3.2 Delayed maximum power

In this scenario, the power increases in the same way as in the normal Bratsberg startup procedure during the first period of time, but changes after 180 s, as seen in Figure 5.14. At this point the setpoint for power production changes to 130 MW, resulting in a major production flow increase seen in Figure 5.13. As the ACUR LE regulation starts, the air pressure in the chamber reduces, as plotted in Figure 5.15. The result is an almost constant rate of change in discharge. As this flow reaches the intended maximum value of 100 m^3/s, the PID in ACUR LE is turned off, and some moderate oscillations occur.

While the production increases slowly during the first three minutes, Turbine 1 is forced to run at low efficiency, seen in Figure 5.16, but as soon as the setpoint hits 130 MW, both turbines run at approximately design conditions. This leads to a total power production of 26.55 MWh during the 15 simulated minutes.

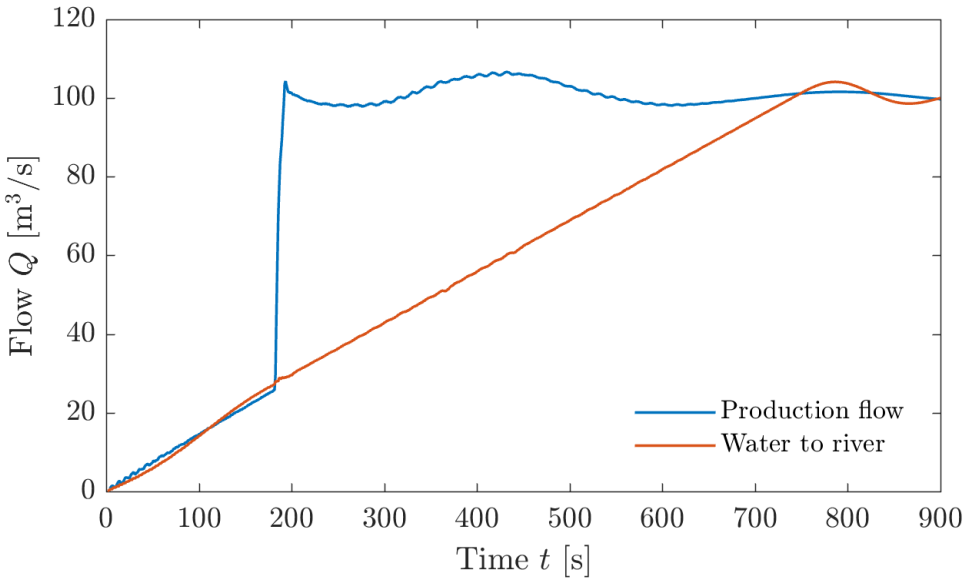

FIGURE 5.13: Linear increase in discharge with massive increase in production flow.

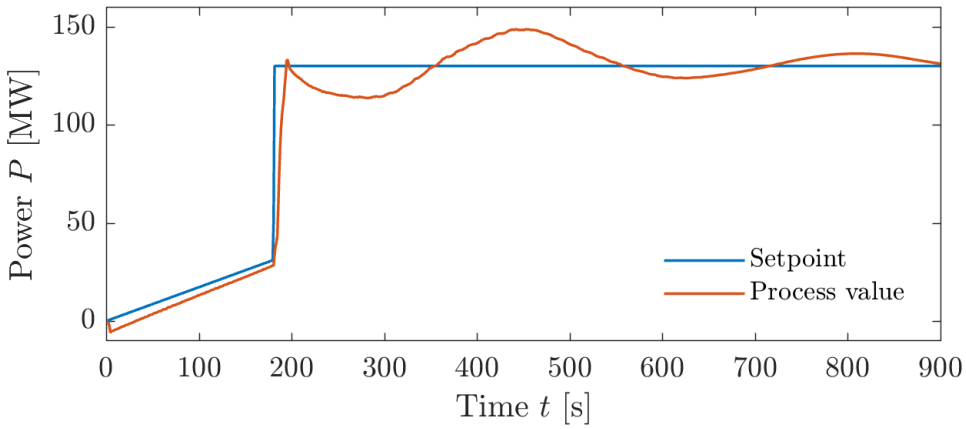

FIGURE 5.14: The power setpoint steps up to 130 MW after 180 s.

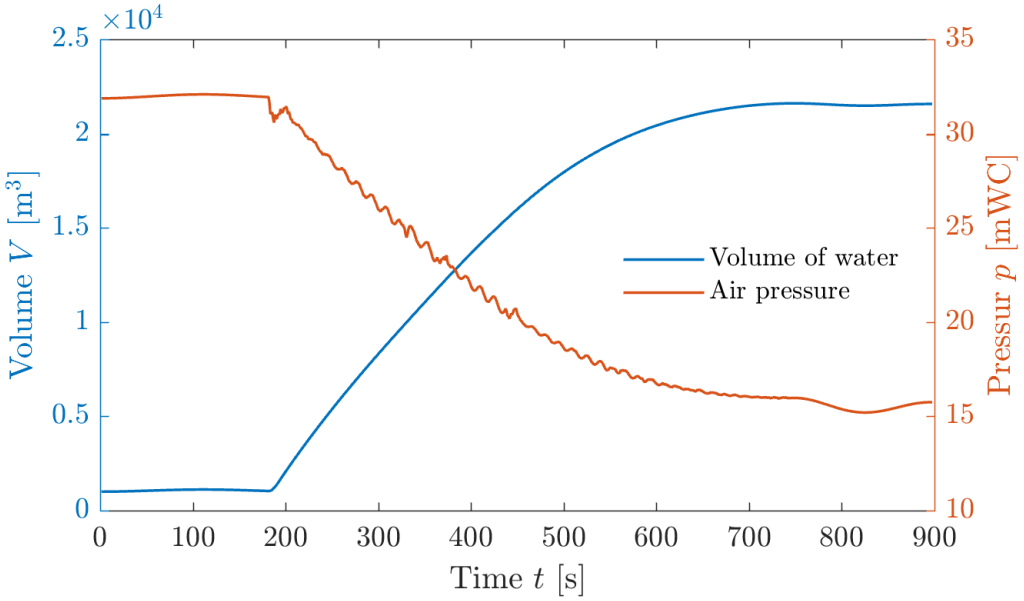

FIGURE 5.15: The water volume increases slowly as the air pressure oscillates and decreases inside ACUR LE.

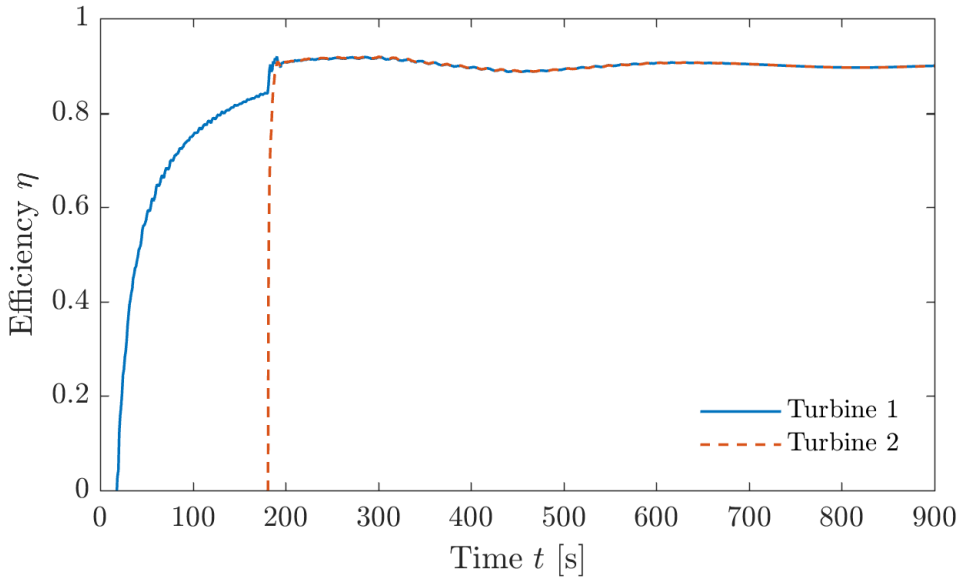

FIGURE 5.16: The efficiency increases slowly for Turbine 1 compared to Turbine 2.

5.3.3 Production increase in two steps

As an alternative to the slowly increasing power given in Section 5.2.1, the power is in this simulation increased in two steps. Initially, one of the turbines starts up and runs at approximately design condition at a discharge of 50 m^3/s, providing power at 65 MW. With decreasing pressure in ACUR LE, as seen in Figure 5.19, the chamber is increasingly filled with water. At 330 s, the production plotted in Figure 5.18 increases to the maximum value of 130 MW as the second turbine is turned on. The process value from the figure illustrates how the power varies tremendously, varying around the setpoint. This causes the altering behavior of the production flow in Figure 5.17, where the wavelike motion is accompanied by a short wavelength oscillation. At around 760 s, where the water to the river has reached the operating flow of approximately 100 m^3/s, the regulation in ACUR LE is turned off, causing some moderate flow and pressure oscillations.

In this simulation, the water storage provided by ACUR LE, visualized through the volume of water in Figure 5.19, is utilized completely. This means that the power increase in Turbine 2 could not have been initiated earlier. As both turbines run at design conditions at all times, the efficiency is generally high, seen in Figure 5.20. This leads to a total power production of 26.45 MWh during these 15 minutes.

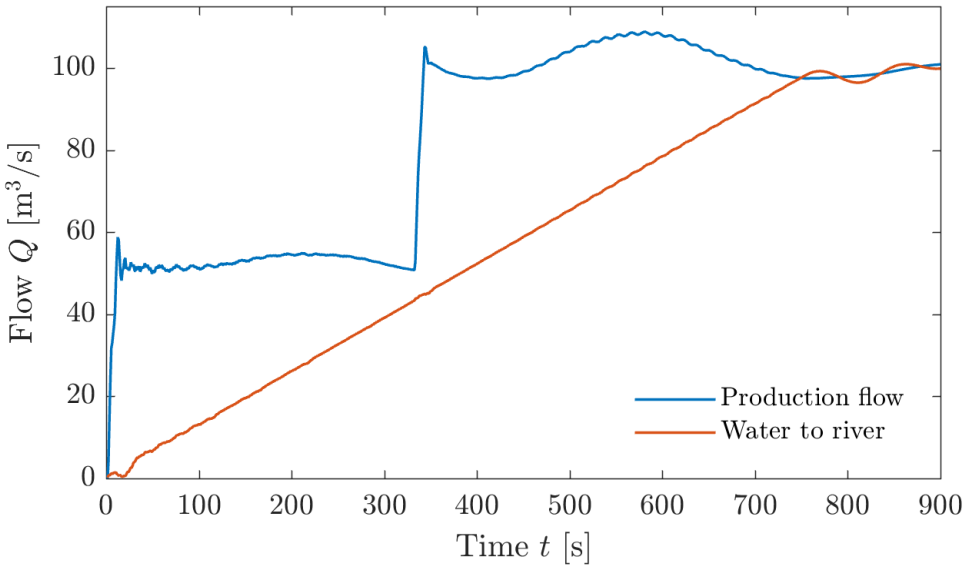

FIGURE 5.17: Production flow increases in steps while the discharge to river increases linearly.

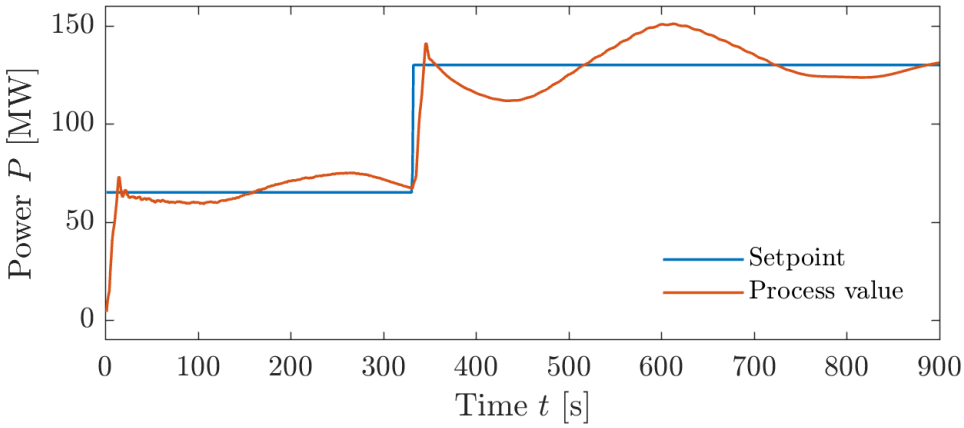

FIGURE 5.18: The power P oscillates and increases in two steps.

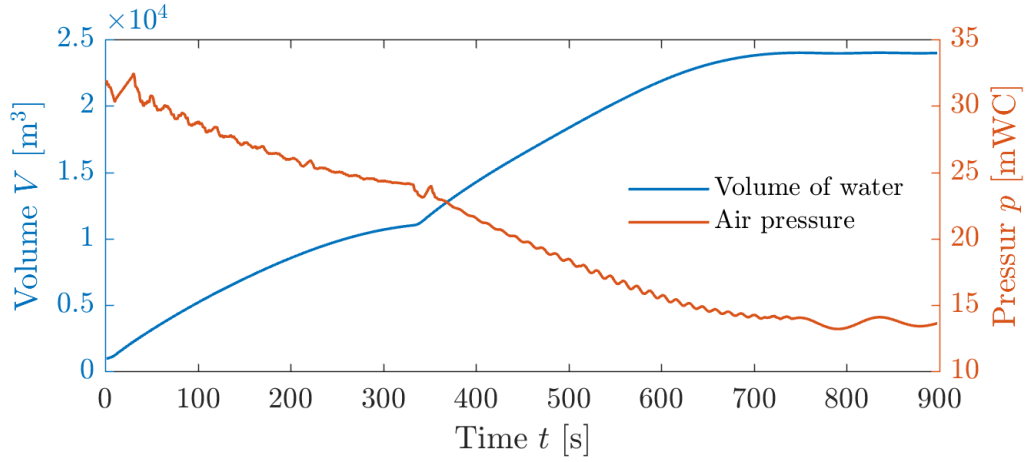

FIGURE 5.19: Water volume and air pressure in ACUR LE changes during the startup.

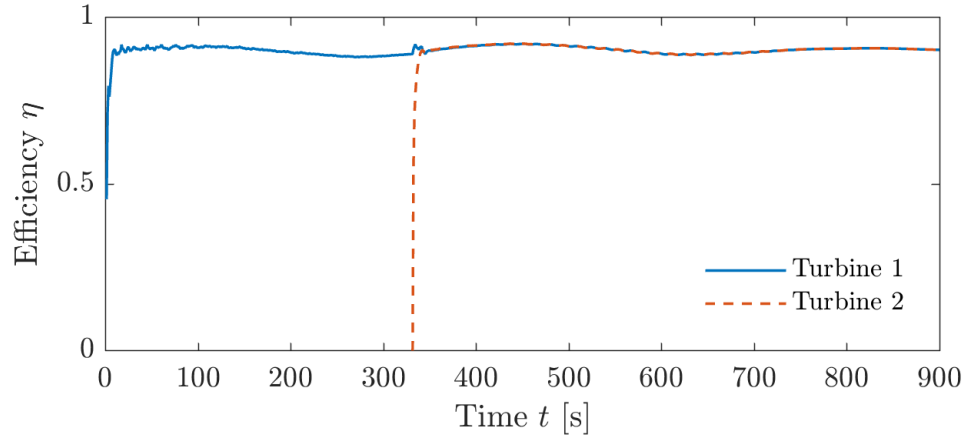

FIGURE 5.20: The efficiency η shoots up to 0.9 instantly before some small oscillations occur.

5.3.4 Production increase in three steps

In this simulation, the production is initially put to the maximum value of 130 MW, visualized in Figure 5.22. While the air pressure in ACUR LE decreases as the chamber fills up with water in Figure 5.23, the discharge flow follows the intended rate of change from Equation 4.13, as seen in Figure 5.21. After 230 s, ACUR LE is almost entirely filled with water. Consequently, one of the turbines is shut off to reduce the production flow while the other turbine runs at approximately design speed. The power is reduced until the water level in ACUR LE has decreased sufficiently, enabling the power to increase again. In this startup simulation, not only the valve but also the compressor is used to manipulate the discharge. This enables the total discharge to surpass the production flow, as seen in Figure 5.21 at approximately 400-600 s. Then, the power and production flow increases again while ACUR LE absorbs water from the tailrace tunnel. The sudden change in power causes oscillations that seem to grow in amplitude. At 760 s, ACUR LE is restarted with the setpoint of 100 m^3/s, but the governor is not able to dampen the oscillation.

Turbine 2 runs at approximately design speed with the highest efficiency for the entire simulation, as seen in Figure 5.24, but Turbine 1 is at times running at low efficiency. Although intended, the process value of power does not follow the setpoint function from Figure 5.22 exact, causing the production flow to oscillate. After 230 s, the setpoint for power in Turbine 1 is adjusted to 0 MW, but the turbine does not shut down completely. As the shutdown happens at the peak of the production flow oscillation, where the flow is approximately 10 m^3/s higher than the intended mean value, the flow stays around 10 m^3/s higher than intended after the shutdown. For this reason, Turbine 1 actually generates some energy. In total, the startup procedure generates around 26.25 MWh.

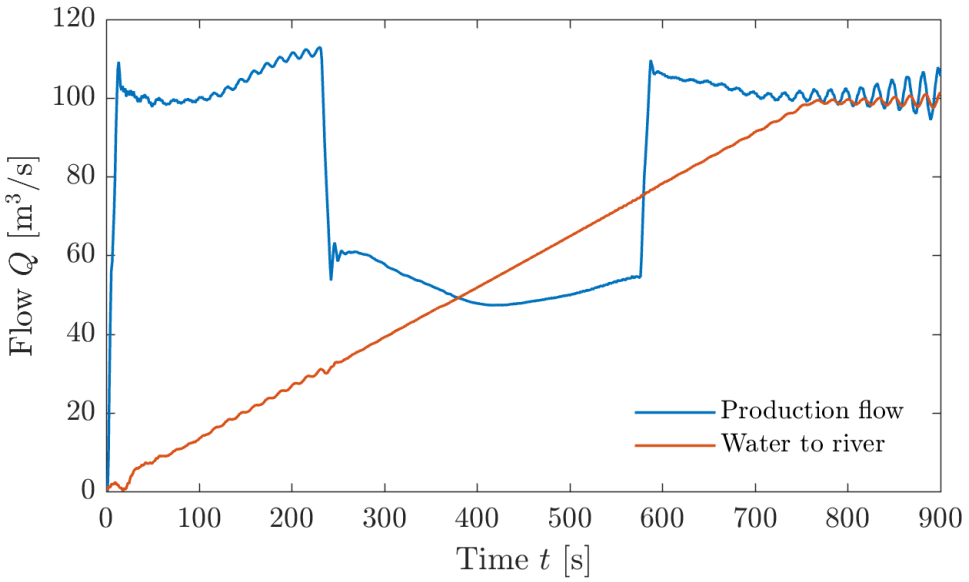

FIGURE 5.21: The discharge flow increases linearly, while the production flow oscillates in three steps.

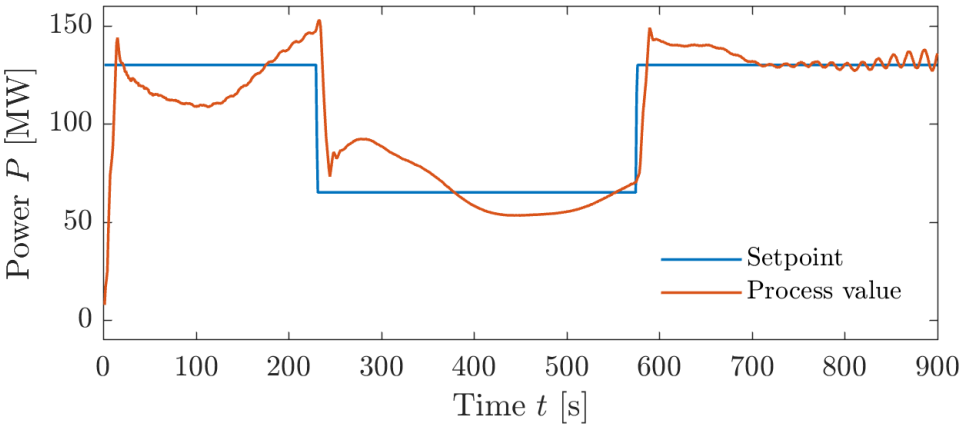

FIGURE 5.22: The power P changes drastically in three-steps.

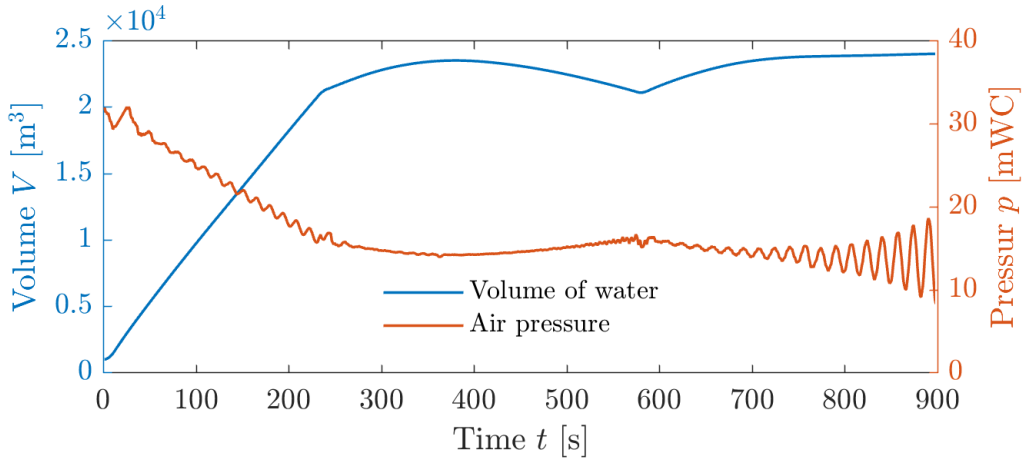

FIGURE 5.23: The water volume in ACUR LE increases, decreases and increases again, while the air pressure changes inversely.

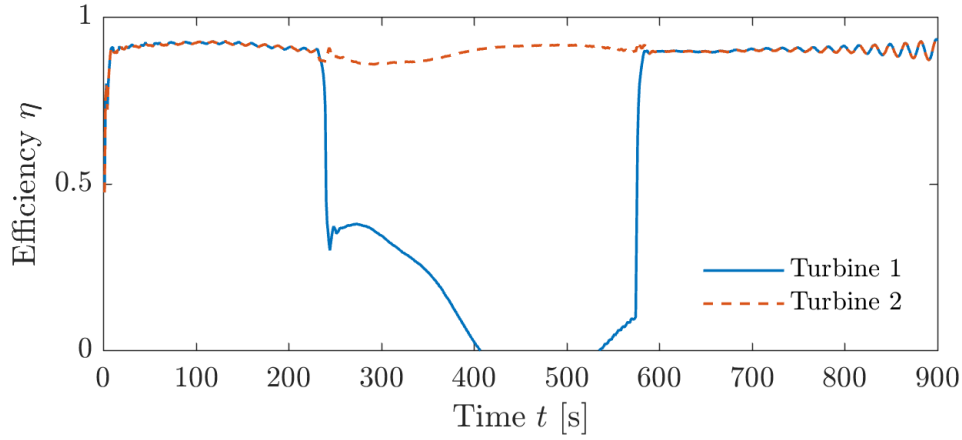

FIGURE 5.24: The efficiency η stays high for Turbine 2, but is at times lower for Turbine 1.

5.4 Startup scenario for Case 2

ACUR LE provides a volume of 50,000 m^3 for water storage, meaning that the power can increase instantly while ACUR LE ensures that the total discharge flow to river follows the given rate of change from Equation 4.13. As seen in Figure 5.26, the power increases to 130 MW during approximately 10 seconds immediately as the simulation begins, causing the production flow to increase equivalently, seen in Figure 5.25. During the first 50 s, the discharge varies in an oscillating manner, before ACUR LE is able to keep the rate of change stable. The volume of water in the chamber increases from the initial value of around 1,000 m^3 to approximately 40,000 m^3 during the startup, as seen in Figure 5.27. Contemporary, the pressure decreases to around 16 mWC. The efficiency η in Figure 5.28 is high and equal at all times for both turbines. This leads to a total power production of 32.53 MWh during the simulated 15 minutes.

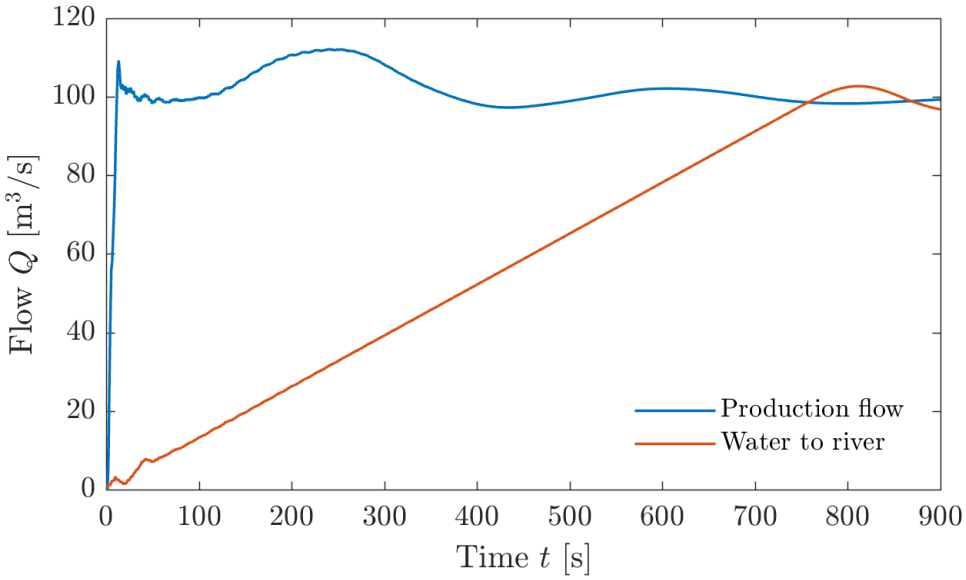

FIGURE 5.25: Linear increase in discharge with high production flow.

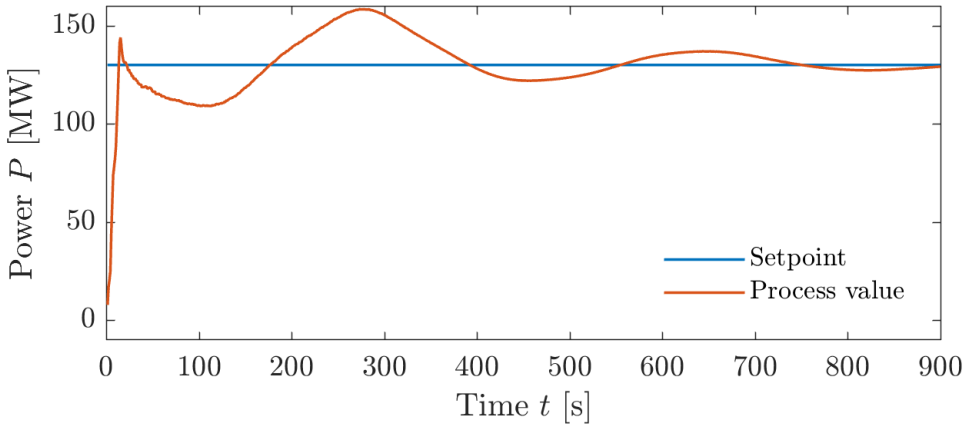

FIGURE 5.26: Instantly high power production that oscillates.

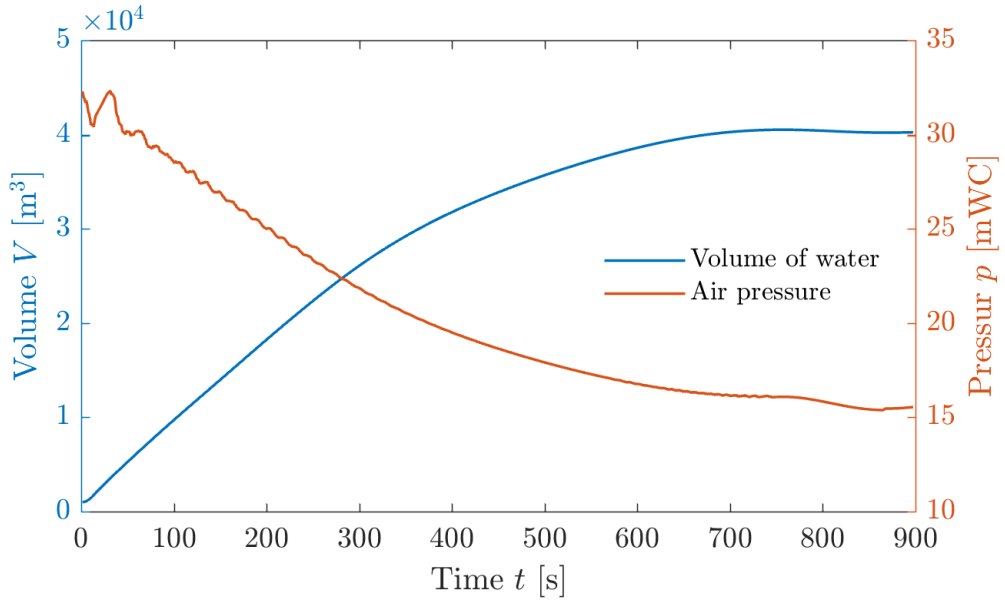

FIGURE 5.27: The air pressure decreases as the water volume increases.

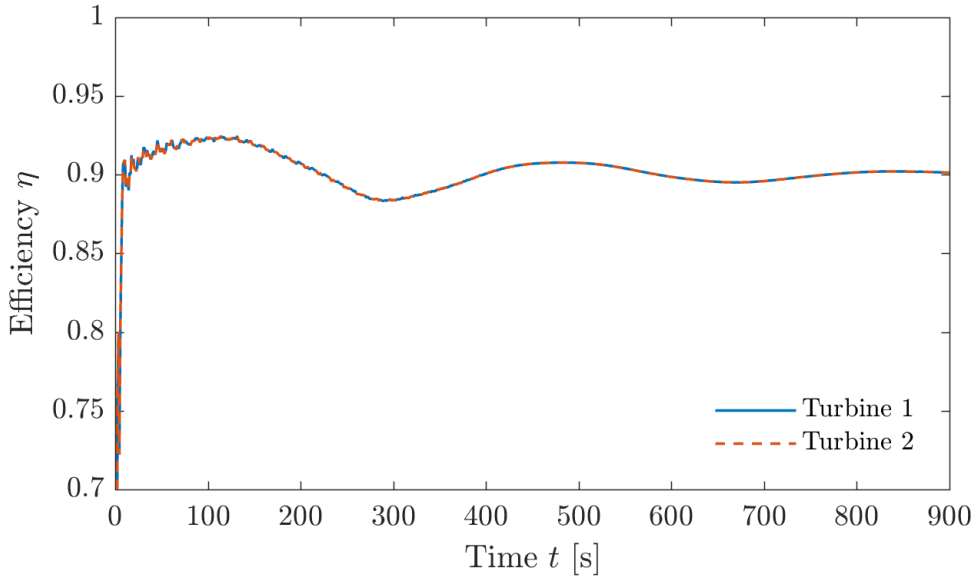

FIGURE 5.28: Magnified view of the small efficiency oscillations.

5.5 Shutdown scenario for Case 1

In this shutdown simulation, the compressor is assumed to be limited to 50 m^3/s, causing the maximum water flow out of ACUR LE to be of the same value. The limiting factor that determines the power ramping rate during the shutdown is the total water volume in ACUR LE for Case 1. As seen from Figure 5.31, the available water volume is utilized completely with the power decrease used in the simulation. ACUR LE manages successfully to decrease the discharge flow with a steady rate of change, seen in Figure 5.29, although some oscillations occur. The turbine efficiency is not plotted for this simulation, and the total energy generated during the shutdown is not considered. As the scenario is related to hydropeaking, the main objective is to shut down the HPP as fast as possible, not to generate electricity.

From 300 s to approximately 440 s, the difference between the production flow and the discharge in Figure 5.29 is intended to be 50 m^3/s but is at times as high as 53 m^3/s. This can be explained from Figure 5.30, where the power process value is lower than the setpoint, causing a lower production flow. Although the maximum compressor throughput is 50 m^3/s in the ACUR LE element controller during the simulation, the delivered air pressure of 30 mWC is higher than the pressure in the chamber, seen in Figure 5.31. This enables a higher mass flow than intended, given by Equation 4.8, which causes the flow of water to be higher than 50 m^3/s.

The oscillations in water flow and air pressure becomes more intense as the rate of change in power is adjusted at 300 s. As ACUR LE stops regulating the air pressure at 820 s, the pressure stabilizes while the production flow grows in amplitude.

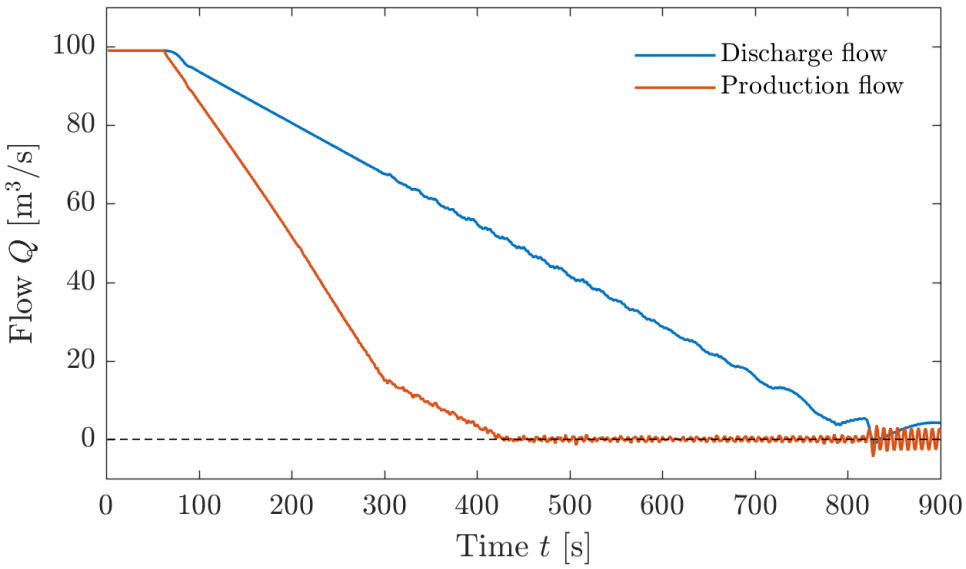

FIGURE 5.29: Almost linear decrease in discharge with a different decrease in production flow.

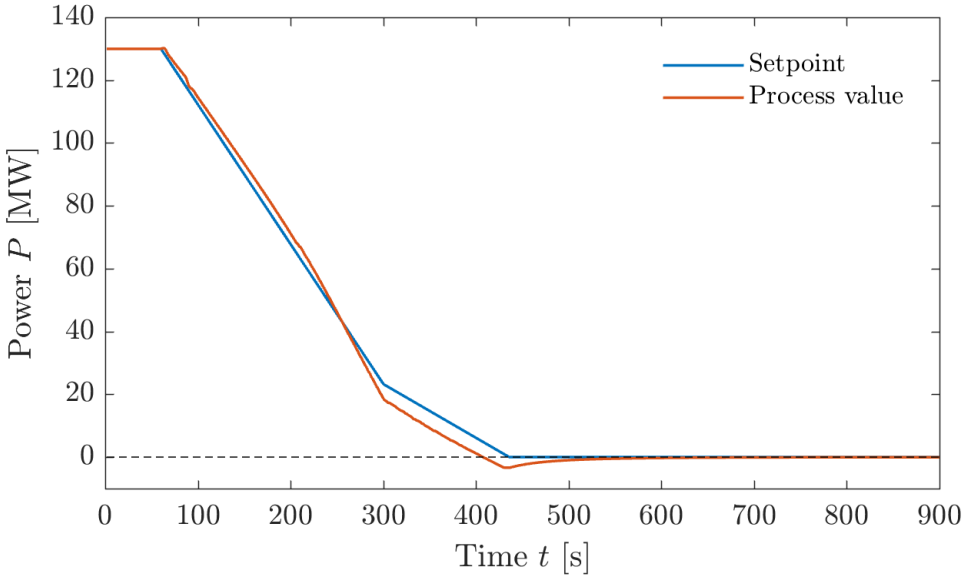

FIGURE 5.30: The power P reduces linearly with two different ramping rates.

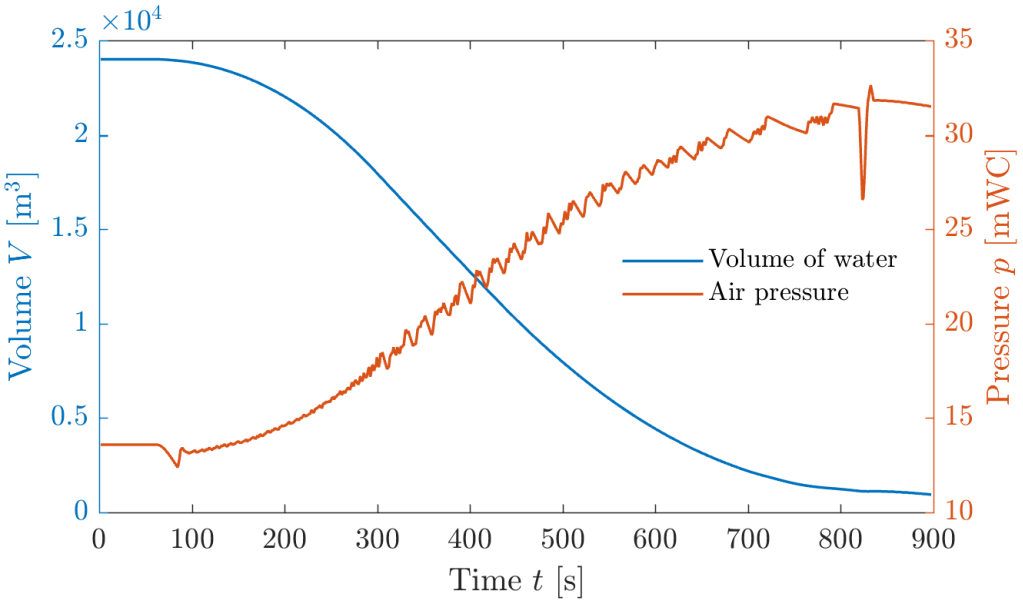

FIGURE 5.31: The water volume decreases as the air pressure increases.

5.6 Shutdown scenario for Case 2

For Case 2, the ACUR LE volume capacity is dimensioned to cover ideal startups and shutdowns, implying that water storage is not a problem for this case. Since the maximum compressor throughput is assumed to be sufficient at all times, the limiting factor in this simulation is the rate of change in air flow through the compressor, given as 25 m^3/s per minute. Therefore, the power can be reduced from 130 MW to 0 MW in just over 3 minutes, as seen in Figure 5.33. The discharge flow to river is reduced from 100 m^3/s to 0 m^3/s in less than 13 minutes, as Figure 5.32 shows. Similarly to the shutdown case in Section 5.5, the efficiency is not plotted for the shutdown scenario with Case 2.

The drop in flow at around 150 s in Figure 5.32 is a result of the drop in power from Figure 5.33 at the same time, due to the complete shutdown of one of the turbines. As the second turbine shuts down completely at 240 s, oscillations occur in the production flow, as well as in the air pressure as seen in Figure 5.34. The oscillations in air pressure diminishes completely as ACUR LE stops regulating at 820 s, while the production flow shows no signs of alteration.

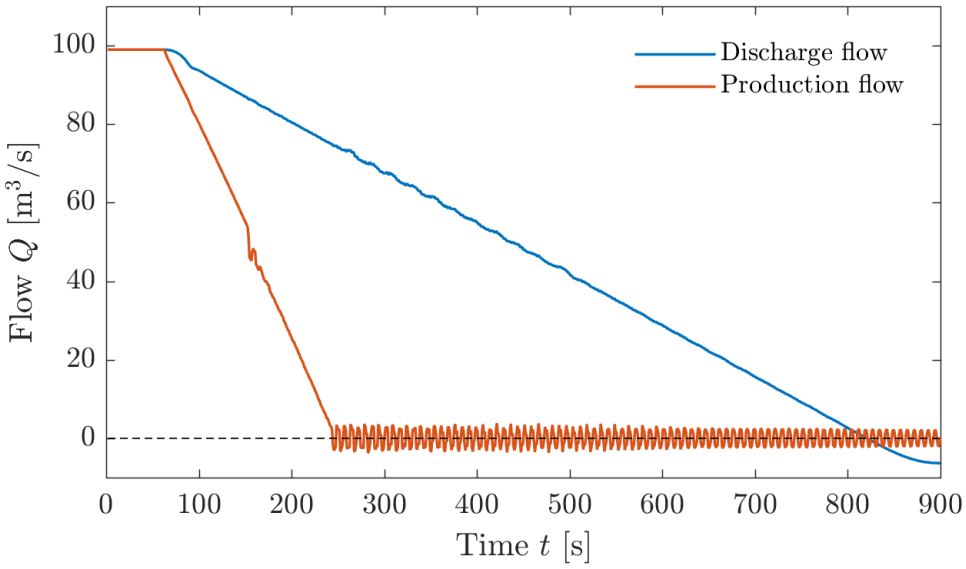

FIGURE 5.32: The production flow reduces quickly while the discharge flow follows the acceptable linear rate of change.

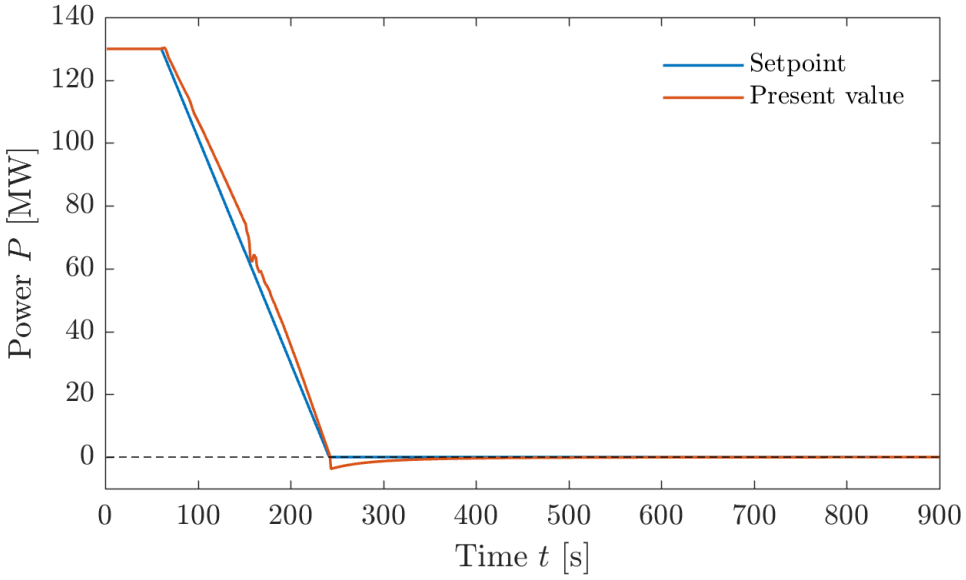

FIGURE 5.33: The power P drops to zero in approximately three minutes.

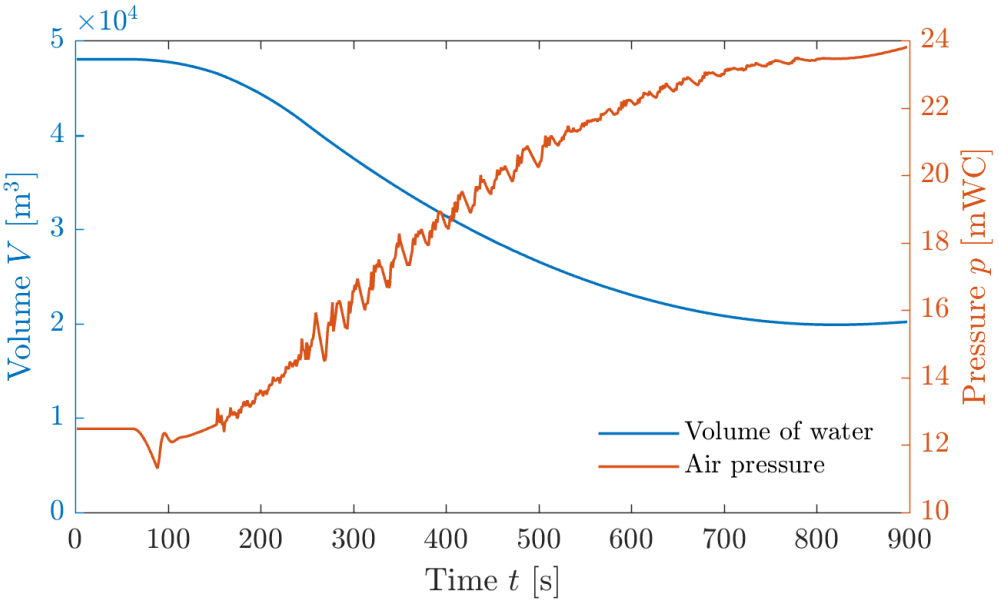

FIGURE 5.34: The air pressure oscillates and increases whereas the water volume decreases.

5.7 Varying power production scenario for Case 2

In this simulation, the energy production is highly variable as in a power balancing scenario. ACUR LE is dimensioned according to Case 2, with the intention of keeping the discharge under control at all times. The power production changes as plotted in Figure 5.36, where the down-ramping function is limited due to the maximum compressor flow increase of 25 m^3/s per minute. However, the same restriction does not apply when the power increases and ACUR LE absorbs water.

This production pattern causes the volume flows to vary as seen in Figure 5.35, where the discharge flow to river changes according to the maximum rate of change from Equation 4.13. After the steep increase in power at 360 s, some pressure fluctuations occur, seen in Figure 5.37. These oscillations increases in amplitude from around 750 s, the moment that the discharge to river becomes equal to the production flow, plotted in Figure 5.35. The same tendency of pressure oscillations is recognized from 1650 s and out, where the two flows become equal once more. This suggests that the PID in ACUR LE struggles to control the discharge flow for small setpoint deviations without creating oscillations.

The ACUR LE water volume covers the difference between production flow and river discharge without any major problems. After 30 minutes, the water level in ACUR LE is higher than it was at the beginning of the simulation, due to the difference in ramping rate for increased and reduced power change. As the power reduction takes more time than the power increase, in general, more water flows into ACUR LE than out. This explains the net volume increase for the water in the chamber, seen in Figure 5.37.

In this simulation, the efficiency stays quite high for both turbines, as seen in Figure 5.38. After 200 s, Turbine 1 shuts down while Turbine 2 keeps running at design condition. From 600 s, the power is reduced by 20 % for both turbines, without any significant efficiency drop. As Turbine 2 shuts down at 840 s, Turbine 1 keeps the power at 80 % with approximately same efficiency. After the second turbine starts up again and both turbines run at design condition, the efficiency oscillates and increases.

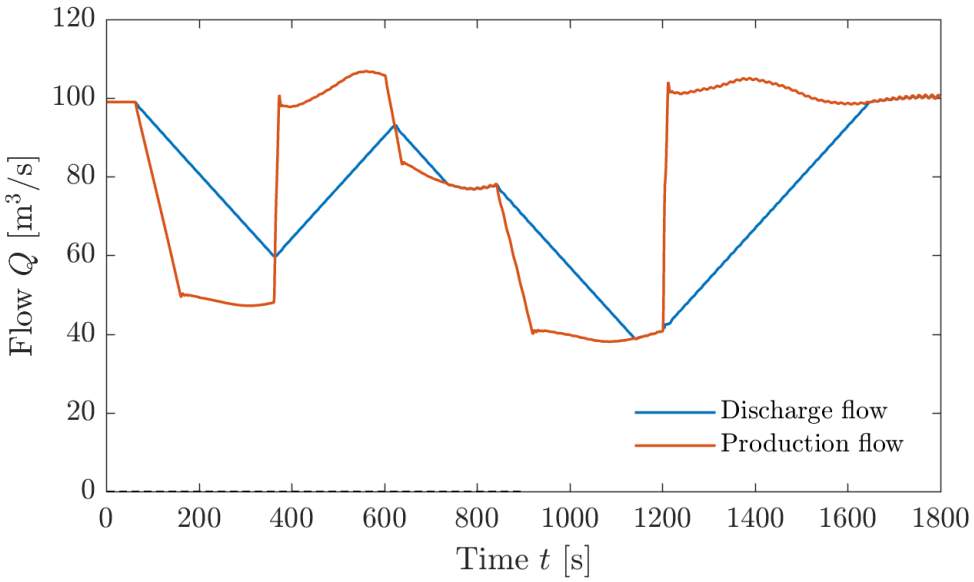

FIGURE 5.35: The production flow varies massively, while the total discharge flow mostly follows linear changes.

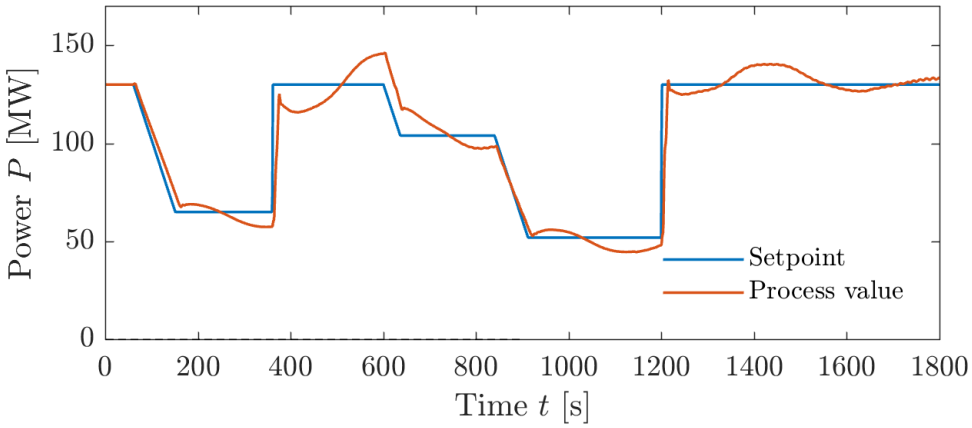

FIGURE 5.36: The power process value oscillates around the different setpoints.

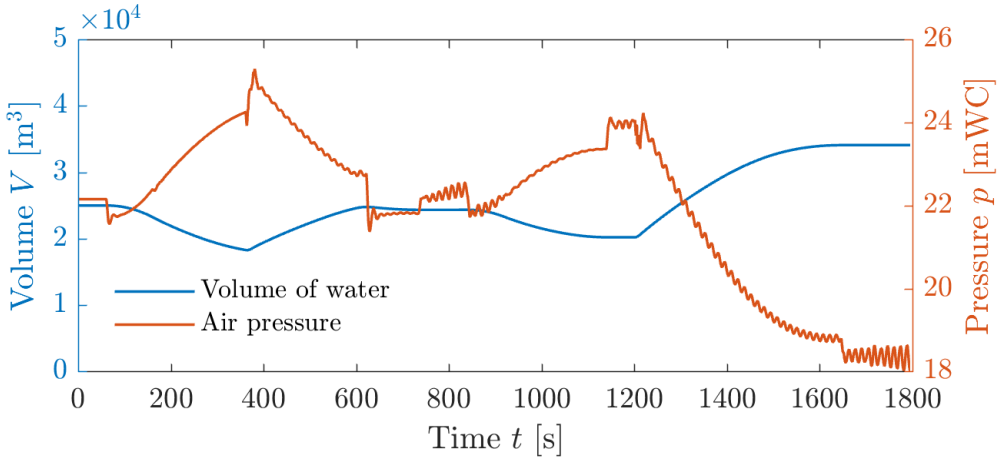

FIGURE 5.37: The air pressure oscillates and changes quickly while the volume of water changes slowly.

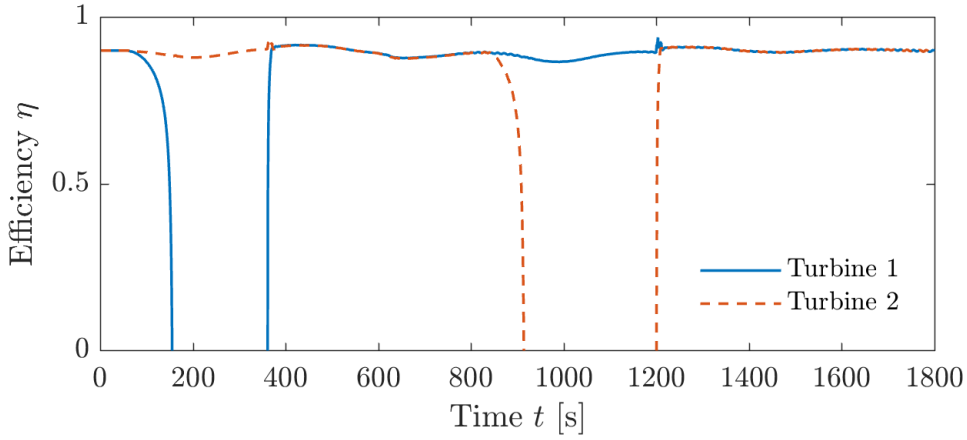

FIGURE 5.38: The efficiency η drops as the turbines shut down.

5.8 Flood simulation scenarios

The flood scenarios cover mitigation and imitation of floods. All simulations are done for Case 2, as described in Section 2.3.2.

5.8.1 Mitigating flood peaks

In this simulation, the Bratsberg model in LVTrans uses the tailrace tunnel setup from Figure 4.4 to investigate flood mitigation. The river flow bypassing the HPP is monitored by ACUR LE, and as the flow increases, ACUR LE begins absorbing water from the tailrace tunnel to counteract the flood peak. The result is a reduction in the total river flow, seen in Figure 5.39. As soon as ACUR LE begins regulating the tailrace water, the flow into the chamber, seen from Figure 5.40, follows the same pattern as the bypass flow. The pressure in ACUR LE oscillates with a high frequency and an increasing amplitude throughout the simulation, until the regulation is turned off after approximately 1400 s, seen in Figure 5.41. These oscillations begin immediately after ACUR LE starts regulating, and the fluctuating behavior does not seem to stop for the flow values in Figure 5.39. A potential reason for this is the flood setup from Figure 4.4, where the bypassing river is represented through pipe and reservoir elements. With two reservoirs connected to the tailrace tunnel, in addition to the free water surface in ACUR LE, oscillations are doomed to happen. In addition, ACUR LE is not able to mitigate the fluctuations between the two reservoirs, enabling the bypass flow to oscillate as seen in Figure 5.39.

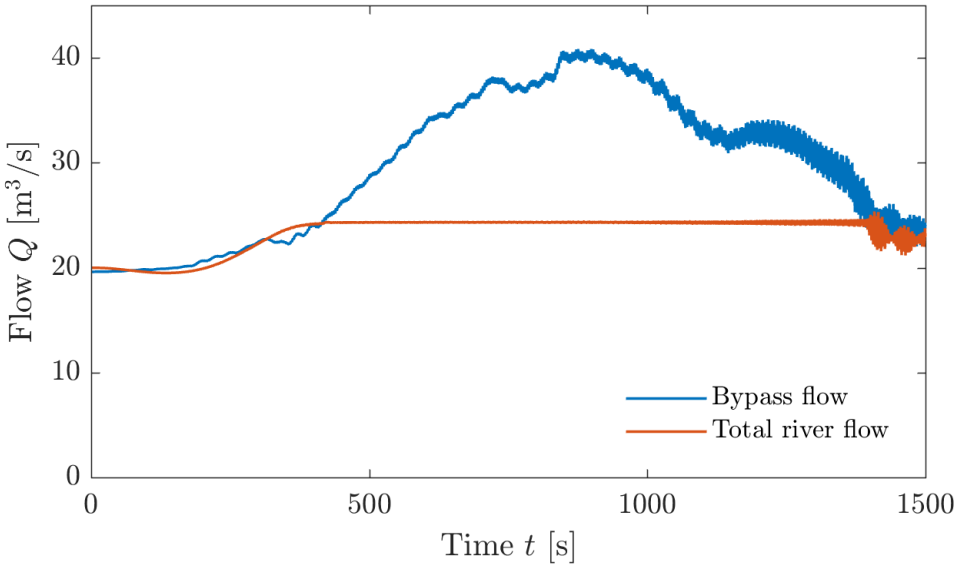

FIGURE 5.39: ACUR LE covers a flood peak by adjusting the total HPP discharge water.

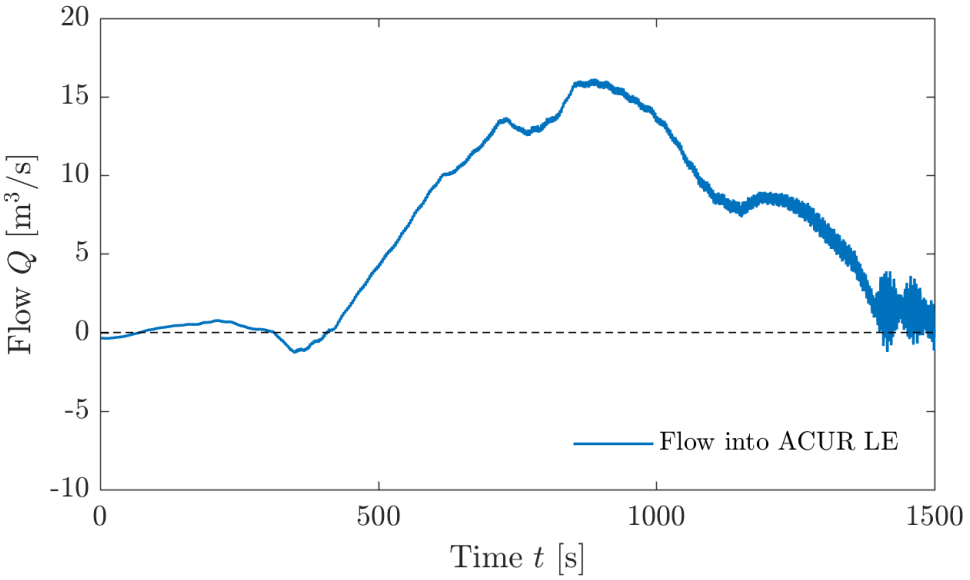

FIGURE 5.40: The net flow into ACUR LE changes during the simulation.

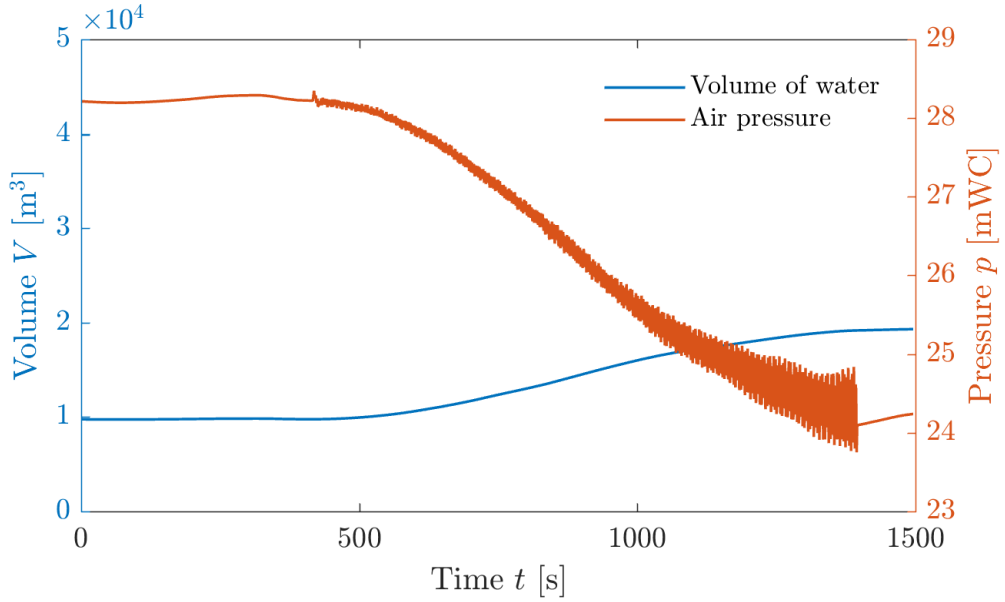

FIGURE 5.41: ACUR LE is filled with water during the flood peak mitigation while the air pressure reduces.

5.8.2 Imitating spring floods

To imitate a flood, the water from ACUR LE is used to increase the total discharge from the HPP while the production stays constant. In this particular simulation, the compressor in ACUR LE is utilized in steps of constant flow increase, giving the total discharge seen in Figure 5.42. The shape of this flow increase could have been different, but the maximum rate of change could not be higher than the compressor is capable of delivering. This operation of ACUR LE reduces the amount of water in the chamber, visualized in Figure 5.43. In the same figure, the pressure is shown to increase in almost linear steps, but with small adjustments as the volume flow increase changes. In this simulation, there are no signs of any significant oscillations. The reason is probably that flow out of the chamber is controlled with a manual approach in the ACUR LE element in LVTrans, without using a setpoint and PID. In addition, the production flow is constant at all times.

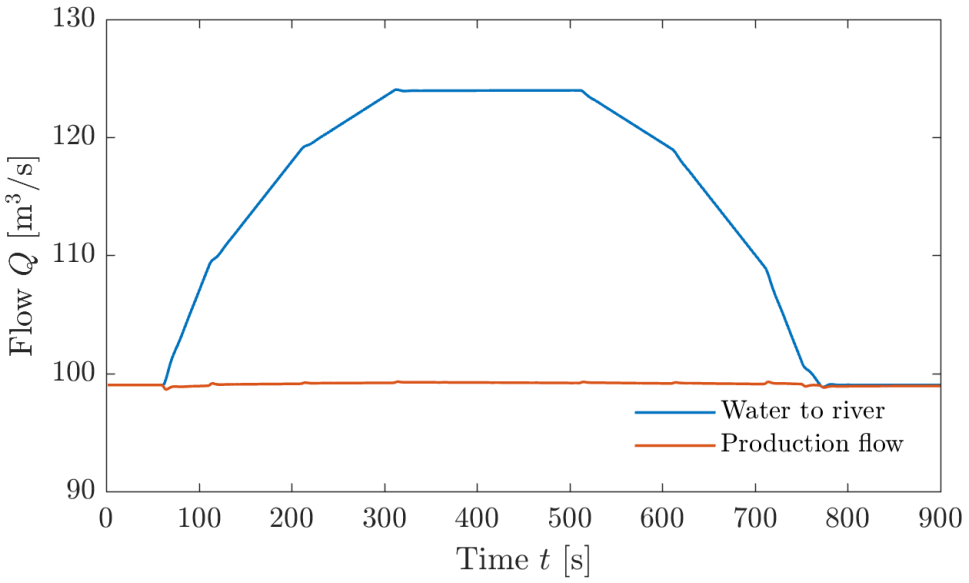

FIGURE 5.42: An artificial flood is created with ACUR LE

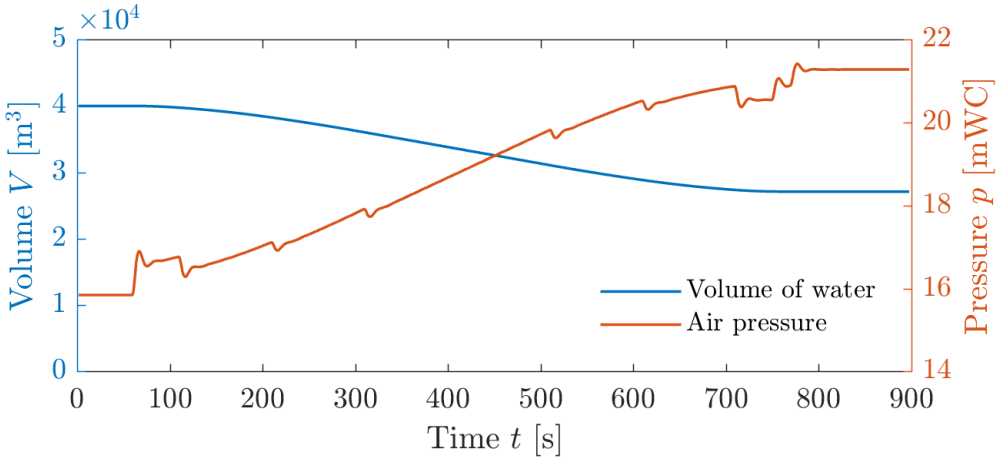

FIGURE 5.43: The volume in ACUR LE decreases while the pressure increases.

5.9 Comparing and discussing the results

The normal startup procedure, described in Section 5.2.1, have been given alternative startup procedures through five simulated scenarios. In all of these simulations, ACUR LE is found to control the total discharge flow successfully, while ensuring that the rate of change stays within the given restriction from Equation 4.13. Regarding the startup scenario for Case 2, ACUR LE provides a surplus of water storage capacity within the chamber. This enables the simulated Bratsberg model to obtain the design values in flow and power within approximately 10 seconds, while the adjacent river experiences a rate of change in flow equivalent to the normal startup at the HPP. The total chamber volume within ACUR LE is for Case 2 about 25 % larger than the volume occupied by water during an ideal startup. This seems to be a suitable dimension with a reasonable safety margin considering the water levels in the chamber. In total, the Case 2 startup scenario represents the most beneficial use of ACUR LE, with the emancipation of hydroelectric production in mind.

In the Case 1 scenario from Section 5.3.1, the power is almost at maximum right from the beginning, until the power production is forced to decrease due to the water storage limitations. From 300 s and out, the setpoint line for power is exactly equal to the setpoint function from the normal Bratsberg HPP startup, seen by comparing Figure 5.10 with Figure 5.2, respectively. However, the actual power for the immediate maximum power scenario is unfortunately much more fluctuating, and causes the production flow to act equivalently. The three-step power scenario from Section 5.3.4 is an alternative usage of ACUR LE with many similarities to the immediate maximum power scenario. These two startup procedures are approximately the same for the first 200 s. As seen from Figure 5.21, the total discharge flow in the three-step scenario follows the rate of change from Equation 4.13 accurately, and is for a period of time surpassing the production flow. Therefore, the realization of this specific scenario is dependent on the compressor being able to deliver the needed flow at the needed time.

The alternative utilization of the ACUR LE volume in the startup procedures is to store water during the last part of the discharge flow increase, as in the simulations described in Section 5.3.2 and 5.3.3. Both startup procedures manage to deliver an even increase in discharge quite successfully, without at any point contributing to an increase in flow in the tailrace tunnel by using the compressor in ACUR LE. Although the two-step production increase scenario from Section 5.3.3 ensures that the turbines run at approximately design condition with high efficiency, the startup from Section 5.3.2 generates a slightly more energy. In this delayed maximum power scenario, there is still a potential for even higher amounts of power, seen by comparing the volume plots for the two scenarios, given in Figure 5.15 and 5.19, respectively.

By evaluating the generated amount of energy during startup as a measure of how efficient the startup procedure is, the Case 2 startup is by far the best, as seen in Table 5.3. The Case 1 startups are all of approximately the same magnitude around 26 MW, significantly higher than for the normal startup at Bratsberg 18.84 MW. The operating procedure from Section 5.3.2 generates more energy than the other startups with Case 1, and bear resemblance to the Case 2 startup regarding in power development. This is seen by comparing Figure 5.14 with 5.26 for Case 1 and 2, respectively.

The shutdown scenarios for Case 1 and 2 are restricted in different ways. For Case 1, the limited water storage volume in ACUR LE prevents a quicker power decrease. In addition, the ACUR LE flow is restricted due to the maximum compressor throughput. Still, the production flow is reduced to zero in approximately half the

TABLE 5.3: Total production for the startup scenarios.

Description:	Production: [MWh]	Section:
Normal startup	18.84	5.2.1
Immediate maximum power	25.77	5.3.1
Delayed maximum power	26.55	5.3.2
Power increase in two-steps	26.45	5.3.3
Power increase in three-steps	26.25	5.3.4
Case 2 startup	32.53	5.4

time compared with the normal Bratsberg HPP shutdown found in Section 5.2.2. In Case 2, maximum rate of change in the compressor is assumed to be 25 m^3/s per minute, and this affects the reduction in power. Nevertheless, the production flow decreases to zero during three minutes, equivalent to one-third of the normal shutdown time at Bratsberg. Undoubtedly, the scenario with Case 2 is favorable in a hydropeaking perspective, but the realization is very much dependent on the abilities of a real-life compressor, unknown to this point. The same goes for the scenario from Section 5.7 with varying power production. The implementation of ACUR LE gives a promising result that illustrates how a power operation resembling hydropeaking is made possible. However, ACUR LE is likely to be be significantly less beneficial given higher compressor restrictions.

In addition to covering startups and shutdowns, the simulations show that ACUR LE is able to mitigate and imitate floods successfully. These scenarios are almost independent of the production flow, with an entirely different purpose than enabling hydropeaking. Still, the startup scenario resembles the flood mitigation as ACUR LE absorbs water from the tailrace tunnel in both cases. In flood imitation, the compressor in ACUR LE is utilized to increase the total discharge flow, much like in shutdown procedures. However, as production flow is kept constant during flood imitation, these scenarios are simpler in operation than shutdowns considering the compressor regulation.

Oscillations arise in all of the simulations, and they often seem to be provoked by large and fast changes in power and production flow. The ACUR LE governor manages to mitigate the fluctuations in some scenarios , especially if the setpoint is given by a function that changes linearly. At times when the previously increasing or decreasing setpoint changes to a constant value, the oscillations often tend to grow in amplitude.

5.9.1 ACUR LE model evaluation

The simulated results are plausible and presumably quite correct based on the intended behavior of ACUR LE, but as they are based on several assumptions and simplifications, the simulations need to be checked against experiments for verification. These assumptions affect the simulations in critical ways, and the reliability of the simulations is dependent on the correctness of the assumptions. For simplicity, all dynamics related to the compressor are in this project neglected, except for some simple restrictions in the delivery of pressurized air. This is a major simplification that embellishes the results.

Further, for simplicity there is assumed no delay or flow increase restrictions regarding removing air from the chamber with the bypass valve. In addition, the air inside ACUR LE is assumed to leave the cavern with a flow as high as 100 m^3/s during a full valve opening. The pressure difference between the air volume in the

ACUR LE and the atmosphere decreases as the chamber fills up with water, but the valve representation does not take this into account. However, ACUR LE is often almost depleted of water in times when the chamber needs to absorb the largest volume flows, while only small flows through the valve is needed in the opposite case. This indicates that the simplification of constant high flow capability does not affect the results severely.

To keep the governor controlling the valve and compressor simple, there has not been assumed any delays as the PID in ACUR LE regulates the mass flow in and out of the chamber. The regulator adjusts the mass flow at each time step $\Delta t = 0.1$ s, enabling ACUR LE to evaluate the needed flow pressure in the chamber precisely. This level of precision could be unlikely in real life, where the regulating abilities are likely to be lower.

The dynamic behavior in the air chamber is described with the polytropic relation between pressure and volume of air. By assuming the temperature to be constant, potentially important effects are ignored. The temperature would likely oscillate and vary in an equivalent way as the pressure did in the simulations, and presumably causing a more unstable system. Still, as these simulations are done at an early stage in the development of the concept idea, the level of accuracy in the described dynamics is assumed to be sufficient. There is already several critical assumptions and uncertainties regarding the compressor and bypass valve, indicating that a more thorough description of the dynamic relations is unnecessary at this point. Besides, the degree of simplification regarding the constant temperature assumption is unknown. The assumption is presumably less severe for ACUR LE than for ACCs in the headrace tunnel, as the pressure differences are lower in the tailrace tunnel.

The simulations are unfortunately unverified by laboratory experiments or real-life events. For this reason, the results should not be considered as anything more than plausible outcomes for the simulated operating procedures at Bratsberg HPP. Still, all the results are regarded as successful and highlight the benefits of implementing ACUR LE in a HPP, making the technical feasibility of ACUR LE look promising. This Master's thesis and the ACUR LE element in LVTrans contributes to the development of ACUR LE. For the intended operation of ACUR LE previously described in Section 2.3, the simulation results are considered to be proof-of-concept. The initialization of active research and development, along with proof-of-concept, defines the third level of the TRLs [11]. For this reason, the maturity in the development of ACUR LE can be described to be at TRL3.

Chapter 6

Conclusion

In this Master's thesis, the benefits of ACUR LE in a hydropower system are highlighted. To meet the future energy demands, HPPs need to evolve and become more flexible in operation. The environmental impacts from hydropower in rivers must be reduced, as the amount of hydropeaking is predicted to increase and large fluctuations affect the river ecosystems.

A numerical model of ACUR LE is developed as an element in LVTrans. The case HPP Bratsberg is modeled in LVTrans with the ACUR LE element implemented, and used to simulate scenarios involving startup, shutdown and flood control. These simulations consider the abilities of ACUR LE to mitigate fluctuations from different operating procedures. With the assumed restrictions related to the compressor and bypass valve, the hydroelectric power operation can be adjusted more freely for startup scenarios compared to shutdown scenarios.

In the startup scenario where ACUR LE is most beneficial, the total discharge flow to river increases linearly over approximately 13 minutes, while the power increases to design operating condition within approximately 10 seconds. Equivalently, the best shutdown scenario reduced the down-ramping time for the power production by two-thirds. Additionally, ACUR LE is found to both mitigate flood peaks and imitate floods successfully.

The simulations are not verified by real-life experiments or events, and the numerical model of ACUR LE contains many assumptions related to the compressor, bypass valve and regulator. These assumptions have simplified the ACUR LE model, but are considered to be reasonable. The simulations performed are a proof-of-concept for ACUR LE, defining the maturity of development to be at TRL3. The outlook for further studies and investigations look promising.

Chapter 7

Further work

While learning more about ACUR LE, several unanswered questions arose on topics beyond the scope of this Master's thesis. This chapter on further work describes the next steps in the development of the ACUR LE, in light of the outcomes from this project.

The compressor dynamics must be investigated in further detail. A cooperation with a compressor manufacturer is likely to be necessary, due to the limited available information in the literature regarding the actual performance of compressors. The compressor to be used in ACUR LE is likely to be specially designed, and the development of a real-size compressor lies many steps ahead. Still, the assumed specifications must be determined at the present stage to create simulations and laboratory experiments based on realistic conditions. Likewise, the valve dynamics should be described, where the first objective must be to find out how the pressure differences affect the flow through the valve. Then the valve dimensions can be determined, as well as the rate of change in volume flow as the valve opening adjusts. From here, a more realistic regulation scenario can be modeled, with a PID governor that takes the compressor and valve limitations into account. In addition, the limitations related to the regulator itself, such as delays, must be considered. It is important to figure out if ACUR LE is still able to mitigate fluctuations and maintain control over the total discharge flow out of the HPP given more realistic conditions for compressor, valve and regulator.

The dynamic behavior as pressurized air enters or leaves the ACUR LE should be described in more detail. A natural next step would be to investigate if the assumption of constant temperature holds, or if the change in temperature must be included in the model. A possibility is to use the MRHT method that describes ACCs, as already mentioned in Chapter 3.4, to include the change of mass in the chamber. The ACUR LE model in LVTrans is fully usable and can easily be modified and used in future simulations. In addition, other simulation tools should be utilizes to simulate ACUR LE in order to supplement and verify the results from the current ACUR LE model in LVTrans. However, to bring the concept idea to the TRL4, laboratory experiments need to be performed [11].

Besides all the technical uncertainties related to the functionality of ACUR LE, the effects of typical hydropeaking operations on adjacent rivers must be studied in more detail. Per now, the main focus for ACUR LE is to mitigate the fluctuations in the river flow to enable varying energy generation. If future research finds the other impacts from hydropeaking to be more important than the rate of change in discharge, the main objective of ACUR LE should be adjusted while the concept solution is re-evaluated. The ability to mitigate flood peaks could be the benefit of ACUR LE that makes the concept idea evolve into a real-life supplement to HPPs. Undoubtedly, this aspect must be thoroughly explored.

Bibliography

[1] W. Lutz, W.P. Butz, and S. K.C. *World Population and Human Capital in the Twenty-first Century: Executive Summary*. Oxford University Press, 2014.

[2] International Energy Agency. World Energy Investment 2018, Executive Summary. Technical report, International Energy Agency, 2018.

[3] UNFCCC: The Paris Agreement. https://unfccc.int/process-and-meetings/the-paris-agreement/the-paris-agreement. Accessed: 17/12/2018.

[4] Renewable Energy Policy Network for the 21st Century. Renewables 2018 Global Status Report. Technical report, Renewable Energy Policy Network for the 21st Century, 2018.

[5] International Energy Agency. Renewable Energy Essentials: Hydropower. Technical report, International Energy Agency, 2010.

[6] International Energy Agency. Status of Power System Transformation 2018. Technical report, International Energy Agency, 2018.

[7] International Energy Agency. Technology Roadmap - Hydropower. Technical report, International Energy Agency, 2012.

[8] Pål-Tore Storli. A novel concept of increasing the flexibility at power plants with outlet to river. *HYDRO 2016, International Conference and Exhibition*, 2016.

[9] HydroFlex. https://www.h2020hydroflex.eu/. Accessed: 01/12/2018.

[10] Horizon 2020 - European Commission. https://ec.europa.eu/programmes/horizon2020/en/. Accessed: 01/12/2018.

[11] ESA. Technology Readiness Levels Handbook for Space Applications. Technical report, ESA, 2008.

[12] J. David. Allan and Maria M. Castillo. *Stream ecology: structure and function of running waters*. Springer, 2007.

[13] Sandra L Postel, Gretchen C Daily, and Paul R Ehrlich. Human Appropriation of Renewable Fresh Water. *Science, New Series*, 271(5250):785–788, 1996.

[14] Electric Power Research Institute. Electric Energy Storage Technology Options. Technical report, Electric Power Research Institute, 2010.

[15] World Energy Council. World Energy Resources Hydropower 2016. Technical report, World Energy Council, 2016.

[16] Georg Premstaller, Valentina Cavedon, Giuseppe Roberto Pisaturo, Steffen Schweizer, Vito Adami, and Maurizio Righetti. Hydropeaking mitigation project on a multi-purpose hydro-scheme on Valsura River in South Tyrol/Italy. *Science of The Total Environment*, 574:642–653, 1 2017.

[17] Andreas Bruder, Diego Tonolla, Steffen P. Schweizer, Stefan Vollenweider, Simone D. Langhans, and Alfred Wüest. A conceptual framework for hydropeaking mitigation. *Science of The Total Environment*, 568:1204–1212, 10 2016.

[18] Otto Moog. Quantification of daily peak hydropower effects on aquatic fauna and management to minimize environmental impacts. *Regulated Rivers: Research & Management*, 8(1-2):5–14, 5 1993.

[19] Julie Charmasson and Peggy Zinke. Mitigation Measures Against Hydropeaking Effects. Technical report, SINTEF, 2011.

[20] N. LeRoy Poff, J. David Allan, Mark B. Bain, James R. Karr, Karen L. Prestegaard, Brian D. Richter, Richard E. Sparks, and Julie C. Stromberg. The Natural Flow Regime. *BioScience*, 47(11):769–784, 12 1997.

[21] M. S. Bevelhimer, R. A. McManamay, and B. O'Connor. Characterizing Sub-Daily Flow Regimes: Implications of Hydrologic Resolution on Ecohydrology Studies. *River Research and Applications*, 31(7):867–879, 9 2015.

[22] Jessica D. Lundquist, Daniel R. Cayan, Jessica D. Lundquist, and Daniel R. Cayan. Seasonal and Spatial Patterns in Diurnal Cycles in Streamflow in the Western United States. *Journal of Hydrometeorology*, 3(5):591–603, 10 2002.

[23] Julie K. H. Zimmerman, Benjamin H. Letcher, Keith H. Nislow, Kimberly A. Lutz, and Francis J. Magilligan. Determining the effects of dams on subdaily variation in river flows at a whole-basin scale. *River Research and Applications*, 26(10):1246–1260, 12 2010.

[24] N. E. Jones. The dual nature of hydropeaking rivers: is ecopeaking possible? *River Research and Applications*, 30(4):521–526, 5 2014.

[25] Marc Pellaud. *Ecological response of a multi-purpose river development project using macro-invertebrates richness and fish habitat value*. PhD thesis, Université de Genève, 2007.

[26] S. Valentin, F. Lauters, C. Sabaton, P. Breil, and Y. Souchon. Modelling temporal variations of physical habitat for brown trout (Salmo trutta) in hydropeaking conditions. *Regulated Rivers: Research & Management*, 12(2-3):317–330, 3 1996.

[27] Tor Haakon Bakken, Torbjørn Forseth, and Atle Harby, editors. *Miljøvirkninger av effektkjøring: Kunnskapsstatus og råd til forvaltning og industri*. Norsk institutt for naturforskning, 6 2016.

[28] S.J. Saltveit, J.H. Halleraker, J.V. Arnekleiv, and A. Harby. Field experiments on stranding in juvenile atlantic salmon (Salmo salar) and brown trout (Salmo trutta) during rapid flow decreases caused by hydropeaking. *Regulated Rivers: Research & Management*, 17(4-5):609–622, 7 2001.

[29] Svein Jakob Saltveit, editor. *Økologiske forhold i vassdrag - konsekvenser av vannføringsendringer*. Norges vassdrags- og energidirektorat, 2006.

[30] T. Meile, J.-L. Boillat, and A. J. Schleiss. Hydropeaking indicators for characterization of the Upper-Rhone River in Switzerland. *Aquatic Sciences*, 73(1):171–182, 2 2011.

[31] Bjørn Ove Johnsen, Jo Vegar Arnekleiv, Lars Asplin, Bjørn T Barlaup, Tor F Naesje, Bjørn Olav Rosseland, and Svein Jakob Saltveit. *Effekter av vassdragsregulering på villaks*. Kunnskapssenter for Laks og Vannmiljø, 2010.

[32] J. H. Halleraker, S. J. Saltveit, A. Harby, J. V. Arnekleiv, H.-P. Fjeldstad, and B. Kohler. Factors influencing stranding of wild juvenile brown trout (Salmo trutta) during rapid and frequent flow decreases in an artificial stream. *River Research and Applications*, 19(5-6):589–603, 9 2003.

[33] NVE: Hydropower potential. https://www.nve.no/energiforsyning-og-konsesjon/vannkraft/vannkraftpotensialet/. Accessed: 17/12/2018.

[34] J.H. L'Abée-Lund and J. Otero. Hydropeaking in small hydropower in Norway-Compliance with license conditions? *River Research and Applications*, 34(4):372–381, 5 2018.

[35] L. Lia, T. Jensen, K.E. Stensby, G. Holm Midttømme, and A.M. Ruud. The current status of hydropower development and dam construction in Norway. *Hydropower & Dams*, 1(3), 2015.

[36] Jessie Cherry, Heidi Cullen, Martin Visbeck, Arthur Small, and Cintia Uvo. Impacts of the North Atlantic Oscillation on Scandinavian Hydropower Production and Energy Markets. *Water Resources Management*, 19(6):673–691, 12 2005.

[37] Maria Catrinu and Jørgen Kjetil Knudsen. Perspectives on hydropower's role to balance non-regulated renewable power production in Northern Europe. Technical report, CEDREN, 2011.

[38] Kjell Erik Stensby. Potential for large scale exchang. *Exchange of balancing services between the Nordic and the Central European synchronous systems, International workshop*, 2011.

[39] Statkraft: The glaciers' inner energy. https://www.statkraft.com/energy-sources/hydropower/the-glaciers-inner-energy/. Accessed: 04/12/2018.

[40] Eivind Solvang, Atle Harby, and Ånund Killingtveit. Økt balansekraftpotensial i norske vannkraftverk. Technical report, SINTEF Energi AS, 2011.

[41] Tor Haakon Bakken, Peggy Zinke, Andreas Melcher, Håkon Sundt, Teppo Vehanen, Klaus Jorde, and Mike Acreman. Setting environmental flows in regulated rivers. Technical report, SINTEF, 2012.

[42] CEDREN. https://www.cedren.no/english/Home. Accessed: 17/12/2018.

[43] Håvard Hamnaberg. Pumpekraft i Noreg. Technical report, The Norwegian Water Resources and Energy Directorate, 2011.

[44] NVE: Hydropower database. https://www.nve.no/energiforsyning-og-konsesjon/vannkraft/vannkraftdatabase/. Accessed: 18/12/2018.

[45] Store norske leksikon: Neavassdraget. https://snl.no/Neavassdraget. Accessed: 14/08/2018.

[46] NVE: Nea hydropower plant. https://www.nve.no/vann-vassdrag-og-miljo/nves-utvalgte-kulturminner/kraftverk/nea/. Accessed: 27/08/2018.

[47] Jo Vegar Arnekleiv, Jan Ivar Koksvik, and Eilif Brodtkorb. Fiskebestandene i Nidelva ovenfor lakseførende del, 1984-1995. Technical report, NTNU Vitenskapsmuseet, 1997.

[48] Jo Vegar Arnekleiv, Jan Iver Koksvik, Nils Arne Hvidsten, and Arne J. Jensen. Virkningene av Bratsbergreguleringen (Bratsberg kraftverk) på bunndyr og fisk i Nidelva, Trondheim (1982-1986). Technical report, NTNU Vitenskapsmuseet, 1994.

[49] Odd Guttormsen. *Vassdragsteknikk II*. Akademika, 2016.

[50] Torbjørn Nielsen. Dynamisk dimensjonering av vannkraftverk. Technical report, NTNU Vannkraftlaboratoriet, 1990.

[51] Torunn Engen Røse. Svingekammer eller luftputekammere i vannkraftverk. Master's thesis, NTNU, 2015.

[52] Ann Kristin Tuseth. Numerisk modellering av luftputekammer. Master's thesis, NTNU, 2013.

[53] E. Benjamin Wylie, Victor L. Streeter, and Lisheng Suo. *Fluid Transients in Systems*. Prentice-Hall, 1993.

[54] Ling Zhou, Deyou Liu, and Bryan Karney. Investigation of Hydraulic Transients of Two Entrapped Air Pockets in a Water Pipeline. *Journal of Hydraulic Engineering*, 2013.

[55] Kaspar Vatland Vereide. *Hydraulics and Thermodynamics of Closed Surge Tanks for Hydropower Plants*. PhD thesis, NTNU, 2016.

[56] H.R. Graze. A Rational Thermodynamic Equation for Air Chamber Design. In *A Rational Thermodynamic Equation for Air Chamber Design*. Conferance on Hydraulics and Fluid Mechanics, 1968.

[57] Kaspar Vereide, Torbjørn Tekle, and Torbjørn Kristian Nielsen. Thermodynamic Behavior and Heat Transfer in Closed Surge Tanks for Hydropower Plants. *Journal of Hydraulic Engineering*, 2015.

[58] Frank P. Incropera and David P. DeWitt. *Fundamentals of Heat and Mass Transfer*. John Wiley & Sons, Inc., 5th edition, 2002.

[59] Gregory K. McMillan. *Centrifugal and axial compressor control*. Momentum Press, 2010.

[60] Heinz P. Bloch. *A Practical Guide to Compressor Technology*. John Wiley & Sons, Inc., Hoboken, NJ, USA, 2nd edition, 2006.

[61] Nve: Bratsberg. https://www.nve.no/energiforsyning-og-konsesjon/vannkraft/vannkraftdatabase/vannkraftverk/?id=38. Accessed: 27/08/2018.

[62] Statkraft: Bratsberg hydropower plant. https://www.statkraft.no/Energikilder/vaare-kraftverk/norge/Bratsberg/. Accessed: 27/08/2018.

[63] LabVIEW - National Instruments. http://www.ni.com/en-no/shop/labview.html. Accessed: 01/09/2018.

[64] Michael J. Moran and Howard N. Shapiro. *Fundamentals of Engineering Thermodynamics*. John Wiley & Sons, 6th edition, 2010.

[65] General Electric Company. Fast, Flexible Power - Aeroderivative Product and Service Solutions. Technical report, General Electric Company, 2013.

[66] Paul C. Hanlon. *Compressor handbook*. McGraw-Hill, 2001.

Appendix A

Derivation of the Method of Characteristics

The method can be derived by using the full 3D Navier-Stokes equation in cylindrical coordinates, and the following theory is provided from *Fluid Transients in Systems* by Wylie and Streeter [53].

To begin with, the equations for motion and continuity are considered:

$$L_1 = g\frac{dH}{dx} + \frac{dV}{dt} + \frac{f}{2D}V|V| = 0 \tag{A.1}$$

$$L_2 = \frac{dH}{dt} + \frac{a^2}{g}\frac{dV}{dx} = 0 \tag{A.2}$$

Then, these to equations are combined linearly and reorganized by the use of an unknown multiplier λ:

$$\begin{aligned} L &= L_1 + \lambda L_2 \\ &= \lambda\left[\frac{dH}{dx}\frac{g}{\lambda} + \frac{dH}{dt}\right] + \left[\frac{dV}{dx}\lambda\frac{a^2}{g} + \frac{dV}{dt}\right] + \frac{fV|V1|}{2D} = 0 \end{aligned} \tag{A.3}$$

Further, from calculus:

$$\frac{dH}{dt} = \frac{dH}{dx}\frac{dx}{dt} + \frac{dH}{dt} \tag{A.4}$$

$$\frac{dV}{dt} = \frac{dV}{dx}\frac{dx}{dt} + \frac{dV}{dt} \tag{A.5}$$

By examining Equation A.3 and the two above, it can be noted that:

$$\frac{dx}{dt} = \frac{g}{\lambda} = \frac{\lambda a^2}{g} \tag{A.6}$$

Now, Equation A.3 becomes an ordinary differential equation:

$$\lambda\frac{dH}{dt} + \frac{dV}{dt} + \frac{fV|V|}{2D} = 0 \tag{A.7}$$

The solution to the ODE is as follows:

$$\lambda = \pm\frac{g}{a} \tag{A.8}$$

By combining this solution with Equation A.6, the following relation appears:

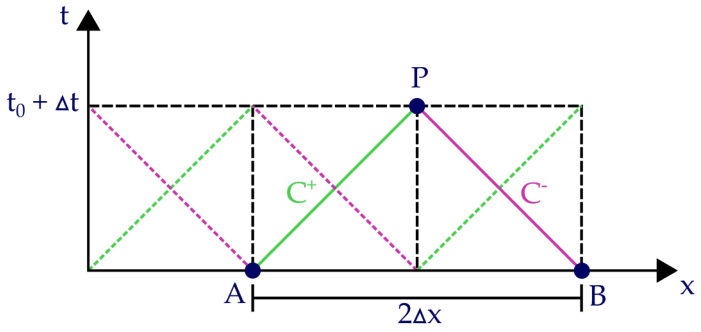

FIGURE A.1: Visualization of the valid regions for the compatibility equations along the characteristic lines.

$$\frac{dx}{dt} = \pm a \tag{A.9}$$

Equation A.8 and Equation A.7 are combined and gives the following two pairs of equations:
First, for C^+:

$$\frac{g}{a}\frac{dH}{dt} + \frac{dV}{dt} + \frac{fV|V|}{2D} = 0 \tag{A.10}$$

$$\frac{dx}{dt} = +a \tag{A.11}$$

Second, for C^-:

$$-\frac{g}{a}\frac{dH}{dt} + \frac{dV}{dt} + \frac{fV|V|}{2D} = 0 \tag{A.12}$$

$$\frac{dx}{dt} = -a \tag{A.13}$$

To visualize the solution of the characteristics method, one can plot the Equation A.11 and A.13 as shown in Figure A.1. The wave velocity a is assumed constant for a given pipe, meaning that the lines in the figure become straight in the xt plane as $dx/dt = constant$. Along these "characteristic" lines, Equation A.11 and A.13, known as the compatibility equations, are valid. This is with the assumption of constant wave velocity a for a given pipe. For this method to work, every pipeline has to be divided into an even number of reaches, N, with the same length Δx. The time step constant is then calculated as $\Delta t = \Delta x/a$.

The next step is to integrate the compatibility equations. If one were to know the values of V and H at point A, seen in Figure A.1, the integrated version of Equation A.10 could be written in terms of the unknown variables V and P at point P. In the same way, would the integrated version of Equation A.12 be written in terms of the same variables, if V and H are known at point B. Thus, we have to equations for two unknown variables.

In this way, the values for H and V are found at point P for time $t = \delta t$. Now, the same method can be used once more to determine the values for the next time step. By alternating the values between two sets of grid intersection points, the dynamics in the pipe are calculated until the desired time duration is covered.

By writing Equation A.10 and A.12 in terms of discharge (in place of velocity), multiplying with $adt/g = dx/g$ and solving for H_P, we obtain:
For C^+:

$$H_P = H_A - B(Q_P - Q_A) - RQ_P|Q_A| \tag{A.14}$$

For C^-:

$$H_P = H_B + B(Q_P - Q_B) + RQ_P|Q_B| \tag{A.15}$$

where B is the pipeline characteristics impedance, defined as

$$B = \frac{a}{gA} \tag{A.16}$$

and R is the pipeline resistance coefficient, defined as

$$R = \frac{f\Delta x}{2gDA^2} \tag{A.17}$$

Equation A.14 and A.15 can be written in a more general an simple form, where
C^+:

$$H_i = C_P - B_P Q_i \tag{A.18}$$

C^-:

$$H_i = C_M + B_M Q_i \tag{A.19}$$

Here, the coefficients C_P, B_P, C_M and B_M are known constant at the point of calculation. They are defined as:

$$C_P = H_{i-1} + BQ_{i-1} \tag{A.20}$$

$$B_P = B + R|Q_{i-1}| \tag{A.21}$$

$$C_M = H_{i+1} + BQ_{i+1} \tag{A.22}$$

$$B_M = B + R|Q_{i+1}| \tag{A.23}$$

After the initial condition, the endpoints of the system are introduced every other time step. Boundary conditions are therefore necessary. As only one of the compatibility equations is available at the single end of a pipe, an auxiliary equation is needed that specifies Q_P, H_P, or a relation between them.

Appendix B

The ACUR LE element controller

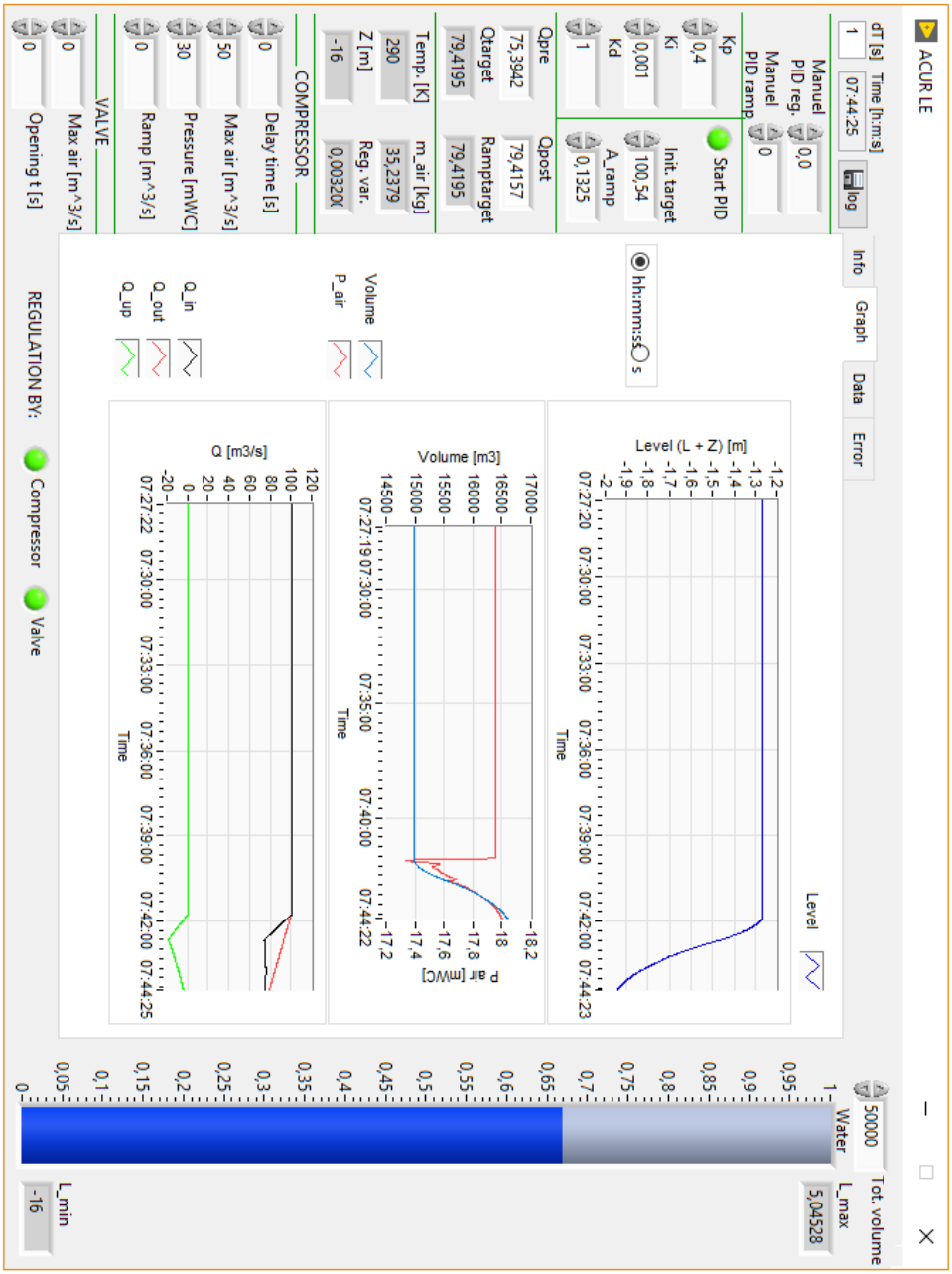

FIGURE B.1: Screen-shot of the ACUR LE element controller in LVTrans during a simulation.

Appendix C

LVTrans code for ACUR LE

```
float64 Ba, Ca, Sb, Sc, dFa, Fa, dQ, Ha, Cv, Q, L, dL;
float64 Hb, dHa, dHb, K, C2, dV, L01, L001, dP1, dP2;
float64 g = 9.81;
float64 Patm = 10.30;
float64 eps1 = 0.00000000000001;
float64 eps2 = 0.00000000000001;
int32 N = 0;

Sc = Cp1/Bp1 + Cm2/Bm2;
Sb = 1.0/Bp1 + 1.0/Bm2;
Ca = Sc/Sb;
Ba = 1.0/Sb;

L01 = L0-Z0;
L001 = L00-Z0;
L = 2.0*L01-L001;

float64 m, R, CAspec, v, CA, dm, reg, mMAX, Qold, PkPa, mkPa;
float64 error, derE;

R = 8314/28.97;


// VALUES WITH PRESSURE IN [kPa]
PkPa = P0*g;
mkPa = PkPa*V0/(R*T0);
if((Reg == 0)&&(now == 0)&&(m_old_in > 0)) mkPa = m_old_in*g;


// MASS AND SPECIFIC VOLUME WITH PRESSURE IN [mWC]
// (FOR SIMPLICITY)
m = mkPa/g;
v = V0/m;
CAspec = P0*v**(C);


// EQUATIONS DESCRIBING THE COMPRESSOR
mMAX = airpressure*maxairflow/(R*T0);
```

```
if(now == 0) Target = inputTarget;
if(now == 0) t_air2 = 0;
if((now == 1) && (t_air1 < airtime)) t_air2 = t_air1 + dt;
if((now == 1) && (t_air1 < airtime)) now = 0;

if((now > 0) && (pTarg > Qpre)) Target = pTarg - Slope*dt;
if((now > 0) && (pTarg < Qpre)) Target = pTarg + Slope*dt;

if((now > 0) && (Slope2 != 0)) Target = pTarg + Slope2*dt;

if((now == 0) && (inputTarget > 0)) rTarg2 = Qpre;
if((now > 0) && (rTarg < Target)) rTarg2 = rTarg + Ramp*dt;
if((now > 0) && (rTarg > Target)) rTarg2 = rTarg - Ramp*dt;
if((Ramp == 0)) rTarg2 = Target;


// EQUATIONS DESCRIBING THE VALVE
if(compGo == 0) mMAX = P0*valveair/(R*T0);


// EQUATIONS DESCRIBING THE REGULATOR
error = Target - Qpost;
if(compGo == 1) error = rTarg2 - Qpost;
if(now > 0) intE2 = intE + error*dt; else intE2 = 0;
derE = (error - pError)/dt;

if(now > 0) Reg = Kp*error + Ki*intE2 + Kd*derE;

Reg = Reg*V0/(totVolume/2);


// CALCULATING LIMITS FOR WATER REGULATION
if((V < 1000) && (Reg < 0)) Reg = 0;
if((V > (totVolume-1000)) && (Reg > 0)) Reg = 0;
if((V0 < 1000) && (Reg < 0)) Reg = 0;


// CALCULATING WATER TANK VISUALIZATION
L_max = L0 + V0/A;
L_min = L0 - (totVolume-V0)/A;
Water = (L - (L_min - Z0))/(L_max - L_min);


RegOut = Reg;

// COMPRESSOR/REGULATOR LIMITS
if(Reg > 1) Reg = 1;
if(Reg < (-1) ) Reg = -1;
if((compGo == 0) && (Qpost < Target)) Reg = 0;
if((valveGo == 0) && (Qpost > rTarg2)) Reg = 0;
```

```
dm = mMAX*Reg;
CA = CAspec*(m + dm)**(C);
P0 = CA/(V0**(C));;

m_old_out = m + dm;


do {
    V = V0-(L-L01)*A;
    Q = 2*(V0-V)/dt - Q0;
    if(Q >= 0.0) Cv = Cvp; else Cv = Cvm;

    dP1 = CA*(V**(-C) - V0**(-C));

    Hb = L+Z0 + P0 + dP1 - Patm
          + f4*Lt*Q*abs(Q)/(At*At*Dt*2*g)
          + Lt*(Q-Q0)/(At*g*dt);
    Ha = Hb + Q*abs(Q)*0.5/Cv;
    Fa = Ha - Ca + Ba*Q;

    dQ = 2.0*A/dt;
    dV = -1.0*A;

    dP2 = A*C*CA*V**(-C-1);

    dHb = 1 + dP2 + f4*Lt*abs(Q)*dQ/(At*At*Dt*g)
                + Lt*dQ/(At*g*dt);
    dHa = dHb + abs(Q)*dQ/Cv;
    dFa = dHa + Ba*dQ;

    dL = -Fa/dFa;
    L = L + dL;
    N++;}

while (abs(dL) > eps2 && N < 100);

V = V0 - (L-L01)*A;
Q = 2*(V0-V)/dt-Q0;

dP1 = CA*(V**(-C) - V0**(-C));

P = P0+dP1;
// T = P*V/(R*(m+dm));
T = T0;

//  VARIABLES TO SIMUALTION WINDOW
pTarg2 = Target;
pError2 = error;
Liq_kote = L+Z0;
```

```
if (Q >= 0.0) Cv = Cvp; else Cv = Cvm;
Hb = L+Z0 + P - Patm + f4*Lt*Q*abs(Q)/(At*At*Dt*2*g)
          + Lt*(Q-Q0)/(At*g*dt);
Ha = Hb+Q*abs(Q)*0.5/Cv;

HPin = Ha;
HPup = Ha;
HPout = Ha;
QPin =  (Cp1 - Ha)/Bp1;
QPout = (-Cm2 + Ha)/Bm2;
QPup = Q;
```

Appendix D

MATLAB script for initial conditions in ACUR LE

```
clear all
close all
clc

% SCRIPT FOR CALCULATING INITIAL VALUES IN LVTRANS
   SIMULATION


%% Values and dimensions desired

% CASE 1
% V_tot = 25000;          % [m^3] total volume (air + water)
% D = 40;                 % [m] equivalent diameter in ACC

% CASE 2
V_tot = 50000;            % [m^3] total volume (air + water)
D = 55;                   % [m] equivalent diameter in ACC

H_river = 6;              % [mWc] river head
Water_in_ACC = 0.96;      % [%] amount of water in ACUR
Z = -16;                  % [m] elevation above datum
T = 290;                  % [K] temperature in water/air/rock

% Tunnel details (between river and ACUR):

f = 0.01;                 % [-] friction factor
L_tun = 2100;             % [m] tailrace tunnel length
D_tun = 8.74;             % [m^2] tailrace tunnel area
c = 1.6668;               % [m/s] speed of water (eq. Q/A)

%% Calculations

g = 9.81;                 % [m/s^2] grav. acc.
H_bar = 101.325/9.81;     % [mWc] barometic pressure head
R = 8314/28.97;           % [J/kg*K] spec. gas const. for air
A = pi*D^2/4;             % [m^2] area in ACC
```

```
L = Water_in_ACC*V_tot/A;           % [m] water level
V_w = L*A;                % [m^3] volume of water
V_A = V_tot - V_w;        % [m^3] volume of air
friction = f*L_tun*c^2/(D_tun*2*g); % [mWc] friction loss
HGL = H_river + friction;           % [mWc] Total HGL
H_A = HGL - (Z + L) + H_bar;        % [mWc] pressure head
Liq_kote = L + Z;         % [m] water level in ACC
h = V_tot/A;              % [m] height of ACC
h_d = (h + Z) - HGL;      % [m] difference, ACC ceil. and HGL

%% Input values to LVTrans

disp('Values into ACC in LVTrans:')
disp( '----------------------------' )
disp(['P_init:           ', num2str(H_A)])
disp(['D:                ', num2str(D)])
disp(['Liq_kote_init:    ', num2str(Liq_kote)])
disp(['V_init:           ', num2str(V_A)])
disp(['Tinit:            ', num2str(T)])
disp( '----------------------------' )
disp(' ')

%% Some comments to the chosen values

disp(['Elevation above datum, Z = ', num2str(Z), ' m.'])
disp(['Total height of ACC, h = ', num2str(h), ' m.'])
disp(['Hydraulic grade line, HGL = ', num2str(HGL), ' m.'])
disp(' ')

if((h + Z) > HGL)
    disp(['ACC ceiling is ', num2str(h_d), ' m above HGL.'
       ])
    disp(['Consider a smaller volume or a larger diameter.'
       ])
end
if((h + Z) < HGL)
    h_d = -h_d;
    disp(['ACC ceiling is ', num2str(h_d), ' m below HGL.'
       ])
    disp('(Consider a larger volume or a smaller diameter.)
       ')
end
```

Appendix E

Limits for minimum water volume in ACUR LE

A sequence of different scenarios for the Case 1 volume, plotted in Figure E.1, is simulated to investigate the total downswing during different water volumes. For the case with an initial water volume of 1000 m^3 and production flow of 30 m^3/s, the chamber would be completely depleted of water during the shutdown. Further, the simulations show that the critical amount of water in the chamber during a full shutdown from the maximum flow is only 4000 m^3.

From these results, the minimum volume limit to prevent a downswing can be estimated, as seen in Figure E.2. The water volume of ACUR LE should for the given volume flow be above the line to prevent a down surge to the bottom of the chamber. The linear regression line is estimated from the volume flows at each 1000 m^3 of ACUR LE that were closest to hitting the zero line, as according to Figure E.1. This equals 30 m^3/s for 1000 m^3, 50 m^3/s for 2000 m^3 and 80 m^3/s for 3000 m^3.

In addition, Figure E.2 contains the calculated minimum water volumes per flow with Equation 3.6. To estimate the equivalent area, Equation 3.7 & 3.8 are used for Estimated limit 1 and 2 from the figure, respectively. While the first estimated limit calculates volumes twice the size compared with the approximated regression line, the second estimated limit corresponds quite accurate.

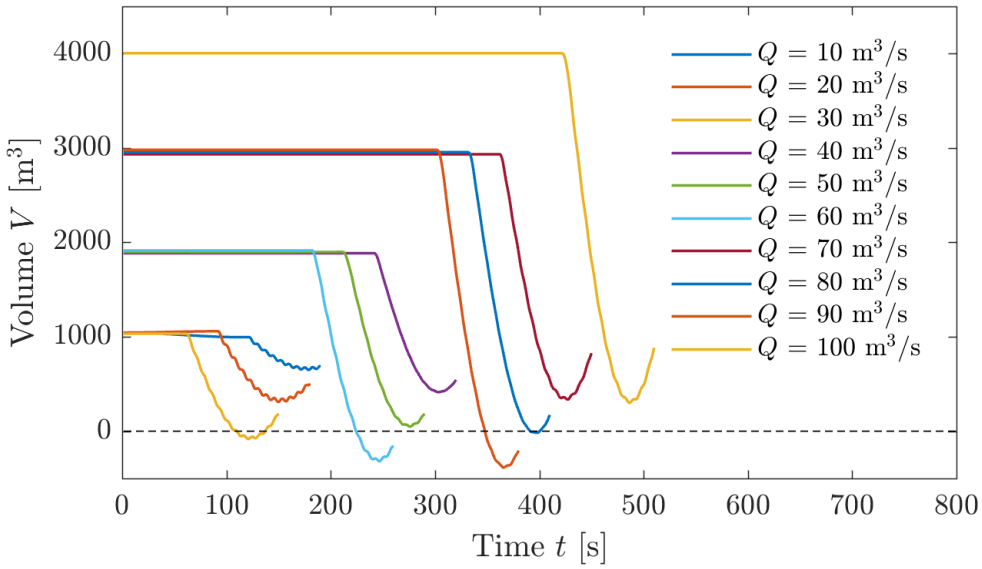

FIGURE E.1: The first downswing of the oscillations that occur during full shutdown for different ACUR LE water volumes.

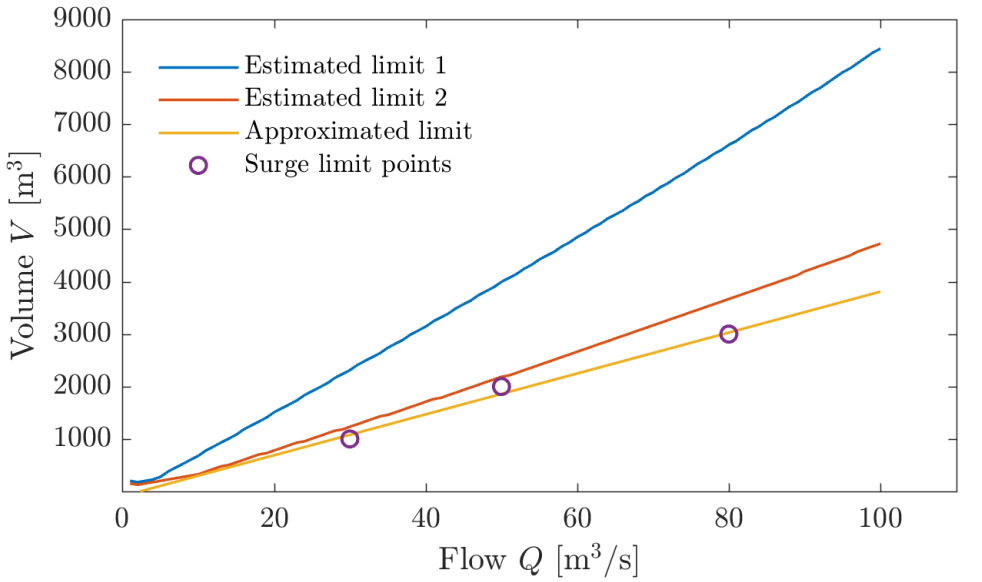

FIGURE E.2: The Case 1 minimum volume limit for different flows, estimated with simulations and theoretical calculations.

Thomas Svensson Moen

Mitigation of Discharge Fluctuations from Hydropower Plants by Active Measures

NTNU
Norwegian University of
Science and Technology